Remineralising composites with improved cytocompatibility and containing antimicrobial agents for conservative treatment of caries

Nicholas J. Walters
BSc (Hons), MSc

UCL

Doctor of Philosophy (PhD)

2016

Candidate declaration

I, Nicholas Walters confirm that the work presented in this thesis is my own, except where otherwise stated within the thesis. Where information has been derived from other sources, I confirm that this has been indicated in the thesis.

Signature: 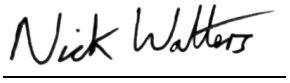 Date: 21st April 2016

Abstract

Objectives. To develop a remineralising dental composite with high strength, conversion and cytocompatibility and antimicrobial potential for more conservative treatment of dental caries.

Methods. The effect of glass filler particle size distributions and glass fibres on wet-point, handling and mechanical properties was assessed. The effect of two photoinitiators at varying concentrations and four co-initiators on conversion, cytocompatibility and mechanical properties was determined. The conversion, depth of cure, shrinkage, mechanical properties, water sorption and cytocompatibility of composites containing varying bulk (urethane dimethacrylate (UDMA), bisphenol A glycidyl methacrylate (Bis-GMA)) and diluent monomers (poly(propylene glycol) dimethacrylate (PPGDMA), tri(ethylene glycol) dimethacrylate (TEGDMA)) were characterised. The conversion, water sorption, calcium precipitation, mechanical properties and shear bond strength of composites containing remineralising and antimicrobial agents (monocalcium phosphate (MCP), tricalcium phosphate (TCP), ε-poly-L-lysine (εPL)) were assessed (storage in water, simulated body fluid (SBF), artificial saliva (AS)). Techniques included Fourier transform infrared spectroscopy, mass and volume determination, biaxial flexural testing, shear bond testing, scanning electron microscopy, energy-dispersive X-ray spectroscopy, Raman spectroscopy, resazurin, WST-8 and MTS assays.

Results. An optimal combination of fillers was established. Conversion was affected by co-initiator to a greater extent than photoinitiator. Composites containing UDMA and PPGDMA had the optimal balance of conversion, mechanical properties, depth of cure and cytocompatibility without increased shrinkage. Composites containing MCP with either TCP or εPL induced rapid hydroxyapatite formation on the surface of the composite within one week in SBF but not in AS or water.

Significance. Composites containing the newly developed liquid phase had high conversion and strength, slightly improved cytocompatibility and acceptable shrinkage. Whilst composites containing MCP and TCP were stronger, the added possible antimicrobial action of those containing MCP and εPL have great potential to defend against recurrent caries by preventing microbial microleakage.

Acknowledgements

This project was conducted at the Division of Biomaterials & Tissue Engineering at UCL Eastman Dental Institute, University College London. It was kindly funded by Engineering & Physical Sciences Research Council (EPSRC) [EP/I022341/1] and Dr. Brian Schottlander (Davis Schottlander & Davis Ltd). Monomers, photoinitiator and glass particles were generously provided by Dr. Stephan Neffgen (DMG Chemisch-Pharmazeutische Fabrik GmbH). Conference attendance was funded using travel grants generously provided by The Worshipful Company of Armourers & Brasiers [two grants totalling £950], Institute of Materials, Minerals & Mining (IOM^3) [three grants totalling £750] and Eastman Graduate Student Fund [£300].

I am especially grateful to my supervisor Prof. Anne Young for her excellent guidance and support throughout my PhD and for teaching me about polymer chemistry and many invaluable biomaterials synthesis and characterisation techniques. The experience I have gained under her supervision will be invaluable to me throughout my career and it was a pleasure working with her. I have also benefitted greatly from the advice and expertise of my secondary supervisors Dr. Paul Ashley and Dr. Vehid Salih, in the fields of restorative dentistry and cell biology, respectively, and for their encouragement throughout my PhD. I would like to thank my other colleagues at UCL Eastman Dental Institute. In particular, I am grateful to: Dr. Graham Palmer, Dr. Nicola Mordan and Dr. George Georgiou, for teaching me numerous techniques and providing invaluable technical support throughout my PhD; Dr. Wendy Xia, Dr. Saad Liaqat and Dr. Piaphong Panpisut, for contributing their time and effort to publications; and Dr. Kirsty Main, Dr. James Phillips and Dr. Nilay Lakhkar, for their helpful advice. I am also very grateful to Prof. Jonathan Knowles, Dr. Farzad Foroutan, Dr. Omaer Syed, Dr. Mustafa Al Qaysi, Dr. Gareth Owens and Dr. Vanessa Sousa Moreno for offering me the chance to be involved with several enjoyable collaborative opportunities.

I will be forever indebted to my mentor and friend, Dr. Eileen Gentleman, who has invested so much time in supporting my career over the last 8 years. I am also grateful to my former colleagues and current collaborators Assist. Prof. Susanna Miettinen, Prof. Minna Kellomäki, Prof. Jöns Hilborn, Dr. Laurent Bozec, Prof. Molly Stevens and Adj. Prof. Vesa Hytönen for supporting my future career path, and to the Jane & Aatos Erkko Foundation for providing generous funding for my postdoctoral research.

Finally, I wish to thank my fiancée, Anna-Elina for her moral support and patience throughout my PhD, my friends and my parents, Eva and Michael, for their unconditional support, which has enabled me to study and develop my career.

Publications & Funding

Publications, conference proceedings and funding relating to the work presented in this thesis are highlighted in red.

† joint first authorship | * corresponding author | ‡ presenting author

Peer-Reviewed Publications

5. **Walters NJ**, Xia W, Salih V, Ashley PF & Young AM*. Poly(propylene glycol) and urethane dimethacrylates improve conversion of dental composites and reveal complexity of cytocompatibility testing. *Dental Materials* 2016;32:264–77, doi: 10.1016/j.dental.2015.11.017.
4. Foroutan F, **Walters NJ**, Owens GJ, Kim H-W, De Leeuw N & Knowles JC*. Titanium-stabilised quaternary phosphate-based sol-gel glasses for bone tissue engineering applications. *Biomedical Materials* 2015;10, in press, doi:10.1088/1748-6041/10/4/045025.
3. Al Qaysi M†, **Walters NJ†**, Foroutan F†, Owens GJ, Kim H-W, Shah R & Knowles JC*. Strontium- and calcium-containing, titanium-stabilised phosphate-based glasses with prolonged degradation for orthopaedic tissue engineering. *Journal of Biomaterials Applications* 2015;30(3):300–310, doi:10.1177/0885328215588898.
2. **Walters NJ** & Gentleman E*. Evolving insights in cell-matrix interactions: Elucidating how non-soluble properties of the extracellular niche direct stem cell fate. *Acta Biomaterialia* 2015;11:3–16, doi:10.1016/j.actbio.2014.09.038.
1. Syed O, **Walters NJ**, Day RM, Kim H-W & Knowles JC*. Evaluation of decellularization protocols for production of tubular small intestine submucosa scaffolds for use in oesophageal tissue engineering. *Acta Biomaterialia* 2014;10:5042–53, doi:10.1016/j.actbio.2014.08.024.

Conference proceedings

13. **Walters NJ‡**, Yu TT, Oommen OP, Hilborn J, Miettinen S* & Gentleman E*. Sequential synthesis of modular poly(ethylene glycol)—peptide hydrogels for nanoscale control over extracellular matrix features. Proceedings of Tissue Engineering & Regenerative Medicine International Society European Chapter Conference; poster presentation; 2016 Jun 28 – Jul 1 Uppsala, Sweden, *in submission*.
12. **Walters NJ‡**, Yu TT, Oommen OP, Hilborn J, Miettinen S* & Gentleman E*. Synthesis of four-arm poly(ethylene glycol)—nitrophenyl carbonate for PEG—

peptide hydrogels. Proceedings of Scandinavian Society for Biomaterials; poster presentation; 2016 Jun 1–3 Reykjavik, Iceland, doi:10.13140/RG.2.1.2946.2806.

11. Koivisto J‡, **Walters NJ**, Parraga J & Kellomäki M*. Macro- and micro-scale mechanical characterisation of hydrogels. Proceedings of BioMediTech Research Day & Kauppi Campus Science Day; poster presentations; 2015 Dec 4 & 2016 Feb 11; Tampere, Finland, doi:10.13140/RG.2.1.2795.6567.
10. Sousa-Moreno V‡, Spratt D, Hassan I, **Walters NJ**, Sutherland J, Mardas N & Donos N*. Peri-implantitis microbiome variability across different disinfection protocols, implant surfaces and their relationship with biocompatibility dynamics: Proceedings of European Association for Osseointegration Conference; oral presentation; 2015 Sep 24–26; Stockholm, Sweden. *Clinical Oral Implants Research* 2015;26(S12):5, doi:10.1111/clr.4_12678.
9. **Walters NJ**‡, Miettinen S & Kellomäki M*. Spermidine cross-linked gellan gum hydrogels with a broad range of moduli for studying the influence of matrix stiffness on adipose-derived stromal cell fate: Proceedings of Tissue Engineering & Regenerative Medicine International Society World Congress; poster presentation; 2015 Sep 8–11 Boston, MA, USA. *Tissue Engineering Part A* 2015;21(s1):258–9, doi:10.13140/RG.2.1.3535.9840.
8. **Walters NJ**‡, Palmer G, Ashley PF & Young AM* (2015). Monocalcium phosphate Induces greater hydroxyapatite mineral formation than tricalcium phosphate on dental composites containing ε-poly-L-lysine: Proceedings of Tissue Engineering & Regenerative Medicine International Society World Congress; poster presentation; 2015 Sep 8–11 Boston, MA, USA. *Tissue Engineering Part A* 2015;21(s1):346–7, doi:10.13140/RG.2.1.3273.8400.
7. **Walters NJ**‡, Dakkouri LI, Ashley PF & Young AM* (2014). Calcium phosphate-precipitating, antimicrobial composite biomaterials: Proceedings of Tissue Engineering & Regenerative Medicine International Society European Chapter Conference; poster presentation; 2014 Jun 10–13 Genova, Italy. *Journal of Tissue Engineering & Regenerative Medicine* 2014;8(s1):263–4, doi:10.1002/term.1932.
6. Khan MA‡, **Walters NJ** & Young AM* (2014). Fibre-reinforced injectable orthopaedic composites with improved toughness and cell compatibility: Proceedings of Society for Biomaterials Conference; oral presentation; 2014 Apr 16–19; Denver, CO, USA, doi:10.13140/RG.2.1.3068.4321.
5. **Walters NJ**‡, Dakkouri LI, Ashley PF & Young AM* (2013). Remineralising dental composite with high conversion and low shrinkage for improved restoration

longevity: Proceedings of European Dental Materials Conference; poster presentation; 2013 Aug 29–30; Birmingham, UK, doi:10.13140/RG.2.1.2019.8566.

4. **Walters NJ**‡, Khan MA & Young AM* (2013). Novel fibre-reinforced remineralising dental and orthopaedic composites with improved toughness and fatigue properties: Proceedings of Swiss Society for Biomaterials Conference; oral presentation; 2013 Jun 25–26; Davos, Switzerland. *European Cells & Materials* 2013;26(4):3, doi:10.13140/2.1.3117.4083.
3. **Walters NJ**‡, Khan MA, Liaqat S & Young AM* (2013). Novel remineralising, antimicrobial dental & orthopaedic resin-based composites: Proceedings of Tissue Engineering & Regenerative Medicine International Society European Chapter Conference; oral presentation; 2013 Jun 17–20; Istanbul, Turkey, doi:10.13140/RG.2.1.2544.1443.
2. **Walters NJ**, Hulsart-Billström G‡, Engvist H & Larsson S* (2013). Premixed calcium phosphate cement as a carrier for bone morphogenetic protein 2: Proceedings of European Calcified Tissue Society Congress; poster presentation; 2013 May 18–21; Lisbon, Portugal. *Bone Abstracts* 2013;1:76, doi:10.1530/boneabs.1.PP87.
1. **Walters NJ**‡ & Young AM* (2012). Low shrinkage dental composites with high strength and toughness: Proceedings of Pan-European Region International Association of Dental Research Conference; 2012 Sep 12–15; Helsinki, Finland. *Journal of Dental Research* 2012;91(C):288, doi:10.13140/RG.2.1.1757.7127.

Acknowledgements for technical contributions to publications (peer-reviewed)

2. Gentleman E, Fredholm YC, Jell G, Lotfibakshaiesh N, O'Donnell MD, Hill RG & Stevens MM*. The effects of strontium-substituted bioactive glasses on osteoblasts and osteoclasts *in vitro*. *Biomaterials* 2010;31:3949–56, doi:10.1016/j.biomaterials.2010.01.121.
1. Gentleman E, Swain RJ, Evans ND, Boonrungsiman S, Jell G, Ball MD, Shean TAV, Oyen ML, Porter AE & Stevens MM*. Comparative materials differences revealed in engineered bone as a function of cell-specific differentiation. *Nature Materials* 2009;8:763–70, doi:10.1038/nmat2505.

Research funding (primary applicant)

2. Journal of Cell Science & The Company of Biologists Travelling Fellowship (£2,500), 2015.
1. Jane & Aatos Erkko Foundation Personal Scholarship (€180,000), 2015–2017

Scientific event organisation funding (primary applicant)

1. Royal Society of Chemistry: Chemistry Biology Interface Division Small Grant for Scientific Activities (£2,000), 2015.

Conference travel funding (primary applicant)

7. Royal Society of Chemistry: Chemistry Biology Interface Division Travel Grant for Postdoctoral Researchers, SCSB 2016 (£400), 2016.
6. The Worshipful Company of Armourers & Brasiers Gauntlet Trust Travel Grant, TERMIS-WC (£250), 2015.
5. Institute of Materials, Minerals & Mining Andrew Carnegie Research Fund, TERMIS-WC (£250), 2015.
4. Institute of Materials, Minerals & Mining Andrew Carnegie Research Fund, TERMIS-EU (£250), 2014.
3. Institute of Materials, Minerals & Mining Andrew Carnegie Research Fund, SSB+RM (£250), 2013
2. The Worshipful Company of Armourers & Brasiers Gauntlet Trust Travel Grant, TERMIS-EU (£700), 2013.
1. UCL Eastman Graduate Student Conference Fund, PER/IADR (£300), 2012.

Educational research funding (beneficiary)

3. PhD Studentship, Engineering & Physical Sciences Research Council (EP/I022341/1, PI: Prof. Anne Young), 2011–2014.
2. MSc Research Project Stipend (PI: Prof. Sune Larsson), 2011.
1. BSc Research Project Scholarship, European Union Socrates-Erasmus Programme (PI: Dr. Demetris Savva), 2005.

Table of contents

List of tables

List of figures

List of equations

List of abbreviations

3-MPTS	3-methacryloxypropyltrimethoxysilane, silane A174
4-META	4-methacryloxyethyl trimellitate anhydride
ACP	amorphous calcium phosphate, $Ca_xH_y(PO_4)_z \cdot nH_2O$ (n = 3–4.5)
ATR	attenuated total reflectance
β-TCP	refer to TCP
BFS	biaxial flexural strength
BHT	butylated hydroxytoluene
Bis-EMA	bisphenol-A ethoxylate dimethacrylate
Bis-GMA	bisphenol-A glycidyl methacrylate
BPA	bisphenol-A
CaP	calcium phosphate
CHXA	chlorhexidine diacetate
CQ	camphorquinone
D-value	mass division diameter
- d10	diameter at which 10% of sample's mass is comprised of smaller particles
- d50	mass median diameter
- d90	diameter at which 10% of sample's mass is comprised of larger particles
D-PBS	Dulbecco's phosphate buffered saline
DCP	dicalcium phosphate, $CaHPO_4$
- DCPA	- dicalcium phosphate anhydrous, also known as monetite, $CaHPO_4$
- DCPD	- dicalcium phosphate dihydrate, also known as brushite, $CaHPO_4 \cdot 2H_2O$
dH_2O	deionised water
DMAEMA	2-(*N,N*-dimethylamino)ethyl methacrylate
DMEM	Dulbecco's modified Eagle medium
DMPT	*N,N*-dimethyl-*p*-toluidine
E	Young's modulus of elasticity
ECM	extracellular matrix
EDAB	ethyl 4-(dimethylamino) benzoate
EDX	Energy dispersive X-ray spectroscopy
εPL	ε-poly-L-lysine, $(C_6H_{12}N_2O)_n$ (n = 23–33)
FBS	foetal bovine serum
FRC	fibre-reinforced composite
FTIR	Fourier transform infrared spectroscopy
GF	glass fibres, diameter 15 μm, length 300 μm
GIC	glass-ionomer cement
$GP_{0.7}$	glass particles, d50 = 0.7 μm
GP_5	glass particles, d50 = 5 μm
GP_7	glass particles, d50 = 7 μm
GPa	gigapascal

HA	hydroxyapatite, $Ca_5(PO_4)_3(OH)$
HEMA	2-hydroxyethyl methacrylate
HGF	human gingival fibroblast
LCU	light curing unit
LED	light-emitting diode
MCP	monocalcium phosphate, $Ca(H_2PO_4)_2$
- MCPM	- monocalcium phosphate monohydrate, $Ca(H_2PO_4)_2 \cdot H_2O$
MPa	megapascal
M_r	relative molecular mass
MTS	3-(4,5-dimethylthiazol-2-yl)-5-(3-carboxymethoxyphenyl)-2-(4-sulfophenyl)-2H-tetrazolium inner salt
MTT	3-(4,5-dimethylthiazol-2-yl)-2,5-diphenyltetrazolium bromide
η	viscosity
Mg-NTG-GMA	*N*(*p*-tolyl)glycine-glycidyl methacrylate magnesium salt
Na-NTG-GMA	*N*(*p*-tolyl)glycine-glycidyl methacrylate sodium salt
OX-50	fumed silica particles, d50 = 40 nm
ρ	density
PAN	polyacrylonitrile
PLR	powder to liquid ratio
PMMA	poly(methyl methacrylate)
PPD	1-phenyl-1,2-propanedione
PPGDMA	poly(propylene glycol) dimethacrylate
PMS	phenozine methosulfate
ppm	parts per million
P/S	penicillin-streptomycin
RI	refractive index
RMGIC	resin-modified glass-ionomer cement
TCP	tricalcium phosphate, $Ca_3(PO_4)_2$
- β-TCP	- β-tricalcium phosphate, $Ca_3(PO_4)_2$
TEGDMA	tri(ethylene glycol) dimethacrylate
T_g	glass transition temperature
TPO (Lucirin)	2,4,6-trimethylbenzoyl-diphenylphoshine oxide
TRIS	Tris(hydroxymethyl)aminomethane
UDMA	urethane dimethacrylate
UFS	uniaxial flexural strength
UV-A	near ultraviolet
WOF	work of fracture
WST-8	sodium 5-(2,4-disulfophenyl)-2-(4-iodophenyl)-3-(4-nitrophenyl)-2H-tetrazolium inner salt
XTT	2,3-bis-(2-methoxy-4-nitro-5-sulfophenyl)-2H-tetrazolium-5-carboxanilide inner salt

1 INTRODUCTION

This Chapter introduces dental anatomy, caries and restorative treatments.

1.1 Dental anatomy

1.1.1 Tooth organisation

Teeth protrude from the maxilla (upper jaw) and mandible (lower jaw) into the oral cavity. Humans develop two sets of teeth during their lifetime and are consequently termed diphyodont. Deciduous (primary) teeth erupt from their location within the bone beneath the gingiva (gum tissue) approximately six months after birth. Permanent (adult) teeth typically begin erupting at the age of ~5–6 years, with mixed dentition present until this process is complete at the age of ~11–12. A full set of deciduous teeth consists of eight incisors, four canines and eight molars, from anterior to posterior (20 in total). A complete adult set consists of eight incisors, four canines, eight bicuspids (premolars) and 12 molars (32 in total)[1].

1.1.2 Tooth structure

A tooth consists of four distinct tissue layers: enamel, dentine, cementum and pulp. The general structure of a tooth is illustrated in Figure 1.1.

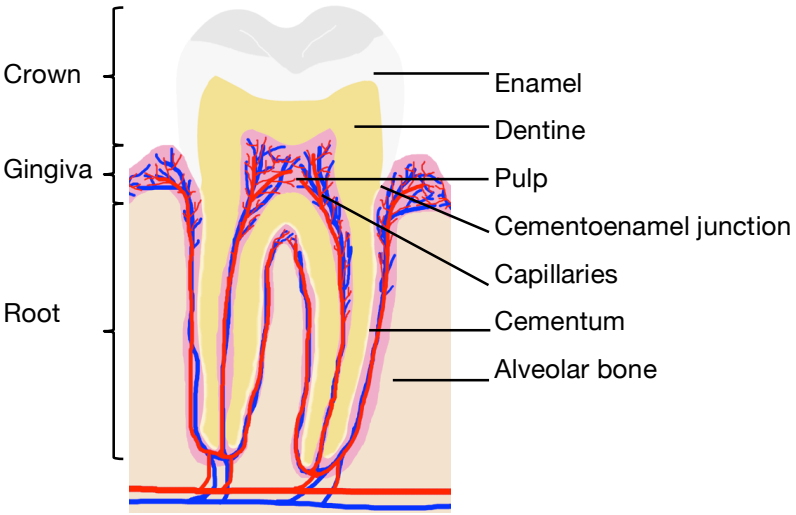

Figure 1.1. Dental anatomy.
Cross-section of a molar.

1.1.2.1 Enamel and cementum

Enamel, the outermost layer, is a strong, hard and highly mineralised tissue consisting of ~96% hydroxyapatite (HA) and fluorapatite mineral phases and ~4% enamelin protein. It is only formed during tooth development, via the process of amelogenesis.

This involves the secretion of extracellular matrix (ECM) protein amelogenin by ameloblast cells. This protein is involved in initiation and organisation of mineral precipitation during tooth development. Enamel colour varies between individuals, from white, through greyish or slightly blue hues, to pale yellow. Due to its semi-translucency, tooth colour is also influenced by the colour of the underlying dentine and any artificial restorations that extend beneath the enamel. Enamel is the only tissue exposed to the oral cavity in a healthy tooth and it varies in thickness, from a thin layer at the cementoenamel junction (CEJ) of ~300 μm^2 (although this varies significantly from patient to patient[3]), up to ~2.5 mm thick at the cusp of the tooth. Enamel forms the occlusal (biting) surface of the tooth's crown, up to the CEJ, to which the gingiva is attached. A glycoprotein film called pellicle is deposited by saliva on the surface of enamel, and acts as a barrier against over-mineralisation of enamel and against demineralisation via caries. Cementum, the outermost subgingival layer is a bone-like tissue which holds the root of the tooth in place below the CEJ and within the bone via the periodontal ligament. It is composed of ~45% HA, ~33% ECM and ~22% water and is subsequently softer than dentine[1].

1.1.2.2 Dentine

Dentine forms the bulk of the tooth structure and consists of ~70% HA, ~10% water and ~20% ECM, most of which is fibrous collagen. It is served by parallel canaliculi, also known as dentinal tubules, which contain cytoplasmic extensions of odontoblasts, the cell bodies of which form the periphery between dentine and the underlying pulp layer. Odontoblasts lay down dentine via the process of dentinogenesis. During tooth development they form primary dentine. Secondary dentine is synthesised in developed teeth, whereas the formation of tertiary dentine is a defensive response to delay caries from reaching the pulp. The diameter of dentinal tubules progressively narrows from ~2.5 μm near pulp to ~0.9 μm near enamel. They maintain dentine quality by acting as a reservoir of ions, proteins and water, provided via the blood supply in the pulp and enabling the deposition of novel mineral[1].

1.1.2.3 Pulp

Dental pulp is a highly vascularised tissue that resides within the pulpal chamber below dentine. The blood supply provides ions and nutrients for the maintenance of mineral and organic tooth components. It also contains nerves, which provide a sensory function in response to temperature, pressure and trauma, and which trigger tertiary dentine production by odontoblasts upon infection of the dentine. The cell body of

odontoblasts resides in the pulp, as does a supply of their multipotent precursors, dental pulp stem cells, which derive from mesenchymal stromal cells (MSC)[1].

1.2 Dental caries

1.2.1 Aetiology

Dental caries (tooth decay) is a disease characterised by pain and eventual loss of dental tissues, caused by bacterial infection. Microbes produce acids upon hydrolysis of nutrients, namely sugars that have accumulated within the pellicle, causing demineralisation of enamel, dentine and cementum. In a caries-free subject, the process of demineralisation occurs continuously. This is countered by remineralisation, induced by precipitation of calcium, phosphate and fluoride ions, which are present in saliva, fluoridated toothpastes and mouthwashes. Inside the tooth, ions are transported via passive mass transport from blood in the pulp via odontoblasts to the dentinal tubules where they form dentinal fluid, which supplies dentine with a source of ions. When oral pH drops below ~5.5, however, the equilibrium is disrupted and demineralisation exceeds remineralisation, resulting in net tissue loss. Erosion of the outer enamel layer is followed by bacterial infection and demineralisation of the underlying dentine. Caries can eventually reach the pulp, where it causes inflammation and pain.

Caries is caused by an imbalance in the oral microbiome, which can be brought about by a high sugar diet and/or poor dental hygiene. Patients with genetic conditions in which proteins that guide tooth tissue formation or make up the ECM are mutated, such as amelogensis imperfecta and dentinogenesis imperfecta, are particularly susceptible to caries. These patients present extreme discolouration of the teeth, which are typically yellow, brown or grey due to the absence of enamel, and suffer from hypersensitivity. Caries can also be exacerbated by medical conditions which reduce the flow rate of saliva, such as Sjögren's syndrome, diabetes mellitus, diabetes insipidus, and sarcoidosis, as well as medications and recreational drugs that cause dry mouth.

The most notable bacterial species responsible for dental caries are *Streptococcus mutans* and *Staphylococcus aureus*, with species from genera *Lactobacillus*, *Bifidobacterium*, *Proprionibacterium* and *Actinomyces* also reported to contribute. All of these bacteria stain Gram-positive and most are facultatively anaerobic. They utilise sugar and starch deposits on and around the teeth as a source of nutrients, most notably fermentable carbohydrates such as glucose, sucrose and fructose. Their

anaerobic respiration produces lactic acid as a by-product, which is responsible for the demineralisation of dental tissues and acts by dissolving the calcium and phosphates that form the bulk of the mineral. Large quantities of bacteria can build up and form a biofilm on the surface of and in-between teeth. This film is called plaque, and it can mineralise over time, forming tartar. Plaque creates an acidic environment on and around the teeth and can cause caries, gingivitis and/or periodontitis if not frequently removed via an oral hygiene regimen. Although saliva counters demineralisation, it is unable to penetrate the biofilm and neutralise the acids formed between the plaque and the tooth[4].

Formation of a cavity is irreversible. Although tertiary dentine can be laid down as a response to infection, the high mineral content makes the dentine and enamel inaccessible to stem cells and odontoblast protrusions that could otherwise potentially regenerate the organic phases of the tissues. Infection of the enamel causes demineralisation, which can eventually lead to infection of the dentine below, and in some cases, the pulp. Since dentine is a softer tissue than enamel, caries tends to progress at a more rapid rate once it has reached the dentine. The progression of caries is illustrated in Figure 1.2.

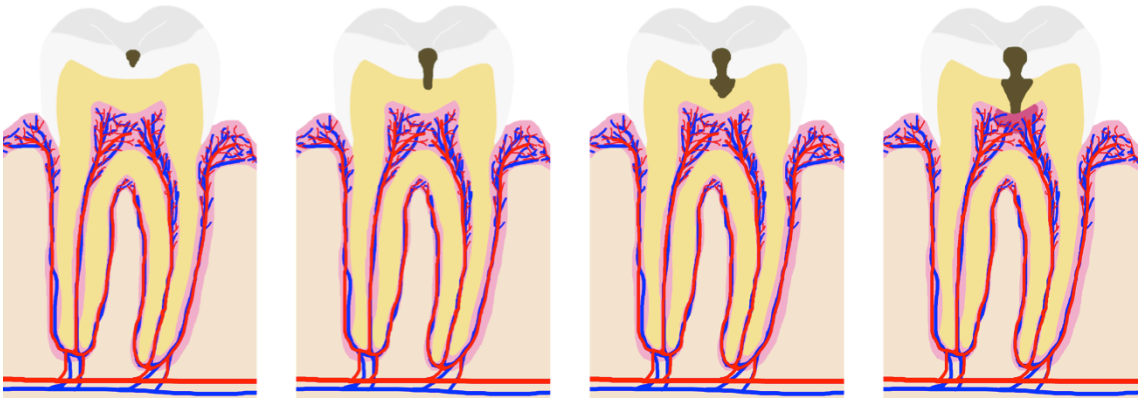

Figure 1.2. Dental caries progression.

Biofilm build-up (shown in dark brown) results in enamel demineralisation, followed by penetration of the dentine. This can eventually reach the pulp, causing inflammation and pain.

1.2.2 Epidemiology

Dental caries is amongst the world's most prevalent diseases and is the most common childhood disease. Between 1999 and 2004, it affected 21% of American children aged 2–11 with adult teeth, 59% of adolescents and 92% of adults and seniors, with around 20% of the total population having had caries that had gone untreated. A significant decline in prevalence between the 1970s and 1999 may be attributed to improved dental hygiene. However, there is still great disparity between different ethnicities,

which is apparent between subpopulations in the USA, e.g. disparities between communities of Caucasian and Hispanic origin, and between populations with low vs. high income. Whilst genetic susceptibility may contribute to this variation, socioeconomic factors are the most significant cause of disparate rates of caries across the world[5].

1.2.3 Prophylaxis

Oral hygiene and dietary modification are prophylactic methods used to prevent dental caries. Routine tooth brushing twice per day and regular use of dental floss prevents build-up of plaque and help to minimise tooth demineralisation caused by the microbes that constitute the biofilm. Since high sugar diets result in high levels of caries, sugar intake should be kept to a minimum, in particular with regards to drinks with high sugar content. A high calcium diet and calcium and fluoride supplements have been shown to decrease susceptibility to caries. Additionally, the widespread inclusion of fluoride in toothpastes and mouthwashes is highly beneficial to caries prevention[6].

1.2.4 Treatment

Dental caries is typically treated by removing infected (and sometimes some affected) dental tissue and replacing the void using dental restorative materials, such as those discussed in Chapter 1.3.

1.3 Dental restorative materials

Humans have been making efforts to restore teeth since prehistoric times. The most ancient known dental filling, discovered in Slovenia, consists of beeswax and dates back to the 6,500 years to the Neolithic period (Figure 1.3)[7].

Figure 1.3. Earliest known example of a dental restoration.
A Neolithic beeswax filling in a left canine found in Slovenia. Figure reproduced from Ref. [7] under the terms of the Creative Commons Attribution License.

Amalgam was developed in the 19th century and is still widely used today. There is, however, an increasing trend towards clinicians and patients favouring white, aesthetic fillings, including composites, glass-ionomer cements (GIC) resin-modified glass-ionomer cements (RMGIC) and compomers. As demand increases, so too does the need to overcome the disadvantages of existing restorative materials. Chapter 1.3

provides a brief introduction to the composition and the advantages and disadvantages of each type of material.

1.3.1 Amalgams

Amalgams are malleable mercury alloys containing silver, tin, zinc and copper. Unfavourable due to their poor aesthetics and destructiveness to healthy tissue, researchers have sought to replace amalgams with more aesthetically suitable materials over the last fifty years. Despite significant advances, amalgam is still widely used, due to its durability, longevity and low cost. One major issue that modern materials overcome with relative success is that amalgam restorations often require removal of sound tooth structure in order to anchor the restoration to the tooth, since it does not bind to the tissue. Furthermore, amalgam expands and contracts in response to heat and cold much more rapidly than the tooth[8], which can exert pressure on the remaining tooth structure.

Mercury is a heavy metal which imparts an advantageous bacteriostatic effect on microbes, but is highly toxic at sufficient doses (acute effects observed at dose of 14–57 mg/kg body weight for an adult[9]) and harmful to living organisms. The use of amalgam was phased out in Norway, Denmark and Sweden over the early 2000s and eventually banned in Scandinavia by 2009. The phasing out of amalgam is justified by two issues, with emphasis on the latter: mercury concentration in the liver is directly proportional to number of amalgam fillings and although levels of mercury leaching are low, its presence in the liver is of concern; manufacture and disposal of mercury-based materials results in environmental contamination of water sources and soil, which in turn are toxic to humans and other organisms in the food chain.

Furthermore, the Minamata Convention on Mercury[10] is an international treaty implemented by the United Nations Environment Programme to protect humans and the environment from mercury contamination. Signed by the UK in October 2013 and by a further 127 countries since, including the US and all EU member states, it aims to phase out the use of dental amalgam. Whilst it does not absolutely preclude the use of amalgam where its use would be beneficial to the patient, it seeks to encourage more conservative use of amalgam for the benefit of most patients and the environment. Composites are in most cases a more appropriate alternative to amalgam.

1.3.2 Composites

Composites were introduced in the early 1960s[11] as an attempt to improve the aesthetics of fillings. They consist primarily of radiopaque glass particle filler bound

together by a network of synthetic polymers, most commonly dimethacrylates and more recently, ring-opening siloranes. Most current commercial composites are supplied premixed in syringes that do not require mixing by the clinician and are cured by photoinitiation using a light-curing unit (LCU). Composites have superior aesthetics and mechanical properties compared to other white dental restorative materials. They have excellent handling properties and depending on formulation, can be layered incrementally or used to bulk fill cavities. As with other aesthetic fillings, they allow minimal enamel and dentine removal and are significantly less destructive than amalgam.

There are two major drawbacks, however, that affect composite longevity. The bond between the tooth and restoration has low durability, since it is based on a physical interaction between the polymer and the collagen fibres in dentine, which are exposed upon acid-etching (described in more detail in Chapter 2.2). Furthermore, upon curing, composites contract by ~2–6 vol% due to polymerisation shrinkage. These factors can cause debonding of the composite and in some cases eventually result in microbial microleakage between the tooth and restoration. Despite their high strength, composites are brittle and have a relatively high fracture and failure rate[12-14]. Dimethacrylate composites are described in more detail in Chapter 1.4.

The general procedure for performing a composite restoration involves the removal of infected and sometimes some affected tissue, followed by etching (discussed in more detail in Chapter 2.2) and treating of the cavity. An adhesive is then applied and cured, followed by incremental layering and curing of the composite. The final layer is sculpted, cured and then polished.

1.3.3 Glass ionomer cements

Introduced in the early 1970s, GICs consist of silicate glass powders and organic acids. They are chemically cured and adhere to the tooth via an acid-base reaction, which forms a more durable chemical bond to the mineral than composite adhesives do to collagen. GICs release fluoride for a relatively long period and can act as a fluoride reservoir, “recharging” in the presence of fluorides in drinking water, toothpastes and mouthwashes. This can help to increase the level of fluorapatite in enamel and has a bacteriostatic and bactericidal effect. Fluorapatite is significantly less soluble than HA and addition of fluoride to tap water has successfully reduced the incidence of dental caries in a large number of case studies[15]. One major drawback of GICs is that they are considerably weaker than composites. As they are brittle, they are not favoured in load-bearing cavities. Whilst they have relatively good aesthetic

properties, they fail to match teeth as accurately as composites due to their lack of translucency. In addition, they have poor wear resistance and longevity[16,17].

1.3.4 Resin-modified glass ionomer cements

RMGICs are hybrids of GICs and composites that contain a dual thermal initiator and photoinitiator curing system. They have aesthetic properties between those of GICs and composites. Their composition is similar to that of GIC, with the addition of monomers such as HEMA and photoinitiators. They also act as a fluoride reservoir. RMGICs have poor wear resistance and are stronger than GICs but weaker than composites, rendering them unsuitable for occlusal surfaces. Whilst they are cosmetically superior to GICs, they also fail to match the aesthetics of composites.

1.3.5 Compomers

Compomers (polyacid-modified composite resins) are GIC-composite hybrids with greater monomers content than RMGICs, resulting in greater strength. Their aesthetics are superior to RMGICs and GICs, but inferior to composites. They release a small quantity of fluoride, though this is thought to be clinically insignificant, and they do not act as a reservoir. Like composites, compomers require use of a bonding agent[14,16,18].

1.3.6 Advantages and disadvantages of restorative materials

The advantages and disadvantages of the aforementioned dental restorative materials are summarised in

Table 1.1. Advantages and disadvantages of dental restorative materials.	**Amalgam**	**Composite**	**Compomer**	**RMGIC**	**GIC**

. This is an approximation based on the literature and discussions with clinicians, including Dr. Paul Ashley (Paediatric Dentistry, UCL Eastman Dental Institute). Aesthetics are increasingly considered to be one of the most important factors concerning dental restorative materials.

Table 1.1. Advantages and disadvantages of dental restorative materials.	**Amalgam**	**Composite**	**Compomer**	**RMGIC**	**GIC**
Aesthetics					
Minimally invasive					
Restoration longevity					
Strength					
Application in load-bearing teeth					
Bond or retention durability					

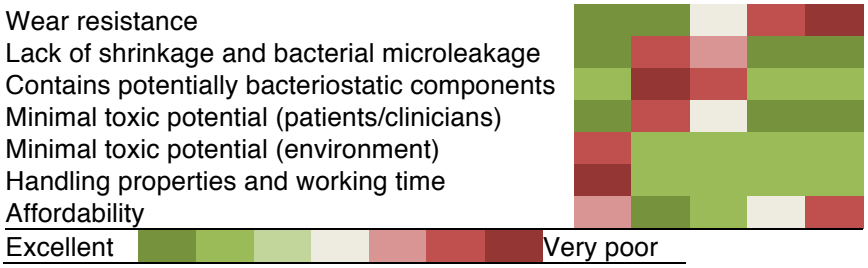

1.4 Aims and objectives

The aim of this project was to develop a novel remineralising dental composite with high strength, improved cytocompatibility and antimicrobial potential for more conservative treatment of dental caries. Such materials have the potential to protect against dental caries whilst allowing minimal removal of healthy tissue[19]. The hypotheses and objectives are summarised sequentially below and are discussed in greater detail in the corresponding chapters.

- The use of long, flexible monomers with high relative molecular mass (M_r) and low double bond concentration should result in high conversion (≥ 70%) compared to many commercial composites (~50%). This in turn should improve mechanical properties and cytocompatibility without detrimentally affecting shrinkage or aesthetics.
- The use of calcium phosphates (CaP) should result in water sorption, followed by CaP release and the precipitation of stable mineral on the composite surface. The water sorption and remineralisation together have the potential to seal the interface between the tooth and restoration, preventing microbial microleakage, recurrent caries and restoration failure. This could enable the removal of less of the healthy tissue, making the procedure less invasive and painful. This could be of particular benefit to paediatric patients and patients in developing countries, where access to costly dental equipment such as drills may be restricted.
- The use of a highly soluble preservative has the potential to aid CaP release and nucleation, as well as protect against microleakage through its antimicrobial action.
- The use of reinforcing fibres should improve the toughness and therefore longevity of the composite, making it ideal for load-bearing restorations.
- The aesthetics of the cured composite must remain of acceptable quality.

The material under development aims to overcome some of the shortcomings of existing composites whilst introducing additional novel features that could contribute to a new generation of multi-action restorative materials. These materials could particularly benefit young and disadvantaged patients, who can be more difficult to

treat due to anxiety[20] and lower access to affordable dental care. They also trigger a shift to “smarter” dental materials which continue to function and “respond” to the clinical situation after application, an approach which is targeted in other biomaterials and drug delivery approaches, e.g. in this case through recurrent caries causing further release of remineralising and antimicrobial agents.

2 COMPOSITES

This chapter describes the composition of dimethacrylate-based composites in greater detail, introducing the mechanism of polymerisation and adhesion and discussing their typical composition. It also describes innovative variations of composites, such as remineralising, antimicrobial and fibre reinforced materials.

2.1 Dimethacrylate polymerisation

The most widely used type of monomer used in dental composites is dimethacrylates, which are linear molecules containing a methacrylate group ($CH_2C(CH_3)C(OH)OR–$) at each end that were developed by Bowen in the early 1960s[11]. Although other types of monomers have been developed with the aim of reducing shrinkage, such as ring-opening siloranes, these are beyond the scope of this thesis. The polymerisation discussed therefore refers to that of chain growth polymerisation of dimethacrylates.

Chain growth polymerisation can be described to occur in three phases, preceded by the formation of free radicals (Figure 2.1). Radicals are formed either via thermal initiation or photoinitiation. The majority of dimethacrylate-based composites are initiated by photoinitiation (discussed in more detail in Chapter 2.3.1), whereas orthopaedic cements are typically initiated via a thermal reaction, which occurs upon contact between an initiator and co-initiator.

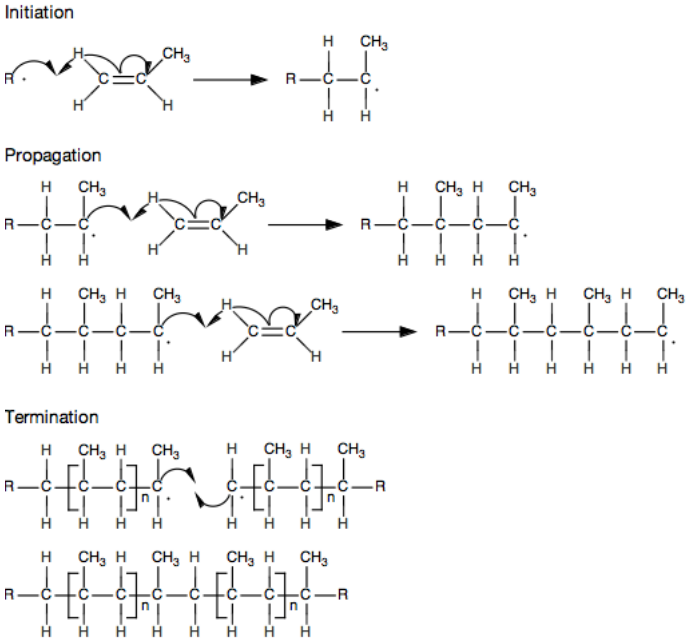

Figure 2.1. Chain growth polymerisation.

Initiation, propagation and termination reactions of chain growth polymerisation in a simple methacrylate system.

The free radicals generated during photoinitiation in turn initiate the polymerisation process. A new C–C bond is formed between a radical and a methacrylate group belonging to a monomer molecule. This occurs when the radical and the alkene group (C=C) of the methacrylate group each donate an electron. Another electron from the alkene group relocates to the C at the opposite terminus of the monomer. The resulting molecule still has an extra electron, meaning it then acts as a radical and reacts with another monomer molecule. This process occurs numerous times and results in chain growth of the polymer. The process is terminated when two radicals react with one another. Any free radicals that may remain after the polymer has formed may either recombine or eventually diffuse out of the polymer.

The situation in a dental composite containing multiple monomers of high M_r is more complicated than the example illustrated in Figure 2.1. Since the monomers are dimethacrylates, the resulting polymer is highly cross-linked. Cross-linking improves mechanical properties, wear resistance and cytocompatibility but increases shrinkage.

2.2 Composite adhesion

Since GICs and RMGICs are able to bond chemically to the tooth structure via an acid-base reaction, they do not require an adhesive agent. They also have a lower failure rate than composites and compomers, which require conditioners, primers and adhesives. The adhesive interacts with the tooth via a weaker, micro-mechanical bond rather than covalent bonding. A conditioner removes the bacterial “smear layer” and etches the tooth. It consists of an acidic gel, such as 37% phosphoric acid, or acidic monomers. Primers consist of bifunctional monomers such as 2-hydroxyethyl methacrylate (HEMA), a surfactant which is hydrophilic at one end and hydrophobic at the other. HEMA is able to bind to both the composite and collagen and expand the matrix. Primers do not contain fillers and in order to reduce their viscosity and improve wetting of the etched tissue, they contain volatile solvents such as ethanol, which evaporate after application. Adhesives contain adhesive monomers, which create a durable bond that links the primer to the composite. They seal the dentine tubules and form a “hybrid layer” between the demineralised dentine and the restoration. As a general rule, preparation of the tooth with more steps results in a more reliable bond (Table 2.1)[21].

In enamel, the conditioner etches gaps around the apatite crystals, allowing the primer to envelop the crystals. In dentine, it demineralises peritubular and intertubular dentine (dentine along the lining of the tubules and between tubules, respectively), exposing

~5–8 µm of collagen matrix, around which primer binds (Figure 2.2). The branched structures created by resin around the tubules are called tags. The more branched the tag, the more durable the bond (Figure 2.3)[21-26].

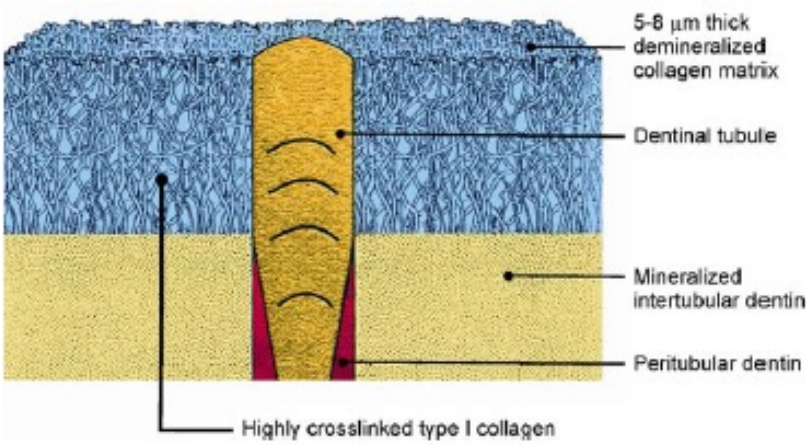

Figure 2.2. Demineralised dentine.

The etched dentine layer consists of ECM components and lacks mineral. The composite binds around the exposed collagen, forming a mechanical bond to the tooth. Reproduced with permission from Ref. [27], © Elsevier Ltd.

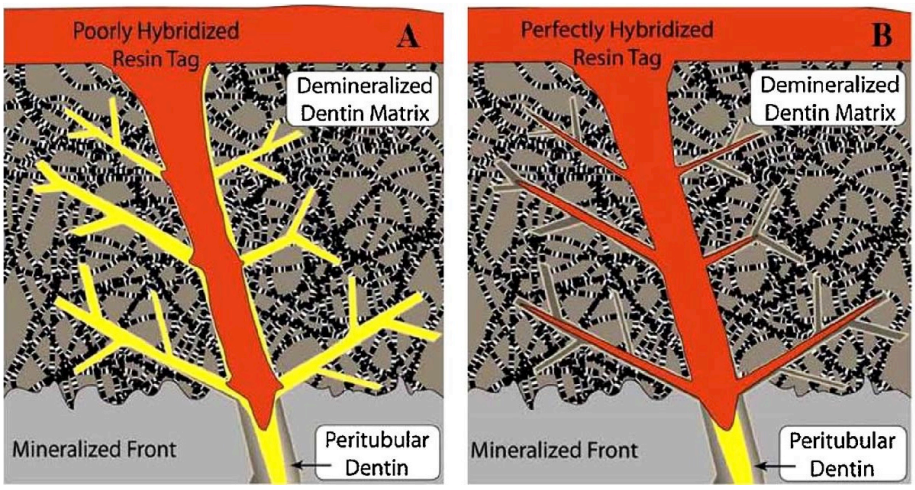

Figure 2.3. Resin tag hybridisation.

(a) Poorly and (b) well hybridised resin tags. Reproduced with permission from Ref. [27], © Wiley Periodicals Inc.

Table 2.1. Tooth preparation techniques and annual failure rates.

Technique	Mean annual failure rate (%)	Preparatory steps
3-step etch & rinse	4.8 ± 4.2	1. Etch & rinse 2.Primer 3. Adhesive
2-step etch & rinse	6.2 ± 5.5	1. Etch & rinse 2. Combined primer & adhesive
2-step self-etch	4.7 ± 5.0	1. Acidic monomer primer 2. Adhesive
1-step self-etch	8.1 ± 11.3	1. Combined acidic monomer primer & adhesive
GIC	1.9 ± 1.8	None

From Ref. [22].

2.3 Composite components

This section introduces the components used in the present research. In some cases, examples of other commonly used components are briefly described. The information in the tables is provided by the corresponding manufacturer.

2.3.1 Liquid phase

The liquid phase of a typical dental composite consists of monomers combined with a photoinitiator system. These compounds are also widely used in dental adhesives and have been comprehensively reviewed[25]. In Chapter 2.3.1, the liquid phase components used throughout the present research are listed and some of their relevant characteristics are introduced.

2.3.1.1 Bulk monomers

Bulk monomers are the main constituent of the liquid phase. They tend to have high viscosity (η), typically due to chemical groups that hinder flexibility. This tends to result in stronger, more rigid materials upon curing. The bulky aromatic groups of commonly used monomer bisphenol-A glycidyl methacrylate (Bis-GMA, Figure 2.4b), for example, hinder mobility and create stiff composites[28]. In addition, hydroxyl groups cause intermolecular binding between molecules, e.g. via hydrogen bonds. The very high viscosity (~700 Pa·s) that results from this, however, impedes diffusion of the reactive species formed during the polymerisation reaction, preventing even propagation of the polymer throughout the full depth of the material as the reaction progresses and resulting in low conversion and depth of cure (DC). In contrast, bisphenol-A ethoxylate dimethacrylate (Bis-EMA, Figure 2.4a) lacks hydroxyl groups and is more flexible and much less viscous (~3 Pa·s) as a result. Similarly, urethane dimethacrylate (UDMA, Figure 2.4c) is much less viscous than Bis-GMA (~8.5 Pa·s). Its viscosity remains high enough to create a packable material that is easy for clinicians to sculpt into shape, yet sufficiently low to achieve a high PLR, since the viscosity of the liquid phase affects the level of wetting of the fillers.

Commercial composites typically contain a mixture of bulk monomers, the ratio of which is not normally disclosed. Filtek Z250 (3M ESPE), for example, contains Bis-GMA, UDMA and bisphenol-A ethoxylate dimethacrylate (Bis-EMA) together with diluent monomer tri(ethylene glycol) dimethacrylate (TEGDMA).

Rigidity of monomers is inherently associated with brittleness. The complete replacement of Bis-GMA with UDMA as the bulk monomer may result in composites

with lower water sorption[29], lower modulus and improved toughness[30] without significantly higher shrinkage[31].

Furthermore, Bis-GMA has historically been synthesised from a bisphenol-A (BPA) precursor, which has been proved to be oestrogenic (oestrogen mimicking), which is of concern to patients, particularly children who are still developing[32]. Although many manufacturers now synthesise BPA-free Bis-GMA via a different route, hydrolysis of Bis-GMA may still result in low levels of BPA leaching from composites.

For these reasons, the total replacement of Bis-GMA with UDMA is investigated in Chapter 5. The chemical structures of Bis-EMA, Bis-GMA and UDMA are illustrated in Figure 2.4 and their physical properties are presented in Table 2.2.

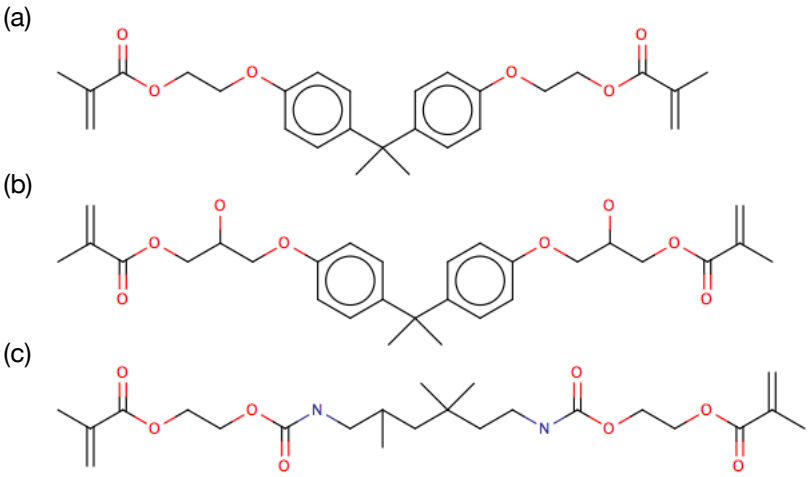

Figure 2.4. Chemical structures of bulk monomers.

(a) Bisphenol-A ethoxylate dimethacrylate (Bis-EMA), (b) bisphenol-A glycidyl methacrylate (Bis-GMA) and (c) urethane dimethacrylate (UDMA).

Table 2.2. Bulk monomer physical properties

Bulk monomer	M_r	ρ (g/cm^3)	RI	η (Pa·s)
Bis-EMA	540	1.12	1.49–1.53	3
Bis-GMA	512	1.16	1.54	700
UDMA	470	1.12	1.48	8.5

2.3.1.2 Diluent monomers

Diluent monomers are incorporated alongside bulk monomers in composite liquid phases in order to reduce viscosity. The ratio of bulk to diluent monomer is typically such that the diluent monomer constitutes around one third or less of the liquid phase. This is in order to maintain optimal physical properties, such as high strength and low shrinkage.

TEGDMA (Figure 2.5b) is the most widely used diluent monomer. Its very low viscosity (~0.09 Pa·s) means that only a small proportion must be used in order to improve the flow and handling properties of the composite. TEGDMA, however, has poor cyto- and genocompatibility[33-37], acts as a vasorelaxant[38-42] and causes apoptosis and necrosis[43,44]. Furthermore, its high double bond concentration increases shrinkage. Its omission from composites would therefore be ideal. The use of poly(propylene glycol) dimethacrylate (PPGDMA, Figure 2.5a) in place of TEGDMA was therefore investigated in Chapter 5. The use of PPGDMA, which is a larger molecule with significantly lower double bond concentration than TEGDMA, has not previously been investigated in dental composites.

The chemical structures of PPGDMA and TEGDMA are illustrated in Figure 2.5 and their physical properties are presented in Figure 2.5.

(a) (b)

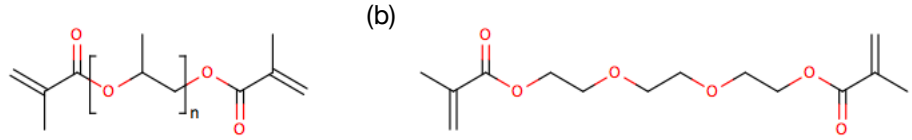

Figure 2.5. Chemical structures of diluent monomers.

(a) Poly(propylene glycol) dimethacrylate (PPGDMA) and (b) triethylene glycol dimethacrylate (TEGDMA).

Table 2.3. Physical properties of diluent monomers.

Diluent monomer	Mr	ρ (g/cm^3)	RI	η (Pa·s)
PPGDMA	600	1.01	1.45	0.09
TEGDMA	286	1.09	1.46	0.05

2.3.1.3 Photoinitiators

Di-2,3-diketo-1,7,7-trimethylnorcamphane, a yellow powder more commonly known as *D*,*L*-camphorquinone (CQ, Figure 2.6a & Table 2.4) is historically the most commonly used photoinitiator in dental composites and adhesives and is used in combination with a co-initiator. It is a type II (electron-transfer) photoinitiator which, upon exposure to blue visible light, interacts with a co-initiator (an electron donor) such as a tertiary amine, yielding radicals by hydrogen abstraction[25]. Each α-dicarbonyl CQ molecule becomes a ketyl radical and each co-initiator molecule becomes an amino alkyl radical. This process is illustrated in Figure 2.7. CQ is well characterised and its use is advantageous, due to its broad absorbance range of 360–510 nm, with peak absorbance in the visible blue light spectrum at 468 nm. Dissolution in monomers such as TEGDMA results in a bathochromic shift (lengthening of the peak absorbance

wavelength) to 474 nm. These wavelengths are covered by LCUs, which are currently the most commonly used light sources and utilise blue light-emitting diodes (LED) with a wavelength range of approximately 400–500 nm[45]. The main disadvantage of CQ is its colour. Depending on the output power and wavelength, this yellowness is bleached by some LED units more efficiently than by others[46]. Furthermore, CQ has been shown to significantly alter metabolism of several structural lipids *in vitro*, which may affect membrane integrity and permeability[47]. A low CQ concentration or replacement with an alternative photoinitiator may therefore be desirable.

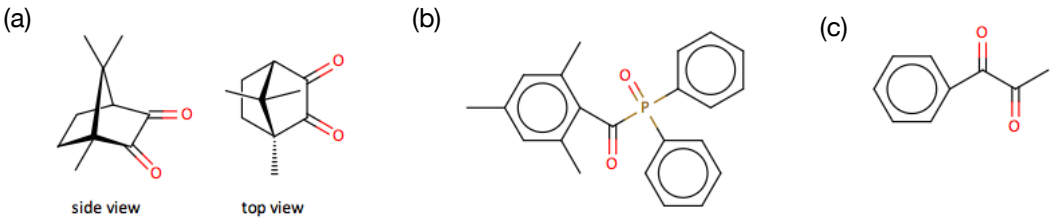

Figure 2.6. Chemical structures of photoinitiators.

(a) Di-2,3-diketo-1,7,7-trimethylnorcamphane (*D*,*L*-camphorquinone, CQ), (b) 2,4,6-trimethylbenzoyl-diphenylphosphine oxide (TPO) and (c) 1-phenyl-1,2 propanedione (PPD).

Table 2.4. Physical properties of photoinitiators.

Photoinitiator	M_r	ρ (g/cm^3)	RI	Absorbance (nm)	
				Range	Peak
CQ	166	0.97	*	360–510	474
TPO	348	1.12	1.48	230–430	385
PPD	148	1.10	1.53	300–480	410

* Unknown

Another class of photoinitiators called acylphosphine oxides, of which 2,4,6-trimethylbenzoyl-diphenylphosphine oxide (TPO, commercial name Lucirin, Figure 2.6b & Table 2.4) is an example, have strong absorption in the near ultra-violet (UV-A) spectrum, with some overlap of the visible blue light spectrum[25,48]. Such molecules are classed as type I (photo-fragmentation) photoinitiators and do not require a co-initiator. Each molecule is cleaved upon irradiation, forming two free radicals. This process is illustrated in Figure 2.8. Some composite manufacturers favour TPO for its less yellow, more off-white colour. When used at high concentrations, however, TPO turns yellow upon polymerisation[49]. TPO requires the use of a quartz tungsten-halogen light source. Since LED LCUs are currently more common and convenient than tungsten-halogen LCUs due to their more compact size, however, TPO was not utilised in the present work.

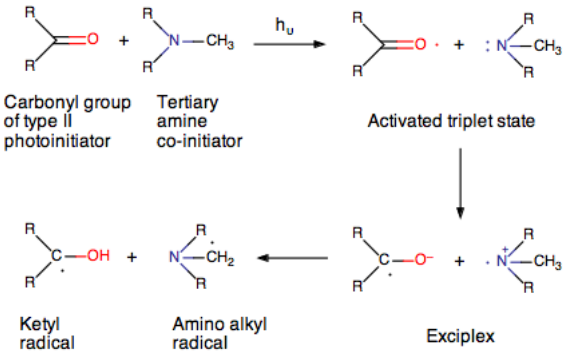

Figure 2.7. Type II photoinitiation by hydrogen abstraction.

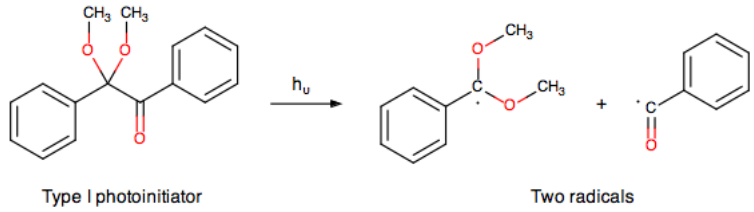

Figure 2.8. Type I photoinitiation by photo-fragmentation.

1-phenyl-1,2 propanedione (PPD, Figure 2.6c & Table 2.4) is an α-diketone which has the favourable property of being able to form free radicals by both type I and type II reactions. It absorbs light with a wavelength of 300–480 nm, with its peak on the edge of the visible light spectrum at 410 nm. PPD is a pale yellow liquid. It has been reported to result in increased mechanical strength and comparable or improved degree of conversion (DC) compared to CQ[25]. The free radicals formed by PPD are less likely to recombine than the two carbonyl radicals of CQ, which are structurally bonded to one another[50], meaning their action may be prolonged compared to CQ. By contrast, however, presence of co-initiators reduces the rate of free radical development compared to CQ. Nevertheless, it has been reported that when PPD and CQ are combined at a ratio of between 1:1 and 1:4, respectively, they act synergistically to improve depth of cure[51].

Since the absorbance range of PPD overlaps that of the conventional LED units used to initiate CQ, they were used in conjunction with one another in Chapter 6, in order to investigate whether any improvement to mechanical properties and DC resulted from using both together. CQ was used alone in the remaining studies.

2.3.1.4 Co-initiators

Various tertiary amines are used in conjunction with type II photoinitiators such as CQ and PPD, for their ability to donate protons to the excited initiator molecules and form

free radicals. Tertiary amines consist of a nitrogen atom surrounded by three side chains (designated 'R groups', Figure 2.9a), which can vary in size and complexity.

N,N-dimethyl-*p*-toluidine (DMPT, Figure 2.9c & Table 2.4) is historically one of the most commonly used co-initiators, though its use has declined due to realisation of toxic effects, caused by its low relative molecular mass (M_r 135) enabling it to readily penetrate cells and by its carcinogenic metabolites[52]. 2-(*N,N*-dimethylamino)ethyl methacrylate (DMAEMA, Figure 2.9b & Table 2.4) and ethyl 4-(dimethylamino) benzoate (EDAB, Figure 2.9d & Table 2.4) are commonly used co-initiators with slightly higher M_r than DMPT (193.2 and 157.2, respectively). DMAEMA has the advantage of containing polymerisable methacrylate groups, which allows it to become incorporated into the polymer during conversion, thus reducing the risk of leaching.

Similarly, *N*(*p*-tolyl)glycine-glycidyl methacrylate (NTG-GMA, Figure 2.9e–f & Table 2.4) is polymerisable, but has the extra advantage of being trifunctional (it contains methacrylate, amine and salt groups). It can be obtained as either a magnesium or sodium salt. It is used in some dental adhesives for its ability to bind to positively charged groups such as the calcium ions that constitute tooth mineral, as well as to the polymer. Being a tertiary amine, it is also able to function as a co-initiator[25]. In the present research, NTG-GMA was compared to DMAEMA, DMPT and EDAB in order to determine whether its significantly higher M_r (329.2) helps to improve cytocompatibility.

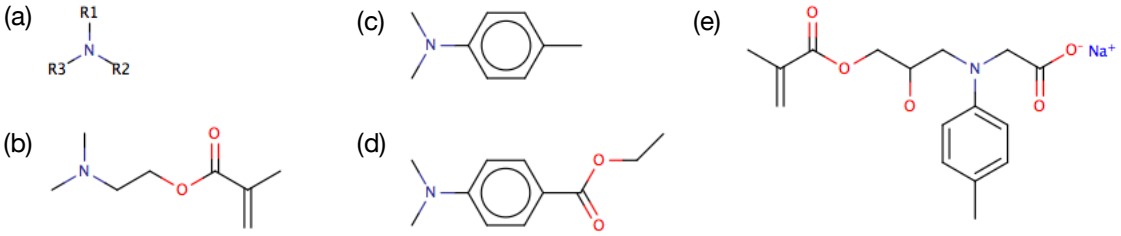

Figure 2.9. Chemical structure of co-initiators.

(a) General chemical structure of a tertiary amine. Chemical structures of co-initiators (b) 2-(*N,N*-dimethylamino)ethyl methacrylate (DMAEMA), (c) *N,N*-dimethyl-*p*-toluidine (DMPT), (d) ethyl 4-(dimethylamino) benzoate (EDAB) and (e) *N*(*p*-tolyl)glycine-glycidyl methacrylate sodium salt (Na-NTG-GMA).

Table 2.5. Physical properties of co-initiators.

Co-initiator	M_r	ρ (g/cm^3)	RI
DMAEMA	157	0.93	1.44
DMPT	135	0.94	1.54
EDAB	193	1.06	1.53
Na-NTG-GMA	329	*	*

* Unknown

2.3.1.5 Inhibitors

Inhibitors are incorporated into composites in order to prolong shelf-life, by preventing monomers from partially polymerising during storage. Monomer components tend to be supplied with low concentrations of inhibitor (typically ~30–250 ppm) but incorporation of additional inhibitor within the liquid phase helps to further prolong longevity of the material. Butylated hydroxytoluene (BHT, Figure 2.10 & Table 2.4) was used in the present work. BHT is analogous to vitamin E and prevents autoxidation by donating a hydrogen atom to convert peroxy radicals to hydroperoxides[53]. Monomethyl ether hydroquinone (MeHQ) is another commonly used inhibitor which was incorporated in some of the monomers by the suppliers (Table 3.1).

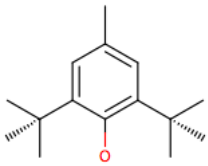

Figure 2.10. Chemical structure of inhibitor butylated hydroxytoluene (BHT).

Table 2.6. Physical properties of inhibitor.

Inhibitor	M_r	ρ (g/cm^3)	RI
BHT	220	1.04	1.49

2.3.2 Filler phase

Dental composites may be classified in terms of their handling, a property which is affected by the powder to liquid ratio (PLR) and the composition of the filler phase. Flowable composites, for example, contain compounds such as HEMA in their liquid phase, which reduce viscosity without requiring a large reduction in filler content. This enables them to be dispensed from fine bore syringes and to flow into poorly accessible cavities. The downside of flowable composites is their relatively high polymerisation shrinkage of ~2–6 vol%, compared to ~2–4 vol% for universal composites, which are suitable for both anterior and posterior applications[54]. Packable composites are highly viscous pastes which often contain a more complex distribution of filler particle sizes in order to achieve more efficient filler loading. These materials are significantly stronger and can be easily sculpted by the clinician in order to create an aesthetic restoration.

Radiopaque glass particles are used as the primary (bulk) filler component in dental composites. The primary roles of glass fillers are their aesthetics and strength. The radiopacity helps to identify the composites in X-ray radiographs. In the more

innovative composites being developed in the present research, additional reactive components are incorporated into the filler phase in order to achieve mineral formation and antimicrobial protection. These are discussed in detail in Chapter 7.

2.3.2.1.1 Bulk filler

Silane-treated glass particles are the most common filler in composites, typically constituting the entire filler phase. It is only in more advanced remineralising, antimicrobial or reinforced composites that fillers with special functionality are usually added. Silane acts as a coupling agent in order to improve the bond between filler and polymer. Si binds covalently to the polymer, whilst O binds to the inorganic filler, as illustrated in Figure 2.11b[55].

Dental composites have in many previous studies been classified in terms of their filler size. The first generation of dental 'macrofill' composites contained particles in the broad range of 10–50 μm. These had high strength but were difficult to polish and suffered from wear, which negatively affected aesthetics. Following this, 'microfill' composites were developed. This name is somewhat misleading, since the amorphous fumed silica particles used (~40 nm on average) were on what is now regarded as the nanoscale. Due to its significantly larger specific surface area (50 ± 15 m^2/g) of fumed silica compared to micro- and macroscopic glass particles, a low PLR was achieved. In order to overcome this, some materials incorporated highly filled, prepolymerised resin filler particles in combination with fumed silica particles. The small filler size of microfill composites improved the polishing and wear but the low filler content weakened them[54].

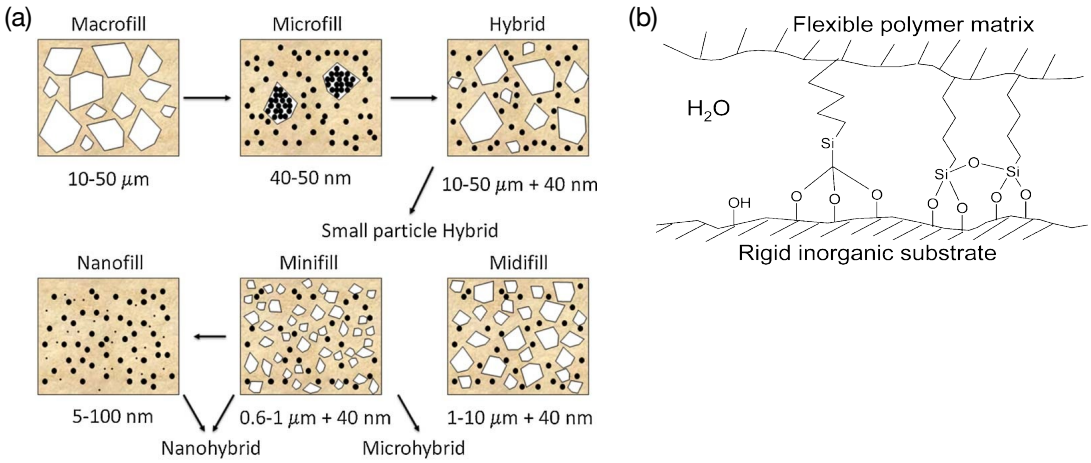

Figure 2.11. Glass filler types and silane coupling.

(a) Chronological development of dental composite filler phases and (b) schematic representation of silane coupling between polymer and filler particles. Reproduced with permission from Refs. [54,55], © Elsevier Ltd.

Several categories of small particle hybrids were subsequently developed in order to create an optimal compromise between mechanical and aesthetic properties. 'Midifills' contained glass with an average particle size of just over 1 μm, in combination with a portion of fumed silica. Refinements in particle milling techniques later enabled development of 'minifills', with 0.4–1 μm particles combined with fumed silica. These later became known as 'microhybrids', most of which are universal composites with high strength, low wear and good polishing characteristic that can subsequently be used for both posterior and anterior restorations. More recently, the concept of microfills has been revisited, with 'nanofill' composites containing primarily 5-100 nm particles and 'nanohybrids' containing prepolymerised nanofillers. Nanohybrids are often indistinguishable from microhybrids in terms of composition[30,54,56-58], although microhybrids tend to achieve slightly higher strength and modulus. The terminology and chronological development of dental composite filler phases is illustrated in Figure 2.11a[54].

The incorporation of fumed silica particles into the filler phase allows for significantly more efficient loading, since the nanofillers occupy the space between the larger particles. Nanofillers form a much smoother surface when polished than larger particles and wear better. This is because large pores do not form when a particle is removed from the surface by wear. Smaller particles may result in increased light transmittance due to lower scattering of light[59] and therefore improve conversion and depth of cure[30,56].

Fumed silica has been used in a wide range of applications for many years, including in dental composites and as a light abrasive agent in toothpastes. When a hydrophilic fumed silica such as OX-50 is incorporated into a nonpolar solvent such as a dental composite liquid phase, it exhibits thixotropic and rheopectic (shear-thinning and thickening) behaviour. The hydrophobic monomers are unable to adsorb on to the hydrophilic surface of the silica and as a result, the particles form aggregates. The aggregates then form agglomerates, which form in order to minimise the amount of free surface energy. The network of agglomerated particles that forms throughout the paste exhibits viscoelasticity (time-dependent creep) which is overcome upon application of shear forces, such as those caused by shrinkage stress. The non-bound silica agglomerates break apart and lead to an apparent reduction in viscosity, an effect that is reversed upon reduction of shear stress. This allows for thorough mixing of the paste at high PLR during manufacture and facile sculpting of the composite by the clinician. The fumed silica network also inhibits sedimentation of particles (including

other, larger fillers) and maintains homogeneity of the paste, which is important for preventing phase separation and improving shelf-life.

In the present work, silane-treated boroaluminosilicate glass particles (Table 3.3) with d50 (median particle size) of 0.7, 5 or 7 μm were utilised. In the present thesis, these are termed $GP_{0.7}$, GP_5 and GP_7, respectively. High purity fumed silicon dioxide particles (Table 3.3) with a mean particle size of ~40 nm was also incorporated into some experimental formulations at 10 wt% of the filler phase, in order to increase filler loading and improve handling properties. This is termed OX-50, based on its commercial name.

2.3.2.1.2 Reinforcing glass fibres

Various fibrous materials including glasses and polymers have been incorporated into dental composites as reinforcing agents. Such materials are known as fibre-reinforced composites (FRC). Long glass fibres are also used as prosthodontic bridges to fix an artificial tooth to adjacent teeth.

For example, high aspect ratio HA nanofibres with an average diameter of 0.1 μm and length of 60–80 μm have been shown to increase flexural strength (FS) of composites by ~22% when incorporated at 10 wt%[60]. Similarly, electrospun polycaprolactam (nylon 6) fibres with a diameter of 0.1–0.6 μm, for example, have been shown to increase composite FS by 36% and work of fracture (WOF, a similar concept to fracture toughness) by ~42% when incorporated at 5 wt%[58].

More complex FRCs have also been investigated[61]. These materials contain fibres with a polyacrylonitrile (PAN) core surrounded by a poly(methyl methacrylate) (PMMA) shell, formed by electrospinning. The outer shell of these nanofibres partially dissolves in the composite liquid phase, allowing semi-impregnation of the PMMA by the matrix at the interface (Figure 2.12). When incorporated at 7.5 wt%, 0.2–0.5 μm diameter nanofibres increased FS and WOF by ~19% and 65%, respectively. When fibres were aligned and elongated using a post-drawing technique, composites containing as little as 1.2 wt% fibres had ~52% and 152% higher FS and WOF, respectively. Nonetheless, the major drawback of electrospun polymers is their nonwoven fabric form, which must be applied *in situ* and be impregnated with the matrix. This restricts their use in dental restorations, a process that is performed under strict time constraints. Despite their impressive improvements to FS and WOF, such materials may be more appropriate for prosthodontic applications.

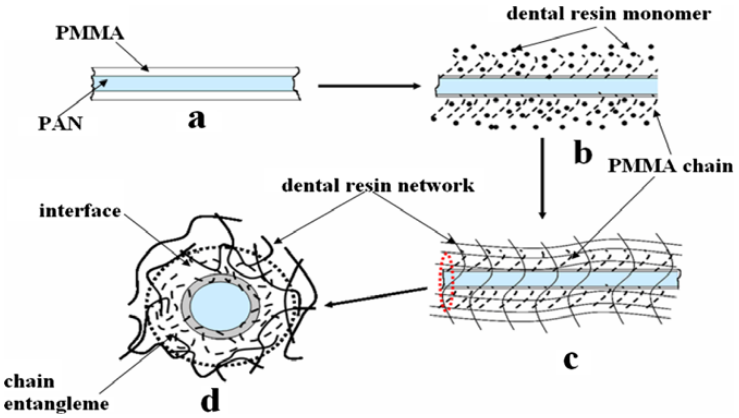

Figure 2.12. PAN core PMMA shell nanofibres.

Schematic of (a) general structure, (b) interaction between PMMA shell and dental resin, (c) semi-interpenetrating polymer network and (d) chain entanglement at the PMMA-resin interface. Reproduced with permission from Ref. [61], © Elsevier Ltd.

An off-the-shelf FRC called everX Posterior is also commercially available (StickTech, Finland, distributed via GC, Japan). This composite contains E-glass (alumino-borosilicate containing < 1 wt% alkali oxides) fibres, similar to those used in other StickTech products such as bridge reinforcements but up to 3 mm in length, compared to several cm for bridges. Experimental work performed by the laboratory that developed everX Posterior has demonstrated that E-glass fibres improve FS and fracture toughness and reduce creep and shrinkage[62-64].

2.3.2.1.3 Remineralising agents

Over the past century, various different calcium phosphate (CaP) phases have been incorporated into a diverse range of dental and orthopaedic restorative materials[65]. The use of CaPs in bone cements[65,66] and adhesives[67] is advantageous due to their ability to dissolve, diffuse and then precipitate in highly saturated physiological solutions such as simulated body fluid (SBF)[68]. They can then undergo phase transition to form more stable mineral phases such as HA[69] and, under certain conditions, promote osteogenesis or dentinogenesis[70,71].

CaPs have also been extensively investigated in dental restoratives[72], including monocalcium phosphate (MCP, $Ca(H_2PO_4)_2$)[19], di calcium phosphate (DCP, $CaHPO_4$)[73], tricalcium phosphate (TCP, $Ca_3(PO_4)_2$)[19], tetra calcium phosphate (TTCP, $Ca_4(PO_4)_2O$)[57], hydroxyapatite (HA, $Ca_{10}(PO_4)_6(OH)_2$)[74] and amorphous calcium phosphate (ACP)[75-77].

The chemical structures of MCP, DCP, TCP and HA are illustrated in Figure 2.13 and their physical properties are listed in Table 2.7. The d50 of the MCPM and β-TCP used in this thesis are also given. In the present research, MCP and TCP were incorporated

into composites with the aim of inducing HA formation in order to remineralise gaps formed upon shrinkage which are susceptible to microleakage. In Chapter 4, a pilot study concerning the effects of CaPs on the physical properties of composites was carried out. The remineralising system was subsequently developed further in Chapter 7.

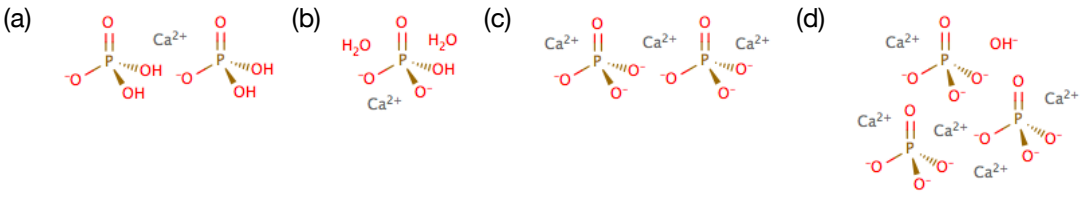

Figure 2.13. Chemical structures of various CaP phases.

a) Monocalcium phosphate (MCP), (b) dicalcium phosphate (DCP), (c) tricalcium phosphate (TCP) and (d) hydroxyapatite (HA). MCP, shown in anhydrous form (MCPA), can also occur in monohydrate form (MCPM). DCP, shown in dihydrate form (DCPD), can also occur in anhydrous form (DCPA).

Table 2.7. Physical properties of CaP phases.

Component	Mr	ρ (g/cm^3)	RI
MCPM	234	2.22	1.52
DCPA	136	2.93	1.61
DCPD	172	2.33	1.54
β-TCP	310	3.06*	1.63
HA	502	3.16	1.65

* True value of whitelockite due to Fe & Mg content (theoretical value of β-TCP is 3.14)

2.3.2.1.4 Antimicrobial agents

Antimicrobial agents that have been investigated in remineralising dental composites and adhesives may be categorised into two main groups. Mobile antimicrobials are free to be released and include chlorhexidine diacetate (CHXA Figure 2.14a, Table 2.8)[18,19,68,78] and silver nanoparticles[79-84]. In contrast, cationic quaternary ammonium monomers are antimicrobial monomers that become immobilised within the polymer upon curing and protect against microbes *in situ*[82,84-89].

ε-poly-L-lysine (εPL, Figure 2.14b, Table 2.8) is a basic, cationic homopolypeptide consisting of multiple L-lysine residues (~25–30 units in the present research). It is water-soluble, stable and biodegradable. The positively charged amine groups of εPL act by permeabilising the cell wall of a wide range of pathogens, including Gram-positive and -negative bacteria, yeasts and moulds[90-93]. Furthermore, εPL is has low toxicity and is poorly absorbed by mammalian cells, even at high doses (e.g. 5 g/kg in

rats). This enables its use as a broad-spectrum preservative in food, cosmetics and toothpaste (the US Food and Drug Administration authorises its use up to 50 mg/kg in food)[93].

The use of εPL in remineralising, antimicrobial composites is investigated in Chapter 7.

(a)

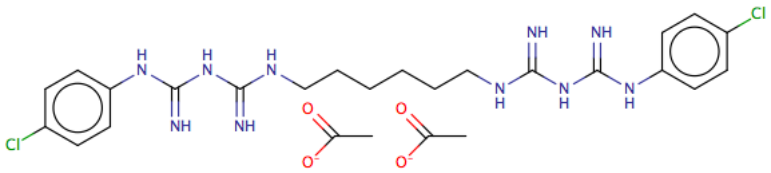

(b)

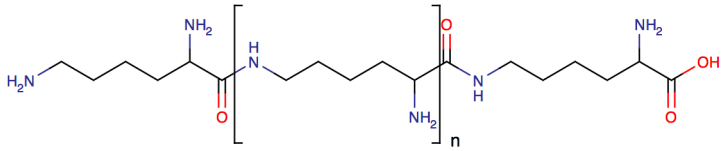

Figure 2.14. Chemical structure of antimicrobial agents.

(a) Chlorhexidine diacetate (CHXA) and (b) ε-poly-L-lysine (εPL) (n ≈ 23–33).

Table 2.8. Physical properties of antimicrobial agents.

Component	**M_r**
CHXA	625.55
εPL	Variable

3 MATERIALS & METHODS

3.1 Materials

The sources of the components used are detailed in Table 3.1. Full names and locations of suppliers are listed in Table 3.2.

Table 3.1. Composite component sources.

Component	Supplier	Product [item code]
Liquid Phase		
Monomer		
Bis-GMA	Polysciences	2,2-Bis[4-(2-hydroxy-3-methacryloxypropoxy)phenyl]propane [03344]
PPGDMA	Polysciences	Poly(propylene glycol) (400) dimethacrylate, 100 ppm MeHQ, 100 ppm BHT [04380]
TEGDMA	DMG	Triethylene glycol dimethacrylate, 200 ppm MeHQ [100102]
UDMA	DMG	Urethane dimethacrylate, 200 ppm MeHQ [100112]
UDMA	Esstech	Urethane dimethacrylate, 100–200 ppm MeHQ [X850 0000]
Photoinitiator		
CQ	DMG	Camphorquinone [100134]
PPD	Sigma-Aldrich	1-Phenyl-1,2-propanedione, 99% [223034]
Co-initiator		
DMAEMA	Sigma-Aldrich	2-(Dimethylamino)ethyl methacrylate, 98%, 700–1,000 ppm MeHQ [234907]
DMPT	Sigma-Aldrich	4,N,N-Trimethylaniline, 99% [D189006]
EDAB	Sigma-Aldrich	Ethyl 4-aminobenzoate [112909]
Mg-NTG-GMA	Esstech	NTG-GMA magnesium salt [X-863-0070]
Na-NTG-GMA	Esstech	NTG-GMA sodium salt [X-863-0050]
Inhibitor		
BHT	Sigma-Aldrich	Butylated hydroxytoluene [W218405]
Filler Phase		
Non-reactive filler		
$G_{0.7}$	DMG	Silane-treated aluminoborosilicate glass particles, d50 = 0.7 μm [021110]
G_5	Sci-Pharm	Silane-treated aluminoborosilicate glass particles, d50 = 5 μm [IF-2019]
G_7	DMG	Silane-treated aluminoborosilicate glass particles, d50 = 7 μm [020684]
OX-50	Evonik	Aerosil® OX-50 hydrophilic fumed silica [OX-50]
GF	MO-SCI	Silane coated, heat treated, aluminoborosilicate glass fibres [GL-0271]
Calcium phosphate		
MCPM	Himed	Monocalcium phosphate monohydrate, d50 = 53 μm [MCP-B26]
DCPA	Sigma-Aldrich	Calcium phosphate dibasic [C7263]
DCPD	Fluka	Calcium phosphate dibasic dihydrate [21184]
β-TCP	Plasma Biotal	β-tricalcium phosphate, d50 = 16.9 μm [P292 S]
Antimicrobial agent		
CHXA	Sigma-Aldrich	Chlorhexidine diacetate salt hydrate [C6143]
εPL	Handary	Epolyly™ P Ultrapure ε-polylysine [0201]

Table 3.2. Composite component supplier locations.

Supplier	Location
DMG Chemisch-Pharmazeutische Fabrik GmbH	Hamburg, Germany
Esscehm Europe Ltd.	Seaham, UK
Evonik Industries AG	Essen, Germany
Fluka Analytical (now Sigma-Aldrich Company Ltd.)	Gillingham, UK
Handary S.A.	Brussels, Belgium
Himed	Old Bethpage, NY, USA
MO-SCI Speciality Products, L.L.C.	Rolla, MO, USA
Plasma Biotal Ltd.	Tideswell, UK
Polysciences Inc.	Eppelheim, Germany
Sci-Pharm (Scientific Pharmaceuticals, Inc.)	Pomona, CA, USA
Sigma-Aldrich Company Ltd.	Gillingham, UK

Table 3.3. Physical properties of glass filler components.

Filler	ρ (g/cm^3)	RI	Dimensions/distribution

Bulk filler			Particle distribution (μm)				
			d10	d25	d50	d75	d90
$GP_{0.7}$	2.8	1.53	1.22	0.84	0.54	0.37	0.29
GP_7			26.5	16.3	7.2	2.4	1.2
GP_5							

Fumed silica			Particle distribution (nm)			Agglomerate distribution (nm)				
			d10	d50	d90	d10	d25	d50	d75	d90
OX-50	2.2	1.46	~20	~40	~70	11.3	20.9	80.3	156	177

Glass fibre			Fibre dimensions (μm)	
			Diameter	Length
GF	2.6	1.55	~15	~300

3.1.1 Composite preparation

3.1.1.1 Liquid phase preparation

Liquid phases were prepared in amber (blue light proof) glass bottles. Inhibitor, co-initiator and photoinitiator were first mixed with diluent monomer using a magnetic stirrer (Stuart UC151 or US151, Bibby Scientific, Stone, UK) until fully dissolved. Bulk monomer was then added and the liquid phase was stirred until homogeneous. The composition of the liquid phase varied depending on study, as outlined in each chapter. Liquid phases were stored at 4 °C and typically used to form composite pastes within 3 months. Autopolymerisation was not observed over extended periods > 1 year. Future studies could test for autopolymerisation by testing the conversion of composite pastes that have been stored for varying time-points by Fourier transform infrared spectroscopy (FTIR, see Chapter 3.2.2.1) or after accelerating the ageing process by using high temperatures.

3.1.1.2 Composite paste preparation

Except where otherwise stated, dental composite pastes were prepared using a centrifugal planetary mixer (SpeedMixer, Hauschild Engineering, Hamm, Germany), in order to minimise air incorporation and to ensure complete wetting of filler particles. The liquid phase was first weighed in a circular mixing vessel with rounded corners and the filler phase was then placed on top. The composition of the filler phase and the powder to liquid ratio (PLR) varied depending on study, as outlined in each chapter. Batches of ~8–10 g composite were typically prepared. An optimised mixing programme was used (2,500 rpm for 10 s, followed by 1,000 rpm for 2 min). Composite pastes were stored in amber glass bottles at 4 °C and typically tested within 1 month. Composites containing a mixture of particle sizes, particularly those containing fumed silica, did not phase separate over extended periods of up to 1 year. The composites tested in Chapter 4 were mixed by hand using a stainless steel spatula and rubber mixing pad, since this work was carried out before the acquisition of the SpeedMixer.

3.1.1.3 Disc specimen production

Except where otherwise stated, disc-shaped specimens were moulded by applying composite pastes to metal circlips (internal diameter 10.2 mm, thickness 1 mm) and pressing them between two sheets of acetate. This prevents oxygen inhibition during polymerisation and expels excess paste, ensuring similar specimen thickness. Specimens were photo-polymerised using a blue light emitting diode curing unit with a wavelength of 450–470 nm and power output with periodic level shifting of 1,100–1,330 mW/cm^2 (Demi Plus, Kerr Dental, Orange, CA, USA), in direct contact with the acetate. The curing duration for each testing method varied and is detailed in each corresponding section.

3.1.2 Storage media preparation

Deionised water (dH_2O, MicroPure, Barnstead, Thermo Scientific, Hemel Hempstead, UK), SBF and artificial saliva (AS) were used as storage media for some techniques, namely mechanical testing and analysis of water sorption and calcium phosphate precipitation.

3.1.2.1 Simulated body fluid

SBF was prepared according to BS ISO 23317:2012[94], using the formulation developed by Kokubo & Takadama (2006)[95]. Briefly, the components in Table 3.4 were gradually added to 700 mL dH_2O in the order displayed in a plastic beaker. Each component was

fully dissolved before the next was added and a temperature of 36.5 ± 1.5 °C was maintained. Before tris(hydroxymethyl) aminomethane (TRIS) was added, the volume was topped up to 900 mL using dH_2O. Temperature was then maintained at a more accurate 36.5 ± 0.5 °C and TRIS was added gradually. pH was not allowed to exceed 7.45. HCl and TRIS were then added alternately, maintaining pH in the range of 7.42–7.45. Once all of the TRIS had been dissolved, HCl was used to adjust the pH to exactly 7.40 at 36.50 °C. The solution was transferred to a 1 L volumetric flask and cooled to 20 °C, before the volume was finally adjusted. SBF was stored at 4 °C and used within 1 month. No spontaneous precipitation was observed during the storage period.

Table 3.4. Composition of SBF.

Component	Mass (g)
Sodium chloride	8.035
Potassium chloride	0.355
Dipotassium hydrogen phosphate trihydrate	0.225
Magnesium chloride hexahydrate	0.231
Hydrochloric acid solution, 1 M	39.00
Calcium chloride dihydrate	0.292
Sodium sulfate	0.072
TRIS	6.118

3.1.2.2 Artificial saliva

AS was prepared according to the formulation used by McKnight-Hanes & Whitford (1992)[96], with the exception of sorbitol, which was omitted because the viscosity of AS containing both sorbitol and cellulose is higher than typical saliva[97]. AS is unable to simulate the action of pellicle, due to the complexity of pellicle's composition and patient to patient variability and from batch to batch, it does not suffer from the high variability seen between patients. Briefly, the components in Table 3.5 were added to dH_2O in the order displayed. Each component was fully dissolved before the next was added. The pH was then adjusted to 6.75 using HCl or KOH. AS was stored at 4 °C and used within 1 month.

Table 3.5. Composition of AS.

Component	Concentration (wt%)
Methyl-*p*-hydroxybenzoate	0.2
Sodium carboxymethyl cellulose	1
Potassium chloride	0.0625
Magnesium chloride hexahydrate	0.0059
Calcium chloride dihydrate	0.0166
Dipotassium phosphate	0.0804
Monopotassium phosphate	0.0326

3.2 Methods

3.2.1 Handling properties & wet-point determination

The wet-point of various liquid and filler phase combinations was determined by gradually adding a small quantity of liquid phase to a known mass of filler phase and mixing, until the filler was sufficiently wetted and a cohesive paste had been formed. The quantity of liquid phase added was recorded and notes were made regarding the handling properties of each formulation. The wet-point (vol%) was then calculated from the total mass of liquid and the density of each component.

3.2.2 Polymerisation properties

3.2.2.1 Degree of conversion

The conversion of composites was determined using Fourier transform infrared spectroscopy (FTIR, System 2000, PerkinElmer, Seer Green, UK). Composite paste was applied to either a single or four stacked circlips of the aforementioned dimensions. These were placed on the diamond of an attenuated total reflectance accessory (Golden Gate ATR, Specac, Slough, UK) and covered with a sheet of acetate. After an initial spectrum of the uncured composite had been obtained, spectra were recorded continuously for 1,000 s (n = 3). The specimens were photo-polymerised from the top for the first 20 s. Spectra were recorded at a wavelength range of 800–1800 cm^{-1} and resolution of 8 cm^{-1}. Absorbance profiles were obtained at 1319 ± 1 cm^{-1} (C–O stretch bond) and 1334 ± 2 cm^{-1} (baseline) and used to calculate conversion at 1 mm and 4 mm depths using Equation 1,

$$C = \left[1 - \left(\frac{A_f}{A_0}\right)\right] \times 100 \qquad \text{Equation 1}$$

where: C is conversion and A_f and A_0 are final and initial absorbance above baseline, respectively[19].

Example FTIR spectra are shown inFigure 3.1.

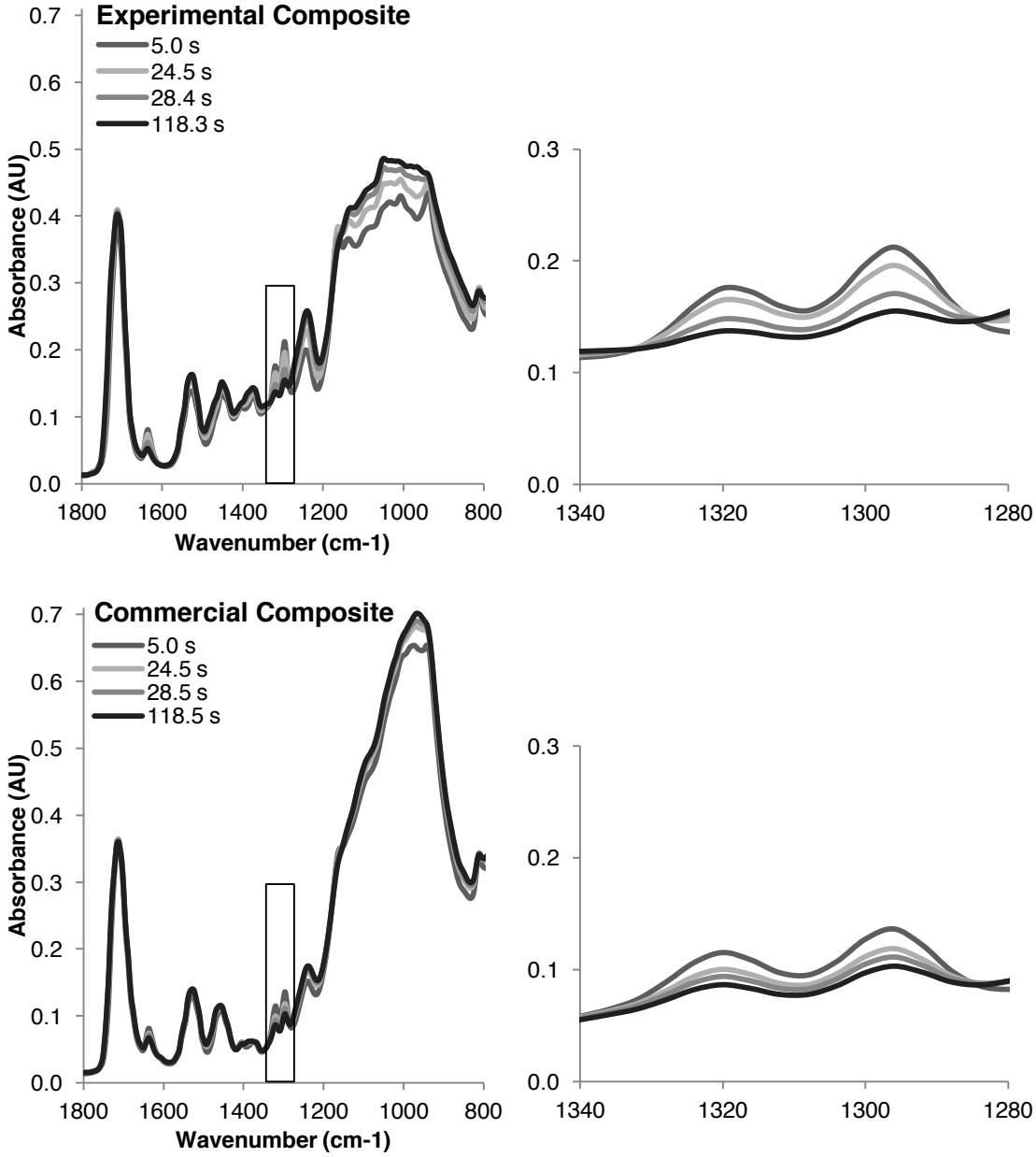

Figure 3.1. Example FTIR spectra.

Spectra of experimental and commercial composites at various time-points, showing C–O stretch bond peak at 1319 cm^{-1} and its baseline at 1334 cm^{-1} in more detail. The broad peak at ~1000 cm^{-1} represents the glass filler particles, the peaks of which vary greatly between manufacturers. Photoinitiation began at 0 s and progressed for 20 s. The spectra of subsequent time-points indicate that polymerisation continues beyond the curing period.

3.2.2.2 Polymerisation shrinkage

Volumetric shrinkage was measured by two methods, in order to compare the reliability and convenience of the techniques.

3.2.2.2.1 Shrinkage based on conversion

Shrinkage was calculated from conversion data using Equation 2[98], which is based on the finding that methacrylate esters typically undergo volumetric shrinkage of ~22.5 cm^3/mol upon polymerisation[99,100],

$$S = \left(mC\rho \sum_i \left(\frac{n_i x_i}{W_i} \right) \right) \times 2250 \qquad \text{Equation 2}$$

where: S, *m*, C, *ρ*, Σ, *i*, *n*, *x* and *W* are shrinkage (vol%), monomer mass fraction within composite, conversion, composite density, sum of all monomers in liquid phase, each monomer in liquid phase, number of C=C bonds per molecule, mass fraction of monomer in liquid phase and molecular mass, respectively.

3.2.2.2.2 Shrinkage based on volume change

* This technique was performed by Dr. Wendy Xia (UCL Eastman Dental Institute) as her contribution to Ref. [101] *

Shrinkage was obtained by measuring the density of polymerised and unpolymerised specimens according to BS EN ISO 17304:2013[101,102]. This technique uses an analytical balance equipped with a density determination apparatus (AG 204 & MS-DNY-43, Mettler Toledo, Beaumont Leys, UK) and is based on Archimedes' principle. Disc specimens were cured for 40 s from each side to ensure complete conversion. Specimen edges were polished to remove loose chips. The mass of three cured and three uncured specimens of each formulation were measured in air and under dH_2O. Each value for mass under water was averaged from 10 readings. The shrinkage of composites and their SD were calculated using the equations provided in the standard.

3.2.2.3 Depth of cure

The depth of cure of composites (n = 3) was measured according to BS EN ISO 4049:2009[101,103]. Briefly, composite paste was applied to a brass split-mould (internal diameter 4 mm, height 6 mm) and photo-polymerised for 20 seconds from the top. The specimen was removed from the mould and a plastic spatula was used to remove any uncured material from the bottom. The depth of cured material was measured using digital callipers to an accuracy of ± 0.01 mm and the reading was halved, as required by the standard, in order to give a value for depth of cure.

3.2.3 Quantification of mass and volume change

Gravimetric analysis and Archimedes' principal were used to quantity mass and volume change of composites in dH_2O, SBF or AS at 37 °C (n = 3). Their mass in air and under dH_2O was measured after 0, 2, 4 and 6 h and 1, 2, 4 and 7 days using an analytical balance equipped with a density determination apparatus (AG 204 & MS-DNY-43, Mettler Toledo, Beaumont Leys, UK). In some studies, measurements continued to 14 days and 1, 2 and 3 months. After each time-point, specimens were re-immersed in the same storage medium. Mass and volume change were plotted against time. The mass of dehydrated specimens was then determined in air and under dH_2O, before being dehydrated again in preparation for SEM and EDX. The density of each specimen was calculated using Equation 3, in order to determine its volume using Equation 4,

$$\rho_c = \left(\frac{m_x}{m_x - w_x}\right)(\rho_0 - \rho_L) + \rho_L \qquad \text{Equation 3}$$

$$V = \frac{m_x}{\rho_c} \qquad \text{Equation 4}$$

where: ρ_c, ρ_0 and ρ_L are the density of the composite specimen, dH_2O or air (g/cm^3), respectively; m_x and m_i are the mass of the specimen in air at each specific time-point 'x' and at the initial time-point, respectively; and V is the volume of the specimen (cm^3).

In Chapter 5, water sorption was simply determined by measuring the mass change of disc specimens cured for 40 s on each side after immersion in dH_2O for 1 week.

3.2.4 Scanning electron microscopy and energy dispersive X-ray spectroscopy

Scanning electron microscopy (SEM, Philips XL30 Field Emission SEM, Amsterdam, Netherlands) was used to visualise mineral formation on the surface of composites. Specimens were coated with 95% gold and 5% palladium (Polaron E5000 Sputter Coater, Quoram Technologies, Laughton, UK) prior to imaging. Energy dispersive X-ray spectroscopy (EDX, INCA Energy 400, Oxford Instruments, Abingdon UK) was used to quantify the ratio of calcium to phosphate in CaP precipitates on the surface of some composites, in order to estimate which CaP phase was present. Elemental proportions were averaged from maps obtained by EDX (n = 3), each containing 25 spectra, attained at 10 μm intervals.

3.2.5 Raman spectroscopy

* This technique was performed by Dr. Graham Palmer (UCL Eastman Dental Institute), a technician with experience in analysing Raman spectroscopy data, as his contribution to Ref. [104] *

The composition of the surface of specimens (n = 3) was analysed by Raman spectroscopy, in order to confirm its chemical composition. A Raman spectrometer (LabRAM 300, Horiba UK Ltd., Northampton, UK) equipped with a 633 nm laser was used with grating set at 1800, a 50x objective and wavenumber range of 700 to 1650 cm^{-1}. Each specimen was mapped in three areas measuring 50 x 50 μm, with spectra obtained in 10 μm steps, providing 25 spectra per area, as previously described[66]. Run time and number were selected to ensure sufficient peak intensity above background and noise. Peak assignments were achieved by comparison with spectra of dental glass, liquid phase, εPL, MCPM, DCPA, DCPD, β-TCP and HA using LabRAM software (Horiba UK Ltd.).

3.2.6 Mechanical and bonding properties

3.2.6.1 Biaxial flexural test

A biaxial flexural test was used to determine the biaxial flexural strength (BFS) and Young's modulus of elasticity (E) of composites. In pilot studies, the modulus of toughness (U_T) was assessed. Composite disc specimens (n = 5–10, depending on study) were cured for 40 s on each side. The majority of specimens were tested dry, 24 h after curing. Others were stored dry for 24 h, before placement in 10 mL dH_2O, AS or SBF at 37 °C for one week or one month. They were then tested (Autograph AGS-X, Shimadzu, Milton Keynes, UK), with a 2 kN load cell and ball-on-ring jig at a cross-head speed of 1 mm/min, until specimen failure. Specimens in Chapter 4 were tested using the same parameters and jig but with a 1 kN load cell and a different test frame (4505 Series Universal Test Frame, Instron, High Wycombe, UK), as they were tested before the acquisition of the Autograph AGS-X. U_T (MPa) was equal to the area under the stress strain curve. BFS (MPa) and E (GPa) were calculated using Equation 5[105] and Equation 6, respectively,

$$\text{BFS} = \frac{P}{t^2}\left[(1+\upsilon)\left(0.485\, ln\left(\frac{a}{t}\right)+0.52\right)+0.48\right] \quad \text{Equation 5}$$

$$E = \left(\frac{\Delta P}{\Delta w_c}\right)\times\left(\frac{\beta_c a^2}{t^3}\right) \quad \text{Equation 6}$$

where: BFS, P, t, υ and a are biaxial flexural strength, failure load (N), specimen thickness (mm), Poisson's ratio (0.3) and jig support radius (4 mm); E, ($\Delta P/\Delta W_c$) and

β_c are modulus, gradient of elastic region and centre deflection function (0.5024)[106], respectively.

3.2.6.2 Shear bond test

* This technique was performed by Dr. Saad Liaqat (UCL Eastman Dental Institute) as his contribution to Ref. [104] *

Shear bond strength (τ) was assessed according to BS ISO 29022:2013[107]. Human dentine was collected from consenting, non-carious, adult human patients and stored at UCL Eastman Biobank (ID № 1304) according to ethical approval and the Human Tissue Act 2004. Uncut teeth were stored in a 0.2% thymol solution at 4 °C for up to 4 weeks prior to use. Dentine was isolated from directly beneath the occlusal part of the enamel, as previously described[108,109]. Briefly, cut sections of human dentine were embedded in epoxy resin (SpeciFix 40, Struers, Rotherham, UK) with dentinal tubules aligned perpendicular to the resin surface. Care was taken to ensure that only superficial rather than deep dentine was exposed. After the resin had set, a cylindrical brass mould (6 mm depth, 3 mm internal diameter) was placed on the surface of the dentine. The end of the tube in contact with dentine was chamfered at 45°, in order to reduce its contact area. The dentine was etched using 37% phosphoric acid for 20 s, before being rinsed with dH_2O and gently dried. Composite pastes were then applied in 2 mm increments, with each layer being cured for 40 s before addition of the next. No bonding agent was utilised. τ was determined using a mechanical test frame (4505 Series Universal Test Frame, Instron) equipped with a flat-edge shear fixture and 1 kN load cell (n = 3). The jig consisted of a metal holder with an adjustable screw for securing the specimen and an adjustable blade, which sheared the composite specimen from the dentine at a cross-head speed of 1 mm/min. τ was then calculated using Equation 7[108],

$$\tau = \frac{F}{A} \qquad \text{Equation 7}$$

where: τ, F and A are shear bond strength, force and area, respectively.

3.2.7 Cytocompatibility

3.2.7.1 Cell culture

Primary human gingival fibroblasts (HGF) were obtained from a commercial source (ScienCell Research Laboratories, Carlsbad, CA, USA). HGF were cultured under standard conditions (37 °C, 95% air, 5% CO_2, 95 % relative humidity) in Dulbecco's modified Eagle medium (DMEM, Gibco, Life Technologies, Paisley, UK) supplemented with 10 % foetal bovine serum (FBS, Gibco) and 1 % penicillin/streptomycin (PAA Laboratories, GE Healthcare, Chalfont St. Giles, UK). Passage numbers 4–8 were used for cytocompatibility studies.

3.2.7.2 Preparation of test solutions

Test solutions were prepared in serum-free DMEM. As is typical in biomaterials testing and as recommended in ISO 10993[110,111], serum-free medium was used in order to prevent adsorption of serum proteins to material components and alteration to release kinetics. Controls consisted of serum-free DMEM. Serum was not added to extracts after extraction and prior to cell culture.

3.2.7.2.1 Liquid phase components

Five ten-fold serial dilutions of each liquid phase component used in Chapter 5 were prepared in serum-free DMEM, ranging from 0.01–100 mM for DMAEMA, UDMA, PPGDMA and TEGDMA, and 0.001–10 mM for CQ and Bis-GMA, due to their lower solubility. The solutions were stored for ~30 mins at 60 °C and then stirred using a sterile spatula, in order to aid dissolution of components with low solubility, particularly the bulk monomers.

3.2.7.2.2 Composite extracts

In order to prepare specimens for extract testing, a 1 mm thick circlip atop a sheet of acetate was filled with composite and covered with acetate. A further three circlips were stacked on top and filled with composite and covered with acetate. The resultant 4 mm deep stack was then photo-polymerised for 20 seconds from the top. The bottom 1 mm thick section was removed from the mould and incubated in 650 μL serum-free DMEM at 37 °C. This provided an extraction ratio of 1 mL / 3 cm^2 surface area, as required by ISO 10993-12:2009[111]. Specimens (n = 3) were agitated at 100 rpm during extraction (orbital shaker, Stuart Scientific, Stone, UK). After 24 h, specimens were transferred to fresh medium and incubated for a further 6 days, yielding extracts from 1- and 7-day time-points.

3.2.7.3 Cytocompatibility assays

HGF were seeded at a density of 30,000 cells/cm^2 in 96 well plates (n = 3 per specimen, time-point and assay). After an initial 24 h seeding period, cell culture medium was replaced with 100 μL of the specimen (component solution, composite extract or control). The solutions were thoroughly mixed using a vortex mixer (Stuart SA8, Bibby Scientific, Stone, UK) in order to ensure even dispersion of dissolved components. Cytocompatibility was assessed after a further 24 h of culture (48 h time-point), in accordance with ISO 10993-5:2012[110]. The specimen was then replaced with serum-free DMEM and cultured for a further 24 h recovery period (72 h time-point). This period was included in order to enable cells to recover after exposure to toxic components, indicating the severity of exposure on cell survival.

Three water-soluble cell metabolic activity assays were used to assess cytocompatibility: resazurin (alamarBlue Cell Proliferation Assay, AdB Serotech, Bio-Rad Laboratories Inc., Hemel Hempstead, UK); water-soluble tetrazolium salt-8 (WST-8, Cell Counting Kit-8, Sigma-Aldrich); and 3-(4,5-dimethylthiazol-2-yl)-5-(3-carboxy-methoxyphenyl)-2-(4-sulfophenyl)-2H-tetrazolium salt (MTS, CellTiter 96 AQ_{ueous} One Solution Cell Proliferation Assay, Promega, Southampton, UK). Medium was aspirated from the cells and replaced with 100 μL fresh cell culture medium containing the corresponding substrate (Table 3.6). After incubation at 37 ˚C, fluorescence (FLx800 Plate Reader, BioTek, Potton, UK) or absorbance (Infinite M200 Plate Reader, Tecan, Männedorf, Switzerland) was measured. Standard curves were obtained by seeding a range of cell concentrations in 96 well plates in serum-containing medium, 2 h prior to each assay, in which time the cells were observed via light microscopy to have attached and spread.

Table 3.6. Cytocompatibility assay parameters.

Substrate	Incubation time (min)	Measurement
Resazurin, 10%	90	*Fluorescence* – excitation: 560 nm, emission: 590 nm
WST-8, 10%	80	*Absorbance* – 460 nm (reference: 650 nm)
MTS, 20%	60	*Absorbance* – 490 nm (reference: 630 nm)

3.2.8 Multifactorial analysis

In order to establish whether any interaction effects occurred between components, pilot studies (Chapter 4.3) were analysed using multifactorial analysis according to Equation 8,

$$P = < P > \pm a_1 \pm a_2 \pm a_3 \pm a_{1,2} \pm a_{1,3} \pm a_{2,3} \pm a_{1,2,3}$$
$$where\ 2a_i = < P >_H - < P >_L \qquad \text{Equation 8}$$

where P = property, $<P>$ = mean property, a = variable, $_H$ = high variable, and $_L$ = low variable.

3.2.9 Statistical analyses

Parametric one-way analysis of variance (ANOVA) and post-hoc Tukey's tests were used (OriginPro software, OriginLab Corporation, Northampton, MA, USA) to determine significance ($p \leq 0.05$) between composite formulations within a single study in Chapter 5–7. Non-parametric two-way ANOVA and post-hoc Tukey's tests were also used in order to determine the significance of the effects of multiple factors, e.g. UDMA vs. Bis-GMA and PPGDMA vs. TEGDMA. Anderson-Darling test was used to determine normality. In all cases, except where otherwise indicated, the data had a Gaussian (normal) distribution. For all techniques, the standard deviation (SD) of each formulation was displayed on graphs, except in the case of polymerisation shrinkage, where the SD was averaged for each study, due to the high variability of the volume change method. Statistical significance is presented on graphs (* $p < 0.05$, ** $p < 0.01$, *** $p < 0.005$ or **** $p < 0.001$).

4 PILOT STUDIES: OPTIMISATION OF COMPOSITIONS

4.1 Introduction to Chapter 4

Chapter 4 concerns the results obtained from various pilot studies which were carried out in order to determine the feasibility of the project and in order to optimise certain aspects of the formulations studied in later chapters. This chapter deals with a wide range of considerations regarding composite formulations and these topics are investigated further in subsequent chapters. The list below summarises the factors that were analysed:

- Wet-point
  - Effect of glass filler particle size
- Mechanical properties
  - Feasibility of using UDMA as bulk monomer
  - Effect of diluent monomer (PPGDMA or TEGDMA)
  - Effect of co-initiator (DMPT, EDAB, Mg-NTG-GMA or Na-NTG-GMA)
  - Effect of PLR (3:1, 3.5:1 or 4:1)
  - Effect of GF (0, 5 or 20 wt% in filler phase)
  - Effect of glass filler particle size
  - Effect of CaPs (MCP and/or β-TCP at 0, 2.5, 10 or 20 wt% each in filler phase, alone or together at 1:1 wt ratio)
  - Effect of εPL (0, 0.5 or 5 wt% in liquid phase)
- Water sorption
  - Effect of CaPs (MCP and/or β-TCP at 0 or 20 wt% each in filler phase, alone or together at 1:1 wt ratio)
  - Effect of εPL (0 or 5 wt% in liquid phase)

4.2 Formulations

Composites in Chapter 4 were hand-mixed and mechanical tests were performed using the 4505 Series Universal Test Frame, since these pilot studies were performed before the acquisition of the SpeedMixer and Autograph AGS-X.

All Chapter 4 materials were left for 24 h to set or post-cure before mechanical testing.

In Chapter 4.3.1, the mechanical properties of commercial composites G-ænial (GC Corporation), Gradia Direct Posterior (GC Corporation), Filtek Z250 (3M ESPE) and

Filtek Z500 (3M ESPE) were first assessed. GIC Fuji IX GP (GC Corporation) and RMGIC Fuji II LC (GC Corporation) were also compared. The GIC was prepared according to the manufacturers' guidelines. The RMGIC was mixed according to guidelines but cured for 40 s for closer comparison to the composites.

The composition of the liquid phase of pilot study experimental formations was varied according to study, but the general formulation consisted of 1 wt% CQ, 1 wt% co-initiator, 5 wt% HEMA, 23.25 wt% diluent monomer and 69.75 wt% UDMA. The ratio of bulk to diluent monomer was 3:1 by weight. PLR and filler phase composition was varied according to study.

Table 4.1. Chapter 4 general composite formulations.

Component type/parameter	Component	Quantity within phase
Liquid phase		
Bulk to diluent monomer ratio		3:1 w/w
Bulk monomer	UDMA	69.75 wt%
Diluent monomer	PPGDMA or TEGDMA	23.25 wt%
Bifunctional monomer	HEMA	5 wt%
Photoinitiator	CQ	1 wt%
Co-initiator	DMPT, EDAB, Mg-NTG-GMA or Na-NTG-GMA	1 wt%
Filler phase		
Glass particles	$GP_{0.7}$, GP_5 or GP_7	Up to 100 wt%
Glass fibres	GF	0, 5 or 20 wt%
CaP	MCPM	0, 2.5, 10 or 20 wt%
	β-TCP	0, 2.5, 10 or 20 wt%
Antimicrobial	εPL	0, 0.5 or 5 wt%
PLR		3:1, 3.5:1 or 4:1 w/w

In Chapter 4.3.2, the mechanical properties of composites containing co-initiators DMPT, EDAB, Mg-NTG-GMA and Na-NTG-GMA at 1 wt% of the liquid phase were compared. The diluent monomer was TEGDMA. The filler phase was 100 wt% GP_5.

Table 4.2. Chapter 4.3.2 composite formulations.

Component type/parameter	Component	Quantity within phase
Liquid phase variable parameters		
Co-initiator	DMPT, EDAB, Mg-NTG-GMA or Na-NTG-GMA	1 wt%
Liquid phase constant parameters		
Bulk monomer	UDMA	69.75 wt%
Diluent monomer	TEGDMA	23.25 wt%
Bifunctional monomer	HEMA	5 wt%
Photoinitiator	CQ	1 wt%
Co-initiator	DMPT	1 wt%
Filler phase constant parameters		
Glass particles	GP_5	100 wt%
PLR		3.5:1 w/w

In Chapter 4.3.3, the effect of PLR and fibre content on mechanical properties was assessed. The mechanical properties of composites containing a PLR of 3:1, 3.5:1 or 4:1 and with GP_5 and GF at 100 and 0% or 80 and 20% of the filler phase, respectively, were compared. The diluent monomer and co-initiator were TEGDMA and DMPT, respectively.

Table 4.3. Chapter 4.3.3 composite formulations.

Component type/parameter	Component	Quantity within phase
Filler phase variable parameters		
Glass particles	GP_5	80 or 100 wt%
Glass fibres	GF	0 or 20 wt%
PLR		3:1, 3.5:1 or 4:1 w/w
Liquid phase constant parameters		
Bulk to diluent monomer ratio		3:1 by weight
Bulk monomer	UDMA	69.75 wt%
Diluent monomer	TEGDMA	23.25 wt%
Bifunctional monomer	HEMA	5 wt%
Photoinitiator	CQ	1 wt%
Co-initiator	DMPT	1 wt%

In Chapter 4.3.4, the effect of glass particle size on wet-point and mechanical properties was assessed. Composites containing 100 wt% of either $G_{0.7}$, G_5 or G_7 were compared. Composites containing $G_{0.7}$ and G_7 at 1:2, 1:1 or 2:1 weight ratios were also compared. For the mechanical test, a PLR of 4:1 was used, except in the case of the composite containing 100 wt% $G_{0.7}$ in its filler phase, which was tested at a PLR of 2.5:1 due to its poor wettability. The diluent monomer and co-initiator were PPGDMA and Na-NTG-GMA, respectively.

Table 4.4. Chapter 4.3.4 composite formulations.

Component type/parameter	Component	Quantity within phase
Filler phase variable parameters		
Glass particles	$GP_{0.7}$	100 wt%
	GP_5	100 wt%
	GP_7	100 wt%
	$GP_{0.7}$:GP_7	1:2 w/w
	$GP_{0.7}$:GP_7	1:1 w/w
	$GP_{0.7}$:GP_7	2:1 w/w
PLR		Variable
Liquid phase constant parameters		
Bulk to diluent monomer ratio		3:1 w/w
Bulk monomer	UDMA	69.75 wt%
Diluent monomer	PPGDMA	23.25 wt%
Bifunctional monomer	HEMA	5 wt%
Photoinitiator	CQ	1 wt%
Co-initiator	Na-NTG-GMA	1 wt%

In Chapter 4.3.5, the interaction effects of glass fibres (5 or 20 wt% of filler phase), CaPs (MCPM and β-TCP combined at a 1:1 wt ratio, total 0, 20 or 40 wt%) and εPL

(0.5 or 5 wt%) and the effect of diluent monomer (PPGDMA or TEGDMA) were assessed in terms of the mechanical properties of composites. GP_7 constituted the remainder of the filler phase. The PLR was 4:1. The co-initiator was Na-NTG-GMA.

Table 4.5. Chapter 4.3.5 composite formulations.

Component type/parameter	Component	Quantity within phase
Liquid phase variable parameters		
Diluent monomer	PPGDMA or TEGDMA	23.25 wt%
Filler phase variable parameters		
Glass fibres	GF	5 or 20 wt%
CaP	MCPM:β-TCP at 1:1 w/w	0, 5, 20 or 40 wt% total
Antimicrobial	εPL	0.5 or 5 wt%
Glass particles	GP_7	Remainder of filler phase
Liquid phase constant parameters		
Bulk to diluent monomer ratio		3:1 by weight
Bulk monomer	UDMA	69.75 wt%
Bifunctional monomer	HEMA	5 wt%
Photoinitiator	CQ	1 wt%
Co-initiator	Na-NTG-GMA	1 wt%
Filler phase constant parameter		
PLR		4:1 by weight

Finally, in Chapter 4.3.6, the effects of individual or combined CaPs (0 or 20 wt% MCPM and 0 or 20 wt% β-TCP) and εPL (0 or 5 wt%) on water sorption over three months and on mechanical properties after one week, two weeks and three months were analysed. GP_7 constituted the remainder of the filler phase. The PLR was 4:1. The diluent monomer and co-initiator were PPGDMA and Na-NTG-GMA, respectively.

Table 4.6. Chapter 4.3.6 composite formulations.

Component type/parameter	Component	Quantity within phase
Filler phase variable parameters		
CaP	MCPM	0 or 20 wt%
	β-TCP	0 or 20 wt%
Antimicrobial	εPL	0 or 5 wt%
Glass particles	GP_7	Remainder of filler phase
Liquid phase constant parameters		
Bulk to diluent monomer ratio		3:1 by weight
Bulk monomer	UDMA	69.75 wt%
Diluent monomer	PPGDMA	23.25 wt%
Bifunctional monomer	HEMA	5 wt%
Photoinitiator	CQ	1 wt%
Co-initiator	Na-NTG-GMA	1 wt%
Filler phase constant parameter		
PLR		4:1 by weight

4.3 Results

4.3.1 Comparison of commercial composites

The mechanical properties of commercial composites are shown in Figure 4.1. The GIC Fuji IX GP and RMGIC Fuji II LC both had very low BFS of 29 and 58 MPa, respectively. Gradia had a BFS of 97 MPa. Its successor G-ænial was slightly weaker at 86 MPa. Filtek Z250 and its successor Z500 had similar strength of ~178 MPa. The two Filtek products also had similar *E* (~4.5 GPa), higher than the remaining products which had similar *E* of ~2.5 GPa. U_T increased from ~1–12 MPa in the same order as BFS increased: Fuji IX GP < Fuji II LC < G-ænial < Gradia < Z250 < Z500.

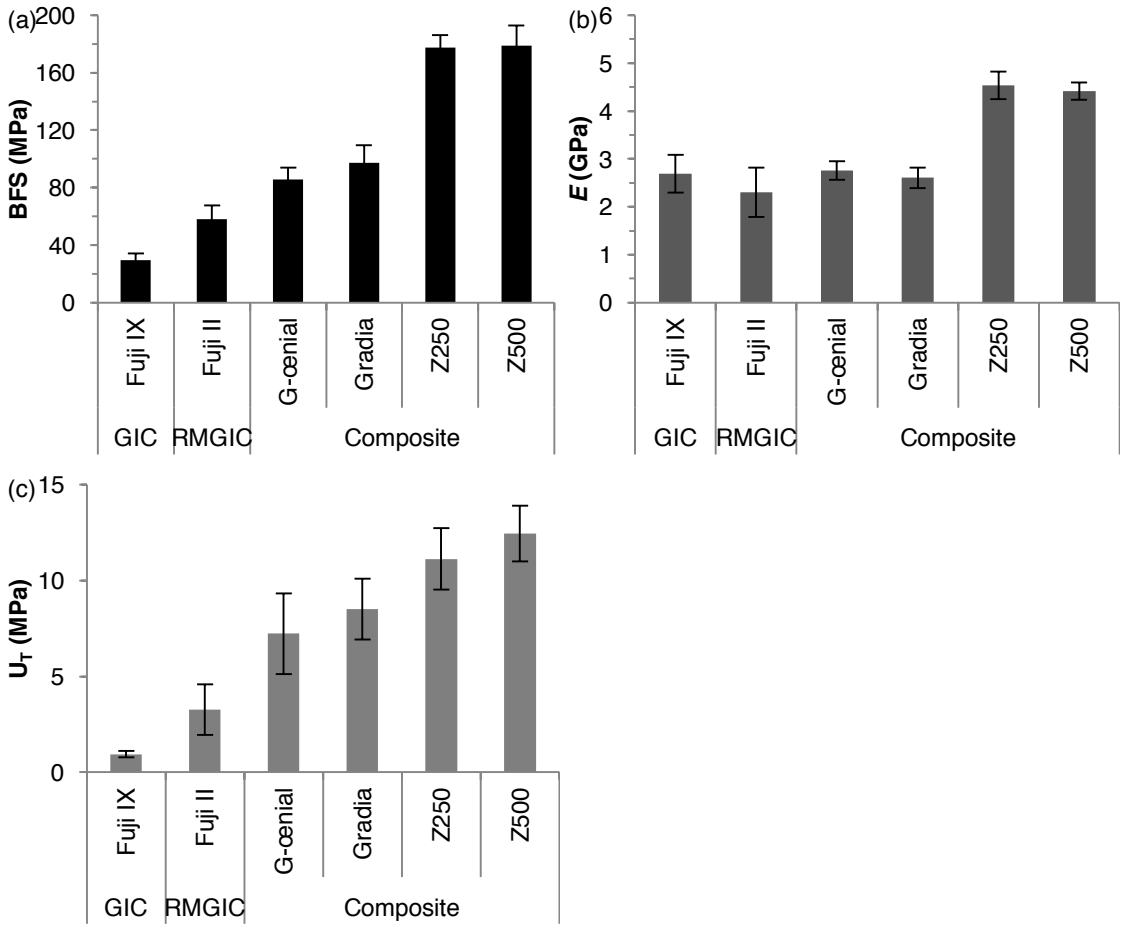

Figure 4.1. Mechanical properties of commercial GIC, RMGIC and composites.

(a) BFS, (b) *E* and (c) UT of dry specimens. Error bars represent 95% confidence interval (n = 4–7).

4.3.2 Effect of co-initiator on mechanical properties

The mechanical properties of composites containing various co-initiators are shown in Figure 4.2. Altering the co-initiator appeared not to have any significant effect on BFS (153–166 MPa) or *E* (4.1–4.5 GPa). Composite containing Na-NTG-GMA had approximately double the U_T (25.3 MPa) value of the remaining composites (13.6–16.3 MPa).

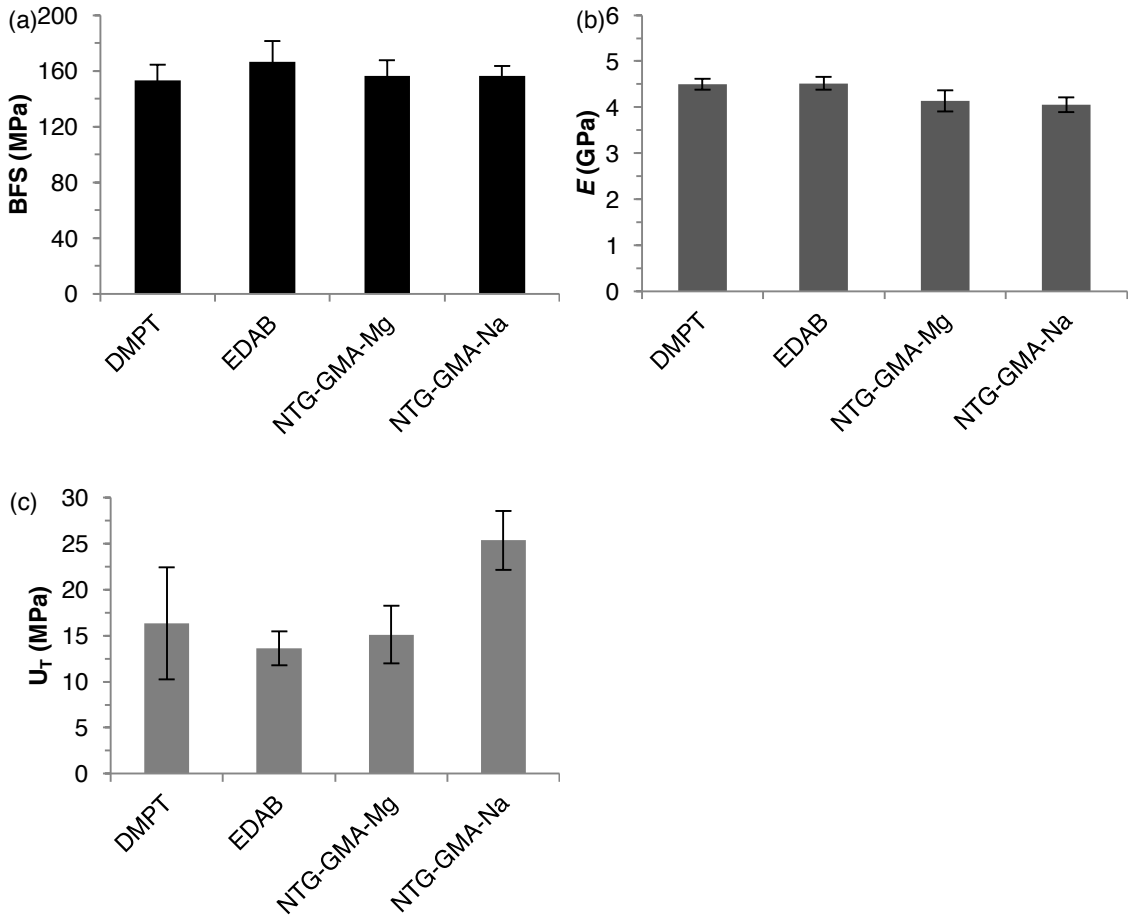

Figure 4.2. Mechanical properties of composites containing various co-initiators.
(a) BFS, (b) *E* and (c) U_T of dry composite specimens containing 1 wt% DMPT, EDAB, Mg-NTG-GMA or Na-NTG-GMA in the liquid phase. Error bars represent 95% confidence interval (n = 5–7).

4.3.3 Effects of PLR and GF content on mechanical properties

The mechanical properties of composites containing varying PLRs (3:1, 3.5:1 or 4:1) and varying GF content (0 or 20 wt%) are shown in Figure 4.3. Neither the PLR used nor the inclusion of fibres had a significant effect on BFS (153–164 MPa). *E* varied from 4.2–5.2 GPa and was slightly higher in composites containing GF. The *E* of composites with a PLR of 3:1 was slightly lower than that of composites with a higher proportion of polymer. GF appeared to improve the mean U_T of composites, though this was not statistically significant due to large variation in results.

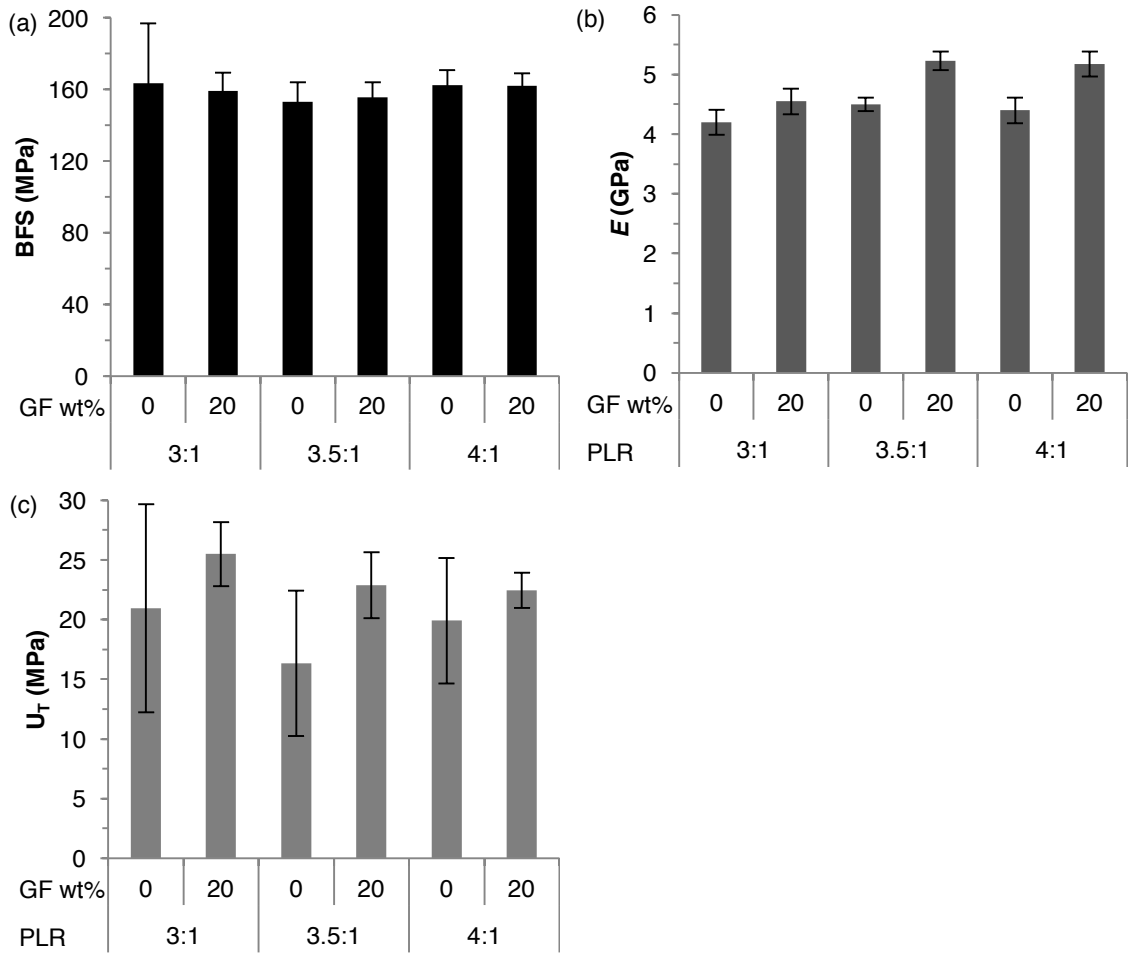

Figure 4.3. Mechanical properties of composites with varying PLR and GF content.
(a) BFS, (b) *E* and (c) U_T of dry composite specimens containing 0 or 20 wt% GF in the filler phase and PLR of 3:1, 3.5:1 or 4:1 by weight. Error bars represent 95% confidence interval (n = 4–6).

4.3.4 Comparison of glass filler particle size

4.3.4.1 Wet-point

The wet-point of composites containing various glass filler particles ($GP_{0.7}$, GP_5, GP_7 or combinations or $GP_{0.7}$ and GP_7 at 1:2, 1:1 or 2:1 wt ratios) are presented in Table 4.7. The wet-point is presented both as the wt% of filler in the composite at the wet-point and the equivalent PLR. It is worth noting that these values represent the absolute limit at which a cohesive paste could be formed but that a slightly lower wt% filler should be incorporated to enable improved wetting and handling properties.

$GP_{0.7}$ had the lowest wet-point (79 wt%), due to its large surface area to weight ratio. GP_7 had a high wet-point (84 wt%), though that of GP_5 was higher (87 wt%). As GP_5 is produced by a different manufacturer than $GP_{0.7}$ or GP_7, it likely has a slightly different formulation with either higher density or greater silane content.

The wet-points of the combinations of $GP_{0.7}$ and GP_7 at wt ratios of 2:1, 1:1 and 1:2 were 81 wt%, 82 wt% and 85 wt% respectively. GP_7 and the $GP_{0.7}$:GP_7 1:2 combination had sufficiently high wet-points for incorporation of additional, unsilanised fillers such as CaPs and εPL but had the best handling properties. Despite its high wet-point, GP_5 was not investigated further due to supply issues.

Table 4.7. Wet-point of composites containing various glass fillers.

Glass particle size (wt ratio)	Wet point	
	wt%	PLR
$GP_{0.7}$	79	3.8:1
GP_5	87	6.7:1
GP_7	84	5.2:1
$GP_{0.7}$:GP_7 (2:1)	81	4.1:1
$GP_{0.7}$:GP_7 (1:1)	82	4.6:1
$GP_{0.7}$:GP_7 (1:2)	85	5.5:1

4.3.4.2 Mechanical properties

The mechanical properties of composites containing various glass filler particles ($GP_{0.7}$, GP_5, GP_7 or combinations or $GP_{0.7}$ and GP_7 at 1:2, 1:1 or 2:1 wt ratios) are shown in Figure 4.4. The PLR was constant at 4:1, except for composites containing only $GP_{0.7}$, which had a PLR of 2.5:1 due to the low wet-point of the filler. Composites containing $GP_{0.7}$ only had marginally higher strength (172 MPa) than those containing GP_5 or GP_7 only (~154 MPa), which may have been due to more complete wetting at the lower PLR used. Composites containing a 1:1 wt ratio combination of $GP_{0.7}$ and GP_7 had the highest BFS (180 MPa), which is likely to be due to more efficient packing of the

particles during mixing. This formulation also had the highest *E* (5.5 GPa) and this did not impact negatively on its U_T (26 MPa).

Subsequent pilot studies utilised GP_7 alone, due to its high wet-point and the greater convenience of using a single glass filler.

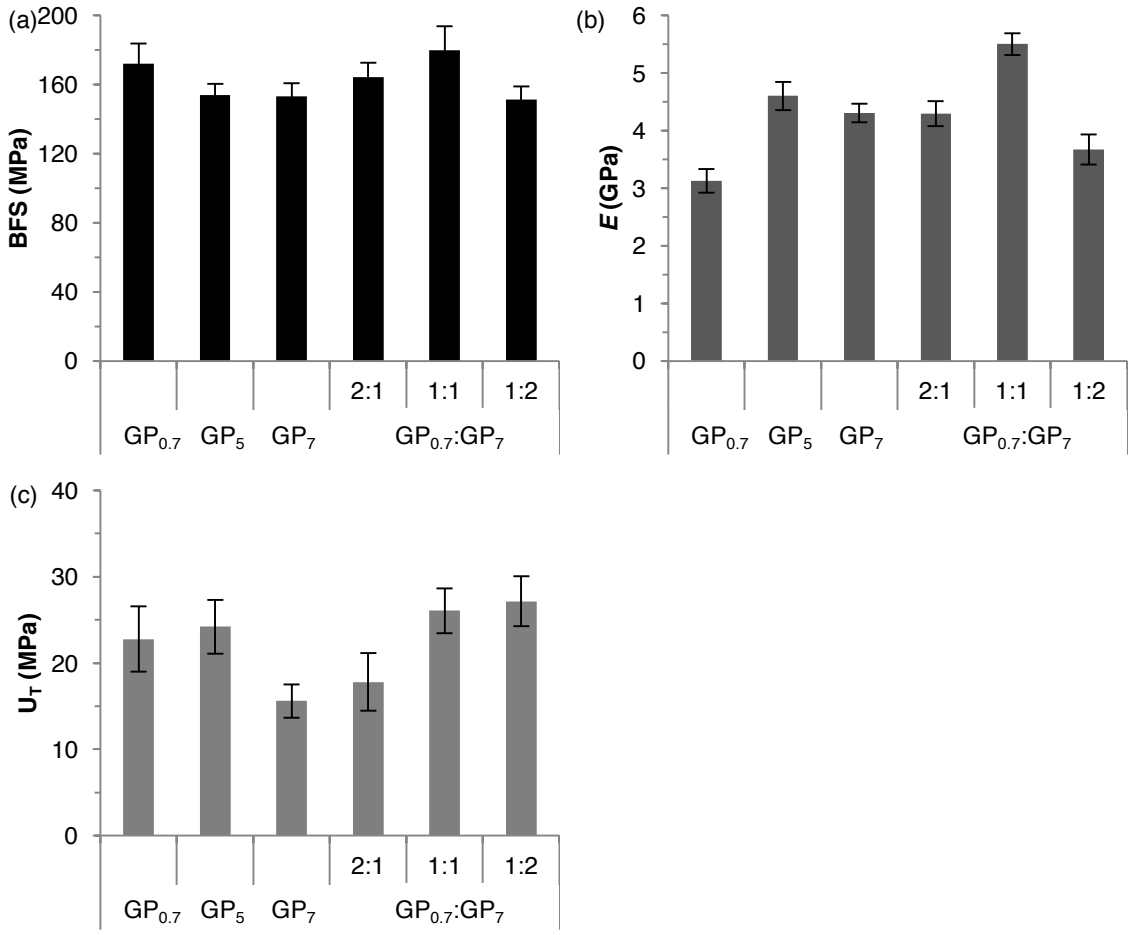

Figure 4.4. Mechanical properties of composites with varying glass filler size.
(a) BFS, (b) *E* and (c) U_T of dry composite specimens containing $GP_{0.7}$, GP_5 or GP_7, or combinations of $GP_{0.7}$ and GP_7 at 2:1, 1:1 or 1:2 wt ratios. PLR was 4:1, except for composites containing $GP_{0.7}$ only (2.5:1). Error bars represent 95% confidence interval (n = 5–7).

4.3.5 Effects of GF, CaP, εPL and diluent monomer on mechanical properties

The mechanical properties of composites containing TEGDMA with varying GF (5 or 20 wt% in filler phase), CaP (5 or 20 wt%, with MCPM and β-TCP at 1:1 wt ratio) and εPL (0.5 or 5 wt%) content are shown in Figure 4.5. Formulations containing 5 wt% εPL generally had lower BFS than those containing 0.5 wt%. CaPs at high levels (20 wt%) weakened the material unless combined with 20 wt% GF. When CaPs and GF were incorporated at 20 wt% each, BFS remained as high (133 MPa) as the formulation with

low levels of all components, suggesting an interaction effect between CaPs and GF. Formulations containing 20 wt% CaPs in general had lower *E* than those with 5 wt%. Increasing GF or CaP content resulted in notable increases in U_T. In the case of the formulation containing 0.5 wt% εPL and 20 wt% each CaPs and GF, toughness was increased by approximately two-fold compared to most other formulations.

The mechanical properties of composites containing PPGDMA with varying GF (0 or 20 wt% in filler phase), CaP (0 or 40 wt%, with MCPM and β-TCP at 1:1 wt ratio) and εPL (0 or 5 wt%) content are shown in Figure 4.6. The trends observed in the previous, similar experiment were mirrored in this experiment. The differences between formulations were the diluent monomer (PPGDMA instead of TEGDMA), the high level of CaP (40 wt% instead of 20 wt%) and the low level of all components (0 wt% in all cases). Incorporating CaPs at 40 wt% and GF at 20 wt% had a significant effect on reducing *E* to ~2–2.6 GPa and increasing U_T to 39 MPa. High BFS (126 MPa) was retained in the formulation containing low εPL and high CaPs and GF.

Parts b, d and f of these figures illustrate the effects of individual components and interaction effects between components on mechanical properties, as calculated using Equation 8. They show the $2a_i$ values, which are achieved by subtracting the average value of the low component concentration from the average value of the high component concentration. Positive values on the graphs indicate that either a single component or a combination of components which interact with one another cause in increase in the corresponding property. Similarly, a negative value indicates a reduction in value. Neutral values or those close to the x axis indicate no significant effect.

Combined analysis of these results from both studies indicates that GF increased BFS and U_T. CaPs decreased BFS and *E*, a trend which was slightly more pronounced in the latter study where CaP content was 40 instead of 20 wt%, but slightly increased U_T. CaPs and GF interacted with one another to slightly improve BFS, without having a notable effect on *E* or U_T. εPL reduced the values of all mechanical properties and did not have any clear interaction with other components. Due to the multiple factors being varied between studies, no conclusions could be made about the effect of varying the diluent monomer, though PPGDMA appeared to perform similarly to TEGDMA.

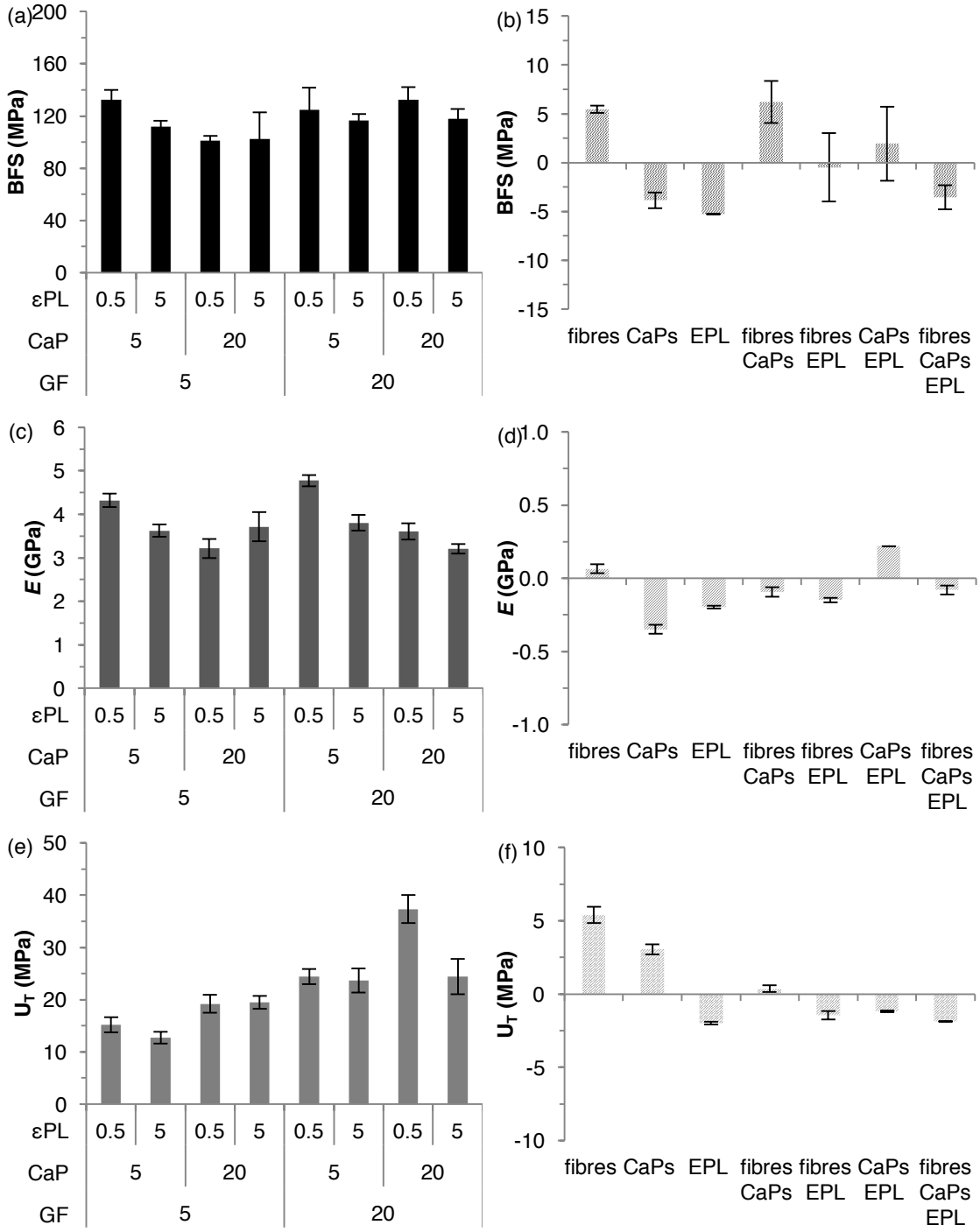

Figure 4.5. Mechanical properties of composites containing TEGDMA with varying GF, CaP and εPL content.

(a,b) BFS, (c,d) *E* and (e,f) U_T of dry composite specimens containing 5 or 20 wt% GF, 5 or 20 wt% CaPs (MCPM and β-TCP at 1:1 wt ratio) and 0.5 or 5 wt% εPL in their filler phases and diluent monomer TEGDMA. (b,d,f) Effects of individual components and interaction effects between components. Error bars represent 95% confidence interval (n = 6–7).

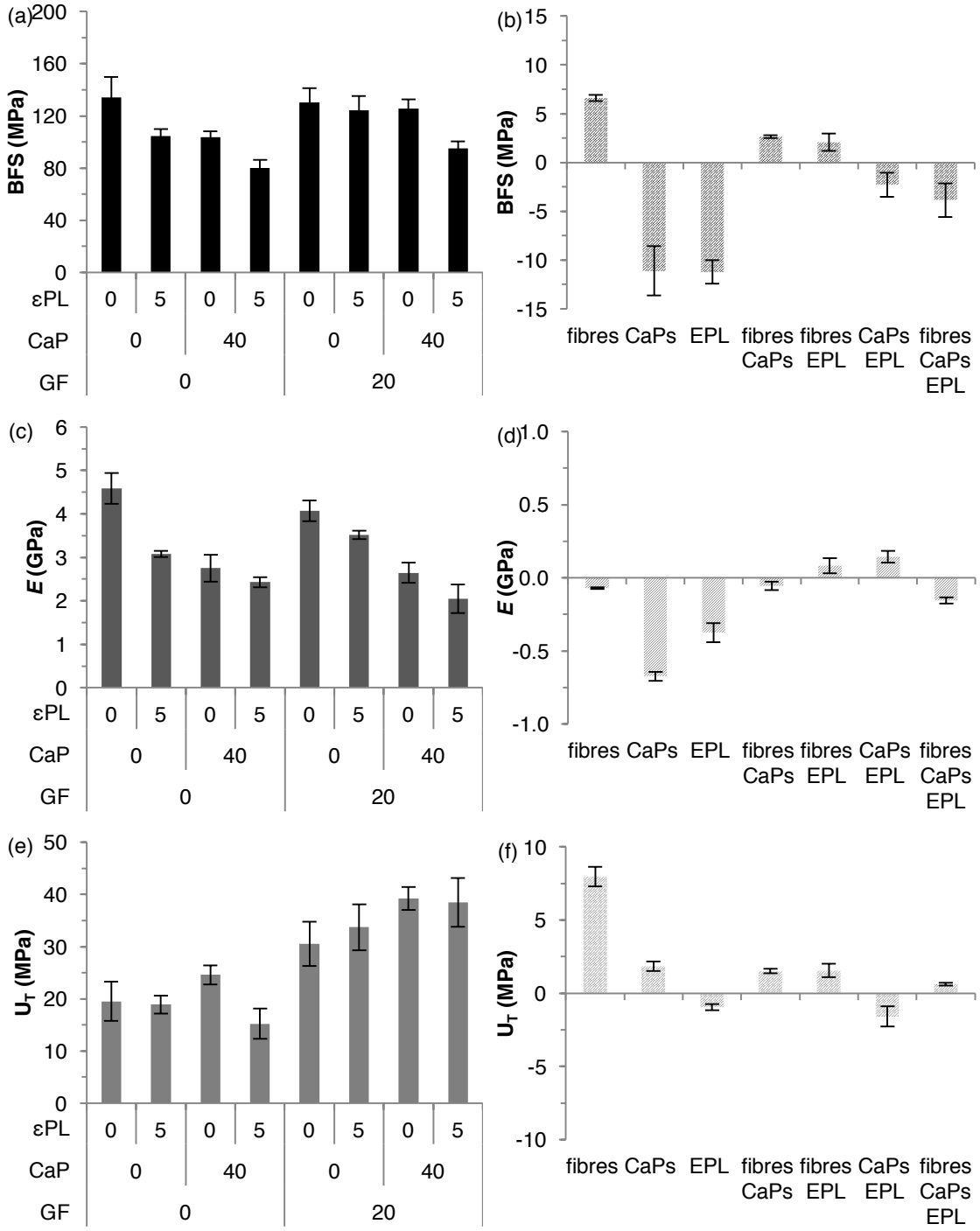

Figure 4.6. Mechanical properties of composites containing PPGDMA with varying GF, CaP and εPL content.

(a,b) BFS, (c,d) *E* and (e,f) U_T of dry composite specimens containing 0 or 20 wt% GF, 0 or 40 wt% CaPs (MCPM and β-TCP at 1:1 wt ratio) and 0 or 5 wt% εPL in their filler phases and diluent monomer PPGDMA. (b,d,f) Effects of individual components and interaction effects between components. Error bars represent 95% confidence interval (n = 5–8).

The effect of composition on U_T can also be easily visualised by comparing stress-strain curves, as shown in the examples given in Figure 4.7. Since U_T is calculated from the area under the curve, stress-strain curves give a clear indication of toughness.

For example, formulations containing GF (e–h) have a much larger area under their stress-strain curves than those lacking GF. Their point of failure is much less pronounced than those of more brittle samples such as (a). CaPs also improve toughness but weaken the materials.

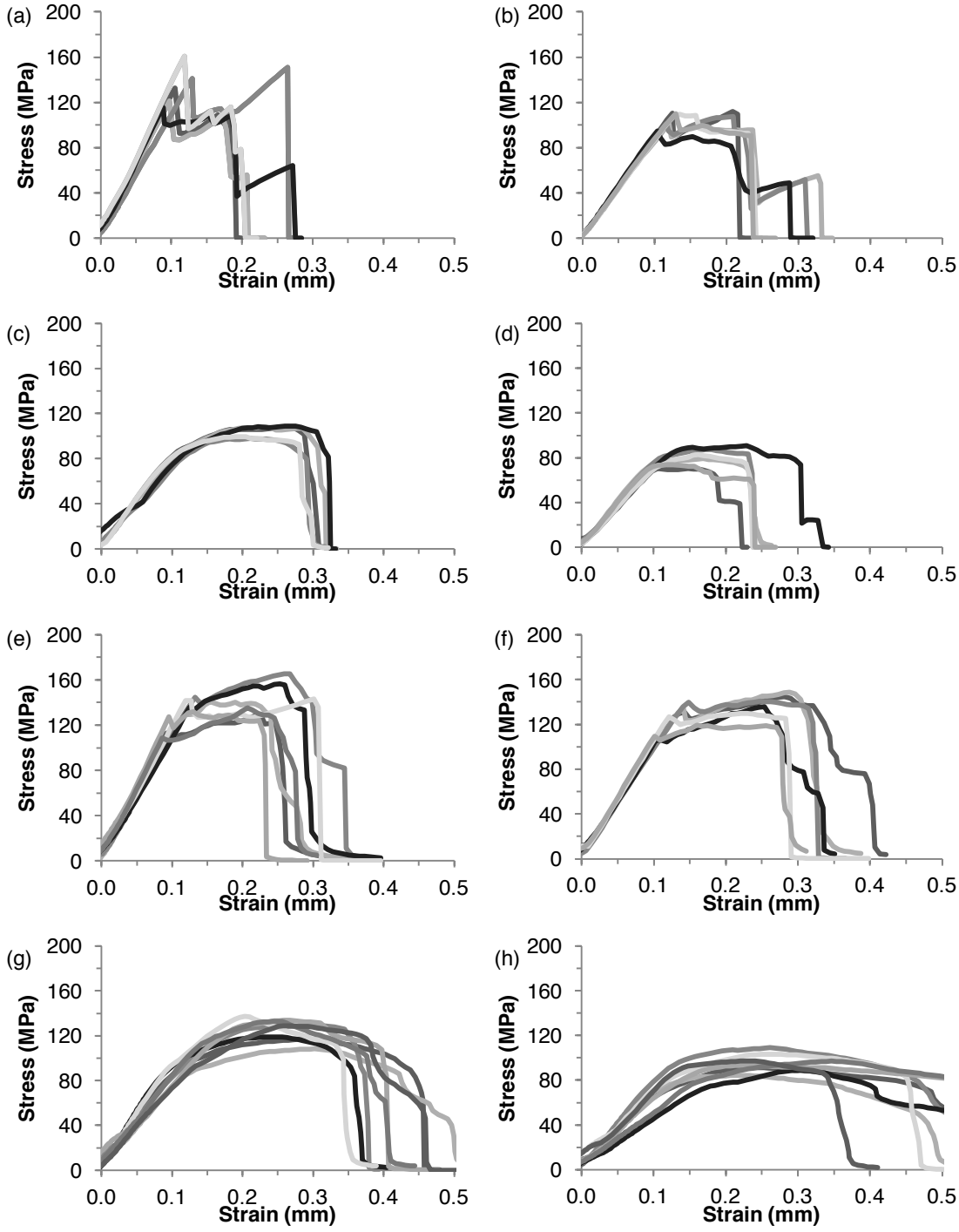

Figure 4.7. Stress-strain curves of composites containing PPGDMA with varying GF, CaP and εPL content.

PPGDMA-based composites with powder phases containing (a–d) 0 or (e–h) 20% GF, (a,b,e,f) 0 or (c,d,g,h) 40% CaPs (MCPM and β-TCP at 1:1 wt ratio) and (a,c,e,g) 0 or (b,d,f,h) 5% εPL (5–8 replicates per formulation are shown).

4.3.6 Effects of MCPM, β-TCP and εPL during storage in artificial saliva

4.3.6.1 Mass and volume change

The mass and volume change of composites containing PPGDMA with varying MCPM (0 or 20 wt% in the filler phase), β-TCP (0 or 20 wt%) and εPL (0 or 5 wt%) content over three months storage in AS are shown in Figure 4.8. This study assesses the individual and combined effects of each CaP on water sorption in AS, compared to previous studies which show the effect of total CaP content where the MCPM:β-TCP is kept constant at 1:1. Due to the large number of sample groups, the figure is split to facilitate viewing. The top two graphs show composites without εPL, whereas groups in the bottom two graphs include 5 wt% εPL.

Composites lacking CaPs and εPL increased in mass by ~0.5 wt% after one week and ~1% after one month. When εPL was incorporated at 5 wt%, mass increased by ~2 wt% after one week and almost 4 wt% after one month. Composites containing 20 wt% β-TCP and lacking MCPM and εPL increased in mass by ~1 wt% after one week and 1.2 wt% after one month. When εPL was incorporated, mass increased by ~3 wt% after one week and ~5 wt% after one month. Composites containing 20 wt% MCPM and lacking β-TCP and εPL increased in mass by 2.5 wt% after one week and 3.2% after one month. When εPL was incorporated, mass increased by ~5 wt% after one week and then plateaued. Composites containing 20 wt% of each CaP and lacking εPL increased in mass by ~7.4 wt% after one week and levelled off. When εPL was incorporated, this value was slightly lower (6.5 wt%). This was the only formulation that did not exhibit a significant increase when εPL was added.

β-TCP alone did not induce extra mass or volume increase, likely due to its low solubility, though it did when combined with εPL, likely due to the high solubility of εPL. MCPM induced significantly more change than β-TCP. This could be due to its higher solubility increasing water sorption, which was further boosted by εPL. The formulation containing both CaPs at 20 wt% each exhibited significantly higher mass and volume increase than all other composites and this was not increased further by εPL. The density of specimens did not change significantly over the course of one month and no trends were observed (0.9978 ± 0.0005 g/cm^3).

An increase in mass may be due to absorbed water expanding the polymer and/or filling pores. Since no precipitation of mineral was observed on the surface of the composite, it is less likely to be due to CaP precipitating from the AS. Mass decrease may be due to diffusion of MCPM out of the material and replacement with water, since

the density of water is less than half that of MCPM (H_2O ≈ 1 g/cm^3; MCPM ≈ 2.2 g/cm^3). β-TCP has relatively low solubility and is therefore unlikely to dissolve or induce water sorption.

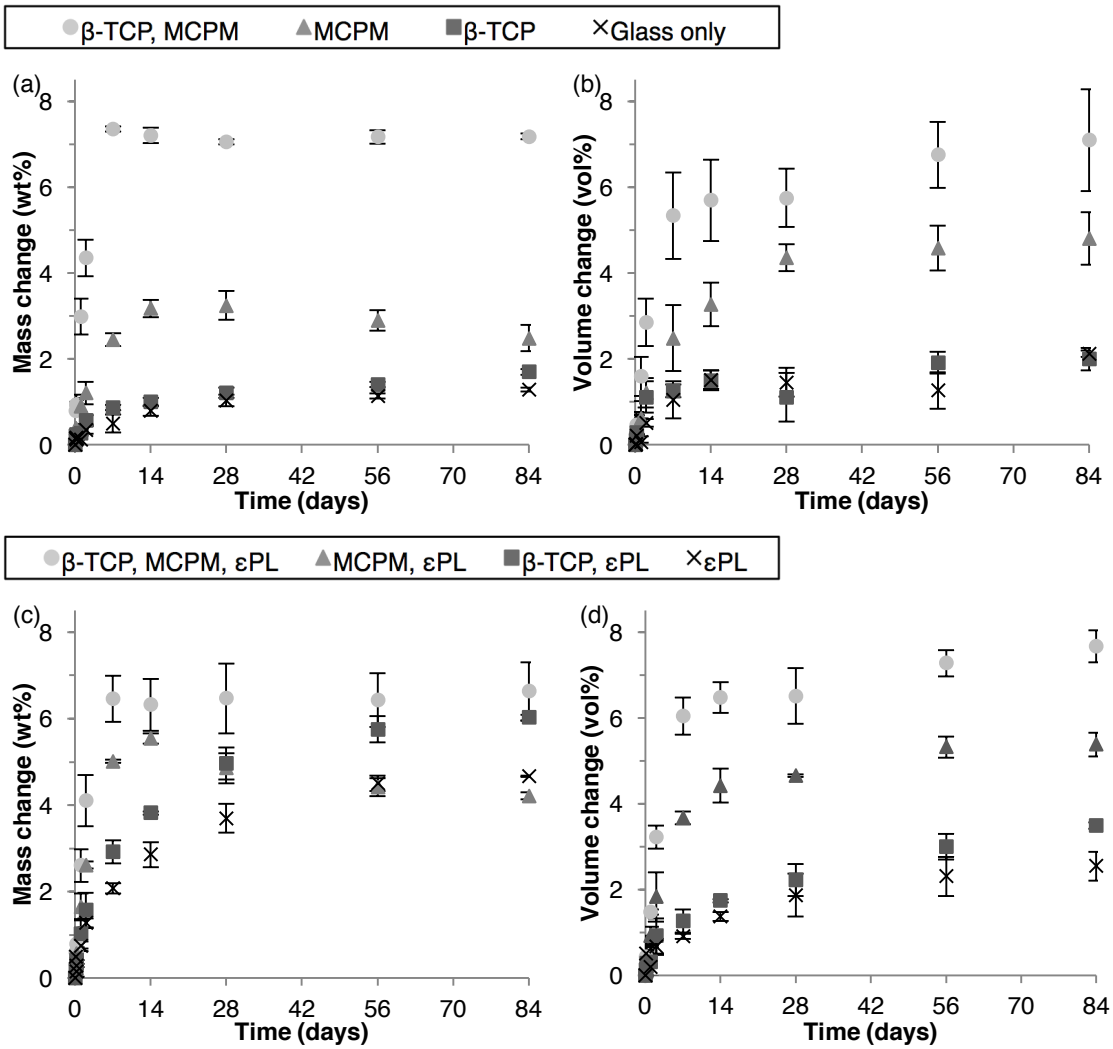

Figure 4.8. Mass and volume change of composites with varying MCPM, β-TCP and εPL content over three months storage in AS.

(a,c) Mass and (b,d) volume change of composite specimens containing 0 or 20 wt% GF, 0 or 40 wt% CaPs (MCPM and β-TCP at 1:1 wt ratio) and 0 or 5 wt% εPL in their filler phases and diluent monomer PPGDMA over 3 months storage in AS. Composites (a,b) without and (c,d) with 5 wt% εPL. Error bars represent SD (n = 3).

4.3.6.2 Mechanical properties

The mechanical properties of composites containing PPGDMA with varying MCPM (0 or 20 wt% in the filler phase), β-TCP (0 or 20 wt%) and εPL (0 or 5 wt%) content after one week, two weeks and three months storage in AS are shown in Figure 4.9, Figure 4.10 and Figure 4.11, respectively. Very similar trends were observed at all time-points, indicating that any effect due to storage in AS would have already occurred within the first week in most cases. There were two exceptions to this. The BFS of composites containing both CaPs reduced slightly between one and two weeks, whilst composites containing all three reactive fillers had increased in strength again by the final time-point. The higher variability at the three month time-point is due to the low number of replicates (n = 3), since specimens were taken from the end-point of the water sorption study.

As observed in the previous pilot study, εPL reduced strength of the material. β-TCP reduced BFS by ~20%, whilst MCPM had a greater effect, reducing it by ~56%. Materials containing both CaPs at 20 wt% each had the lowest BFS (34 and 49 MPa with and without 5 wt% εPL). The *E* and U_T of composites followed the same trends as BFS.

Parts b, d and f of these figures illustrate the effects of individual components and interaction effects between components on mechanical properties. MCPM significantly reduced BFS, *E* and U_T, whereas β-TCP and εPL each reduced these values to a lesser degree. No clear interaction effects were observed.

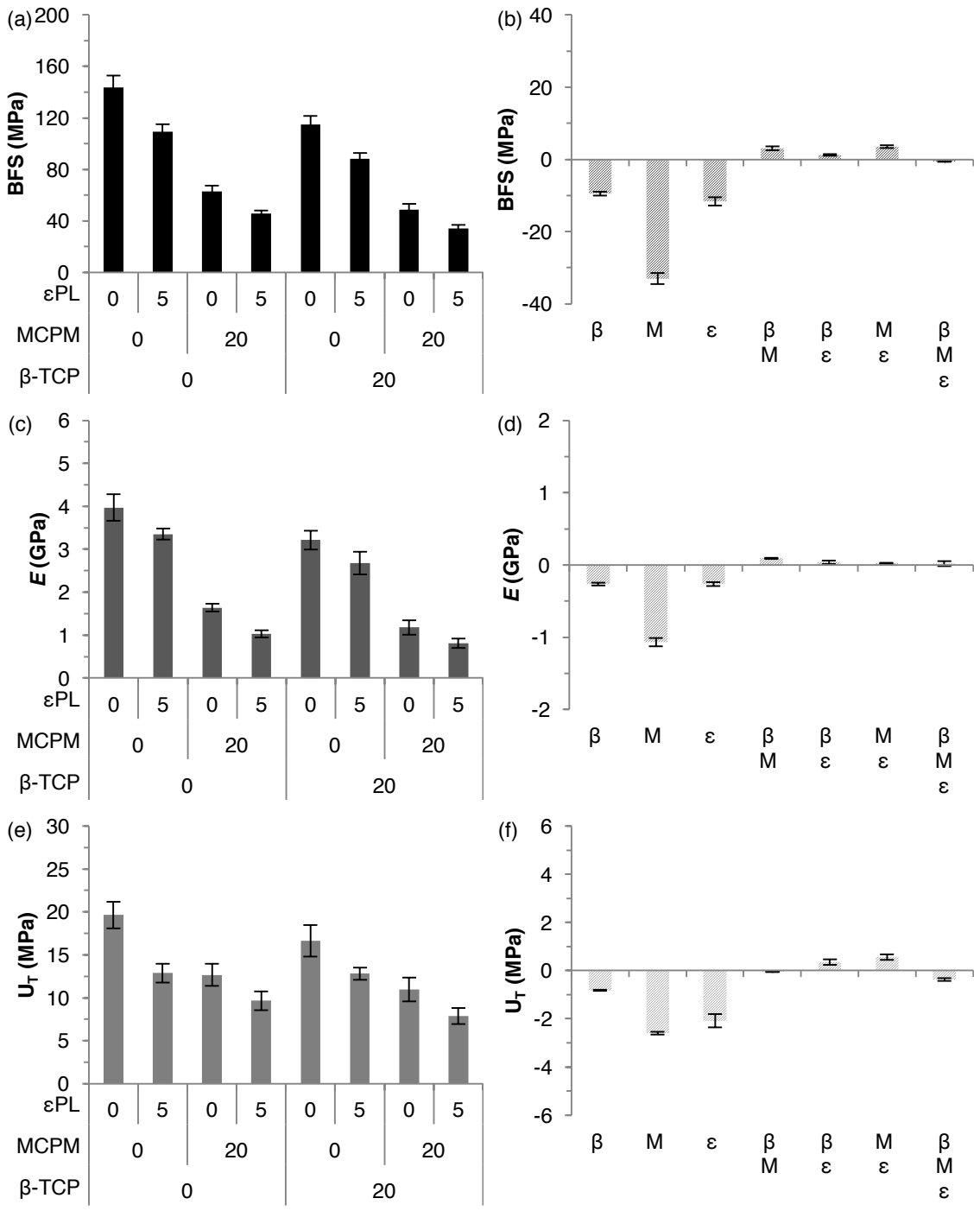

Figure 4.9. Mechanical properties of composites with varying MCPM, β-TCP and εPL content after one week storage in AS.

(a,b) BFS, (c,d) *E* and (e,f) U_T of composite specimens containing 0 or 20 wt% MCPM, 0 or 20 wt% β-TCP and 0 or 5 wt% εPL in their filler phases after 1 week storage in AS. (b,d,f) Effects of individual components and interaction effects between components. Error bars represent 95% confidence interval (n = 8–9).

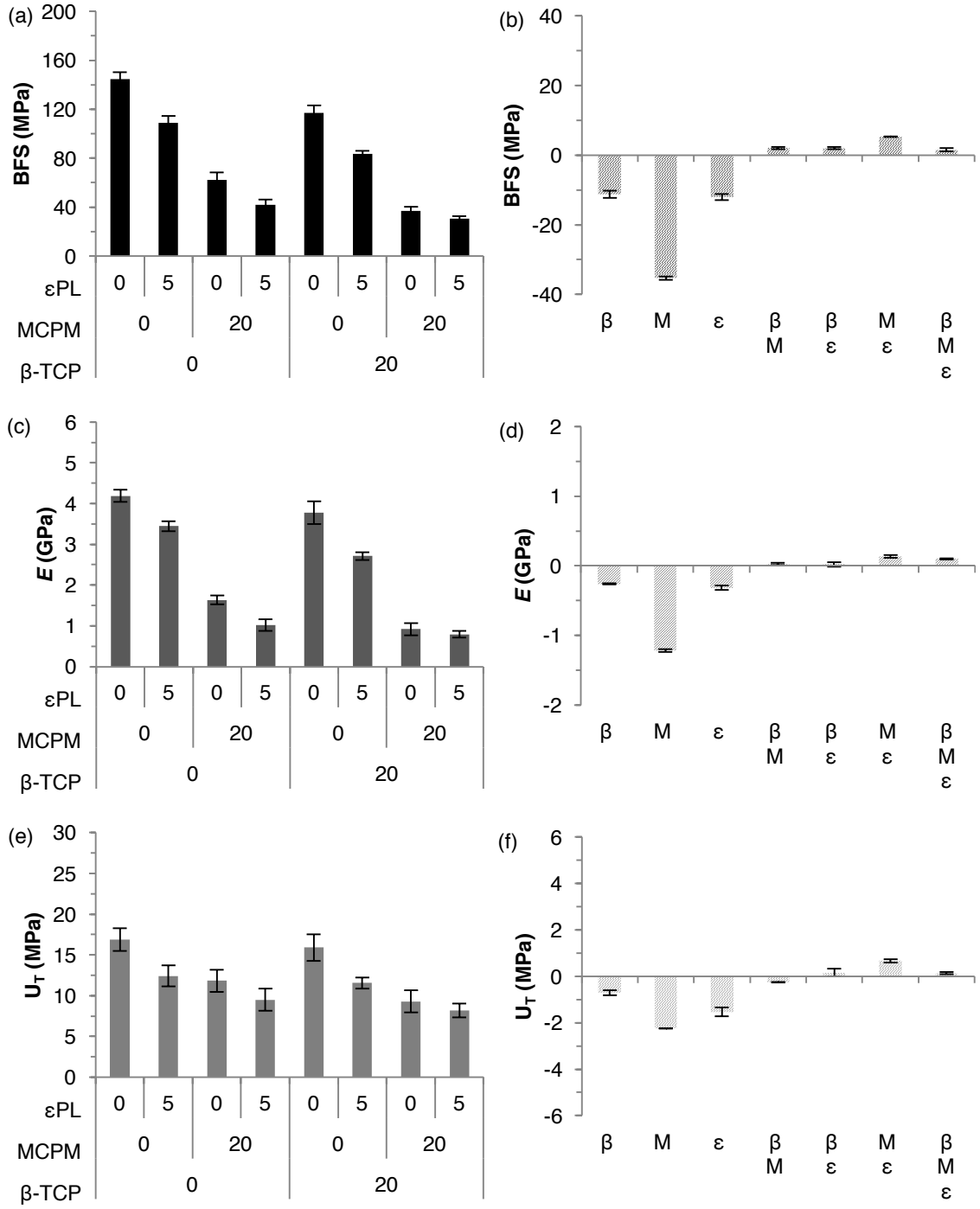

Figure 4.10. Mechanical properties of composites with varying MCPM, β-TCP and εPL content after two weeks storage in AS.

(a,b) BFS, (c,d) *E* and (e,f) U_T of composite specimens containing 0 or 20 wt% MCPM, 0 or 20 wt% β-TCP and 0 or 5 wt% εPL in their filler phases after 2 weeks storage in AS. (b,d,f) Effects of individual components and interaction effects between components. Error bars represent 95% confidence interval (n = 7–9).

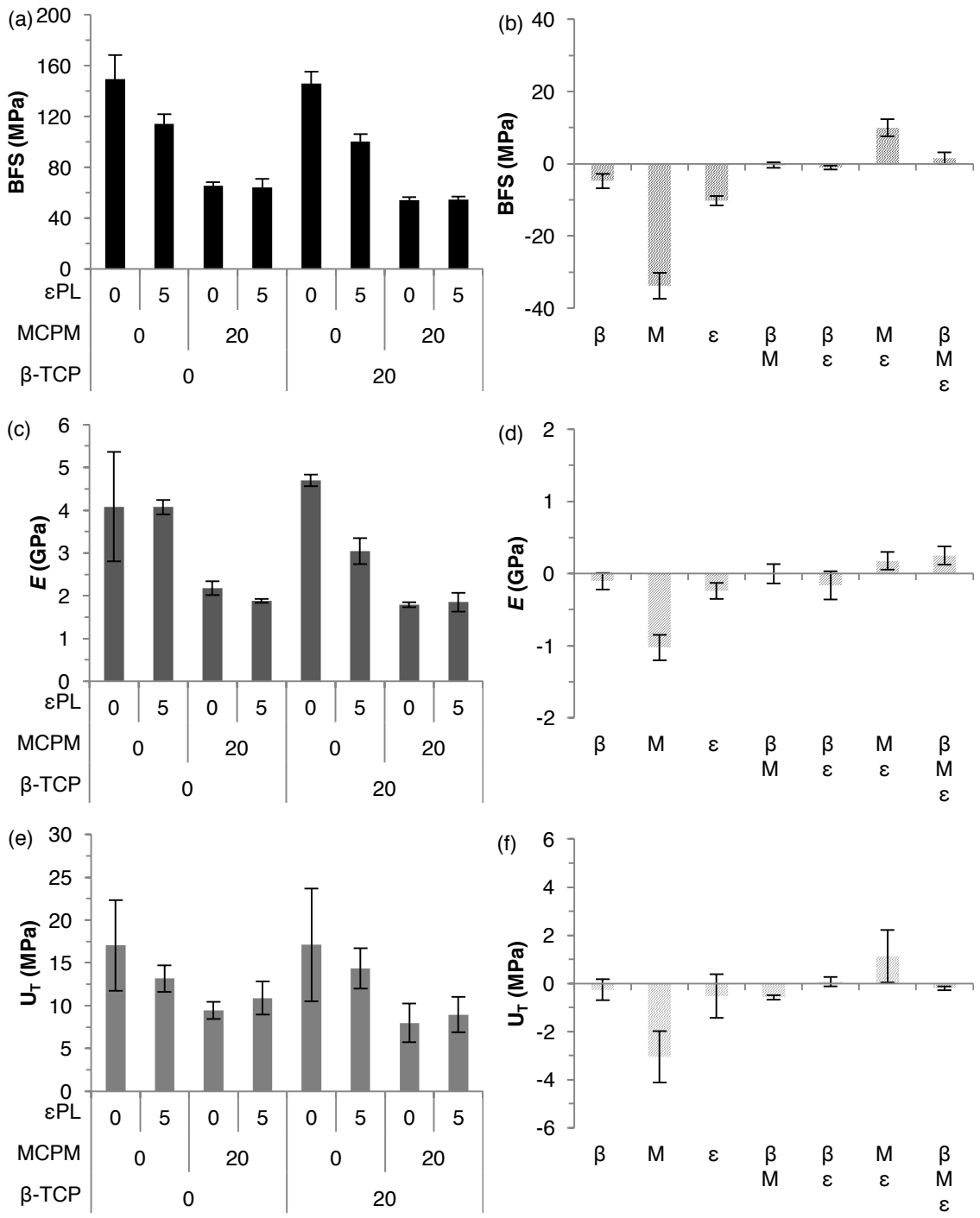

Figure 4.11. Mechanical properties of composites with varying MCPM, β-TCP and εPL content after three months storage in AS.

(a,b) BFS, (c,d) *E* and (e,f) U_T of composite specimens containing 0 or 20 wt% MCPM, 0 or 20 wt% β-TCP and 0 or 5 wt% εPL in their filler phases after 3 months storage in AS. (b,d,f) Effects of individual components and interaction effects between components. Error bars represent 95% confidence interval (n = 3).

4.4 Discussion

This series of pilot studies was developed to give primary indications as to the effect of each component on the properties of the composites. Statistical analysis was not performed in detail in the current chapter but in Chapters 5–7 instead, where some of these properties were investigated in greater detail. Furthermore, the hypotheses that formed the basis for this chapter have already been discussed throughout the introduction and description of the components (Chapters 1–2) and are described in greater detail in Chapter 5–7, with detailed references to supportive literature.

It was hypothesised that composites containing diluent monomer PPGDMA would have greater cytocompatibility than those containing TEGDMA without having significantly reduced mechanical properties, due to its higher molecular mass enabling greater flexibility and conversion. Since PPGDMA has not previously been investigated in dental composites, this hypothesis was completely novel and based on the chemical properties of the monomers in question. Composites containing 25 and 75 wt% diluent and bulk monomer, respectively, in their liquid phases have comparable mechanical properties regardless of whether PPGDMA or TEGDMA is used as diluent monomer. PPGDMA should theoretically have higher conversion than TEGDMA, due to its increased flexibility. This should theoretically result in improved cytocompatibility without increasing shrinkage, due to the lower double bond concentration of PPGDMA than TEGDMA. The use of PPGDMA in place of TEGDMA is therefore investigated in greater detail in Chapter 5.

Although Bis-GMA was not compared to UDMA in this series of pilot studies, the use of UDMA as the sole bulk monomer resulted in relatively high strength composites. The use of UDMA in place of Bis-GMA may be beneficial, since it is a more flexible molecule. This should result in reduced viscosity, improved handling properties and greater conversion[28,112]. The use of UDMA in place of Bis-GMA is therefore also investigated in greater detail in Chapter 5.

It was also hypothesised that different co-initiators would induce varying levels of conversion. No significant difference in BFS was noted between different co-initiators (DMPT, EDAB, Mg-NTG-GMA and Na-NTG-GMA). Composites containing Na-NTG-GMA-Na had double the toughness of those containing the other co-initiators, which is likely due to its ability to bind to the polymer, which may in turn improve cytocompatibility and adhesiveness. The lack of difference in strength of composites containing different composites may be because all were combined at a sufficiently high concentration (1 wt%), above the threshold at which increasing the concentration

further would have a strong effect. A more effective comparison may be drawn by incorporating the co-initiators at a constant molar concentration, as opposed to proportion by mass. The effects of photoinitiator and co-initiator are therefore investigated in greater detail in Chapter 6.

It is worth noting that when comparing components in these pilot studies, they were incorporated at a fixed wt% of the liquid phase. This makes direct comparison difficult. For example, Na-NTG-GMA has M_r of 329, almost 2.5 times greater than that of DMPT (135). This means that Na-NTG-GMA achieved similar properties to DMPT despite being incorporated at only 40 mol% of the concentration than DMPT was used at. Similarly, fewer molecules of PPGDMA than TEGDMA were present when the mass ratio of bulk to diluent monomer was kept fixed at 3:1. For this reason, subsequent studies were improved by using a fixed molarity or molar ratio in order to give a clearer insight into the effects of each component.

It was hypothesised that differences between glass filler particle sizes and surface treatments (which likely vary between manufacturers) would have a significant effect on the wet-point of the composites[54]. Glass particle size had a significant effect on wettability of the filler phase, due to the relationship between surface area per g of filler and the proportion of monomer required. Silanisation and density of the glass may also play an important role, since differences in the handling properties of GP_5 and GP_7 were noticeable despite their similar particle sizes.

Furthermore, it was hypothesised that glass fibres would improve the toughness of composites[62-64]. GF alone slightly improved U_T without affecting strength. Both CaPs reduced BFS when used alone or together. However, when CaPs and fibres were combined at high levels, U_T was significantly improved. This is likely to be due to an interaction between the CaP fillers and the CaP that exists in GF. CaPs may therefore be used in combination with fibres to provide a toughening and remineralising capability to the composite. Despite this, GF were not studied further due to concerns over poor wear resistance, due to the large size of the fibres.

β-TCP and MCPM have previously been shown to promote DCPD and HA mineral precipitation on the surface of composites in SBF[68]. Due to their high solubility, MCPM, and to a greater extent εPL, induced water sorption and release of CaPs out of the material in AS. In a super-saturated solution such as SBF or dentinal fluid, this may result in precipitation of stable HA. Clinically, this could occur at microscopic debonding sites between the tooth and the restoration and help to remineralise and potentially even “self-repair” the material, ultimately resulting in reduced rates of recurrent caries

and restoration failure. At the high levels studied here, these components contribute to the weakening of the material in artificial saliva. These components could, however, be more finely tuned and incorporated at more moderate levels, in order to achieve this remineralising effect.

The use of antimicrobial εPL may also help to prevent recurrent caries. Unpublished data suggests that εPL is released in sufficient quantities and over a prolonged period of one month to have an inhibitory effect on microbes (personal communication with Dr. Anne Young, Dr. Wendy Xia and Dr. Mohammed Adnan Khan due to a pending patent application[113] and development of a commercial product preventing publication of these data). εPL may be advantageous over CHXA due to its more complete release. It may also cause less tooth discolouration than CHXA, although the concentration of CHXA released from composites is significantly lower than that incorporated into commercially available Corsodyl gum treatment mouthwash. Although it causes a slight decrease in BFS, if used at moderate levels this should not be detrimental to the material. Furthermore, by inducing water sorption, εPL may act synergistically with CaP to encourage CaP release and subsequent remineralisation. The use of εPL in dental composites is novel. The effects of MCPM, β-TCP and εPL are therefore investigated in greater detail in Chapter 7.

5 EFFECT OF MONOMER VARIATION ON CYTOCOMPATIBILITY AND MATERIAL PROPERTIES

Note: Chapter 5 is the subject of the following publication (Ref. [101]):

Walters NJ, Xia W, Salih V, Ashley PF & Young AM. Poly(propylene glycol) and urethane dimethacrylates improve conversion of dental composites and reveal complexity of cytocompatibility testing. *Dental Materials* 2016;32:264–77, doi: 10.1016/j.dental.2015.11.017.

5.1 Introduction to Chapter 5

Despite being favoured by clinicians for their high strength compared to other tooth-coloured filling materials and supreme aesthetics compared to all other filling materials, the physical characteristics of dental composites are limited by the close interplay between monomer conversion and characteristics such as polymerisation shrinkage, water sorption, mechanical properties, elution of toxic components and biocompatibility. In order to achieve optimal biocompatibility, mechanical properties and aesthetics[114], a high degree of conversion is ideal, since these properties are directly affected by the level of residual monomer remaining in the composite after curing. Conversely, however, high conversion results in high volumetric shrinkage of dimethacrylate-based composites. For the patient, this can result in microbial microleakage, subsequent recurrent caries and, ultimately, failure of the restoration. Monomers with low double bond concentration can therefore be used in order to minimise shrinkage. This is of particular importance for bulk fill materials, which are applied in thicker increments. The incremental layering of composites, which requires curing each increment before applying the next, is time-consuming for clinicians. This is especially true of deep posterior cavities, which would require multiple increments. As a result, bulk fill materials are often used to overcome this issue. Bulk fill composites utilise photoinitiators which are effective at depths of ~4–5 mm in combination with monomers that have low double bond concentration.

The research presented in Chapter 5 aimed to improve the conversion, strength and cytocompatibility of dimethacrylate-based composites without detrimentally affecting their shrinkage or depth of cure. This was approached by replacing Bis-GMA with UDMA and TEGDMA with PPGDMA. It was hypothesised that the greater cross-linking density and flexibility of UDMA than Bis-GMA[28,112] would help to improve conversion and therefore better cytocompatibility without increasing conversion or depth of cure.

Similarly, PPGDMA was hypothesised to achieve similar improvements due to its significantly lower double bond concentration and greater flexibility than TEGDMA. Human gingival fibroblasts (HGF) were cultured in solutions of each individual liquid phase component at varying concentrations, as well as in extracts of each composite formulation, in order to investigate the effect of each monomer on cytocompatibility. Due to variability between different assays arising from the targeting of different metabolic enzymes[115], three cell viability assays were compared.

5.2 Formulations

Composites were prepared using a filler phase with a fixed formulation, consisting of 10 wt% OX-50, 30 wt% $GP_{0.7}$ and 60 wt% GP_7. This was combined with four dimethacrylate-based liquid phases. The liquid phases consisted of bulk monomer UDMA or Bis-GMA combined with diluent monomer PPGDMA or TEGDMA, prepared according to Chapter 3.1.1.1. The bulk to diluent molar ratio was 3.5:1. This corresponded to the wt ratios show in Table 5.1. The liquid phases also contained 40 mM (0.58–0.61 wt%) CQ, 60 mM (0.82–0.86 wt%) DMAEMA and 100 ppm BHT. Pastes were prepared according to Chapter 3.1.1.2 and disc specimens produced according to Chapter 3.1.1.3 were used for studies, except where otherwise indicated in specific method subsections. PLR was kept constant at 40 vol% liquid (19.3–20.3 wt%, depending on liquid phase density). Dental composites were designated abbreviations based on their bulk and diluent monomer content: UP, UT, BP and BT, where U, B, P and T represent UDMA, Bis-GMA, PPGDMA and TEGDMA, respectively. Formulations are summarised in Table 5.1. Filtek Z250 was used for comparison.

Table 5.1. Chapter 5 experimental formulations.

Variable liquid phase parameters			
Formulation	**Bulk monomer**	**Diluent monomer**	**Bulk:diluent monomer wt ratio**
UP	UDMA	PPGDMA	3.09:1
UT		TEGDMA	5.96:1
BP	Bis-GMA	PPGDMA	3.44:1
BT		TEGDMA	6.67:1

Fixed liquid phase parameters	
Bulk to diluent monomer ratio	3.5:1
CQ	40 mM
DMAEMA	60 mM
BHT	100 ppm

Fixed filler phase and PLR parameters	
$GP_{0.7}$	30 wt%
GP_7	60 wt%
OX-50	10 wt%
PLR	40 vol% liquid

5.3 Results

5.3.1 Handling properties and wet-point

The experimental formulations all had wet-points of 33.3 ± 0.4 vol% liquid. When produced at their corresponding wet-points, composite pastes containing Bis-GMA were perceived to be considerably less malleable during specimen moulding than those containing UDMA. Composites produced at 40 vol% liquid were slightly more malleable, though those containing Bis-GMA were still less malleable than those containing UDMA. The handling properties of Z250 were between those of Bis-GMA- and UDMA-containing composites. A difference in handling properties was not observed between PPGDMA- and TEGDMA-containing composites.

5.3.2 Polymerisation properties

5.3.2.1 Conversion

On average, UDMA-containing experimental composites had 1.2 and 1.3 times higher conversion than Bis-GMA-containing composites at 1 and 4 mm depth, respectively (average p-value of both depths = 0.001) (Figure 5.1a). Use of PPGDMA in place of TEGDMA increased conversion by a further 1.1 and 1.2 times at 1 and 4 mm, respectively (average p-value of both depths < 0.01). Of all four experimental formulations, UP had the highest conversion, at 68% and 65% at 1 and 4 mm. The conversion of UP at both depths was significantly higher than that of BP, BT and Z250 ($p < 0.001$). At 1 mm, it was significantly higher than that of UT ($p < 0.05$). Z250 had the lowest conversion of 50% and 39% at 1 and 4 mm, whilst that of BT was comparable. The conversion of Bis-GMA-containing composites (BP, BT and Z250) was significantly lower at 4 mm than at 1 mm.

5.3.2.2 Shrinkage

The shrinkage at 1 mm depth of UDMA-containing experimental composites was estimated to be ~1.2 times higher, on average, than of Bis-GMA-containing composites ($p < 2 \times 10^{-5}$), when calculated based on conversion values obtained at 1 mm depth (Figure 5.1b). TEGDMA-containing composites were estimated to have ~1.1 times higher shrinkage than PPGDMA-containing composites ($p < 0.04$). The shrinkage of Z250 could not be calculated by this method because its exact composition is not publicly available. The values obtained by measuring volume before and after curing, however, indicated no statistically significant effect of monomer on shrinkage (including Z250), due to the high standard deviation of the technique.

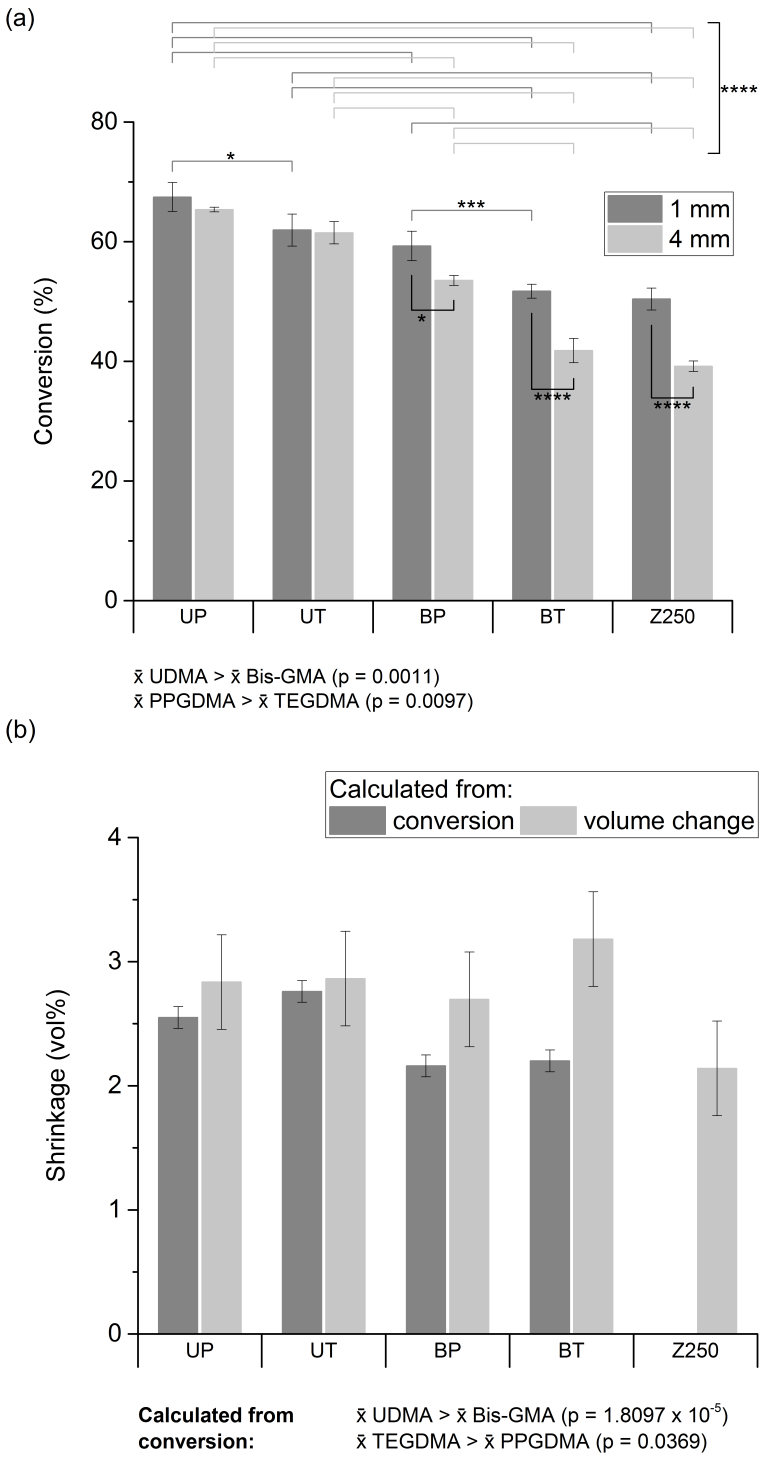

Figure 5.1. Polymerisation properties of composites with varying monomers.

(a) Conversion at 1 and 4 mm depth. Columns represent mean, error bars represent SD.

(b) Shrinkage of 1 mm thick composite discs, calculated from conversion or volume change. Columns represent mean, error bars represent mean SD of the corresponding technique (± 0.05 and ± 0.23 vol% for conversion and volume change, respectively).

(c)

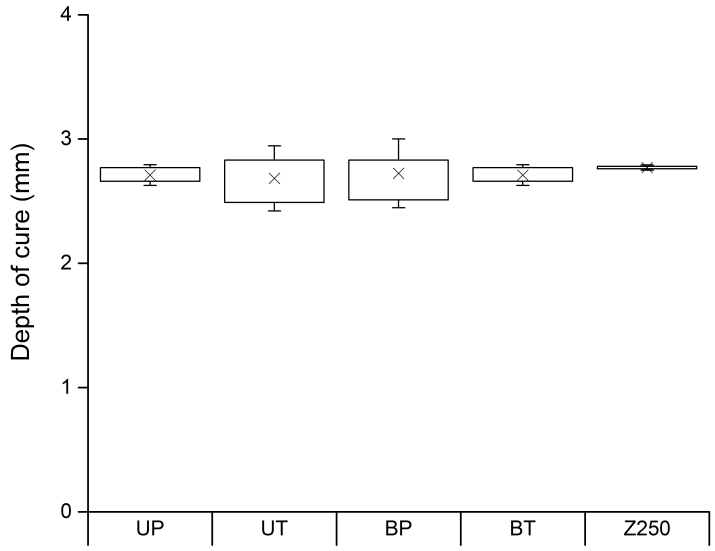

* p < 0.05 *** p < 0.005 **** p < 0.001

(d)

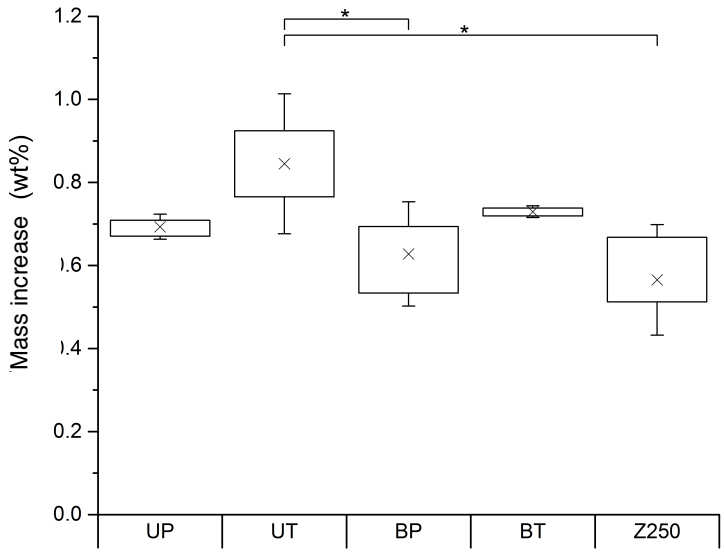

x̄ TEGDMA > x̄ PPGDMA (p = 0.0192)

Figure 5.1 (continued). Polymerisation properties of composites with varying monomers.

(c) Depth of cure of composites.

(d) Mass increase of composites after immersion in dH_2O for one week.

(c, d) Crosses represent mean, boxes represent 25–75 percentiles, error bars represent SD.

5.3.2.3 Depth of cure

All composites had highly comparable depths of cure of 2.7 ± 0.25 mm, regardless of monomer composition (F = 0.96) (Figure 5.1c).

5.3.2.4 Water sorption

TEGDMA-containing composites had, on average, 1.2 times higher water sorption than that PPGDMA-containing composites ($p < 0.02$) (Figure 5.1d). UDMA induced ~1.1 times greater water sorption than Bis-GMA, though this was not deemed statistically significant. UT absorbed significantly more water than Z250 and BP ($p < 0.05$).

5.3.3 Mechanical properties

Experimental composites containing UDMA had significantly higher strength (153–158 MPa) than those with Bis-GMA ($p = 1x\ 10^{-7}$). BP (127 MPa) was significantly stronger than BT (99 MPa) ($p < 0.05$) (Figure 5.2a). Composites containing PPGDMA had slightly lower *E*, on average, than those with TEGDMA (6.15 and 6.75 GPa, respectively) ($p = 0.009$) (Figure 5.2b). Z250 was the strongest composite (173 MPa) and had the lowest modulus (5.3 GPa).

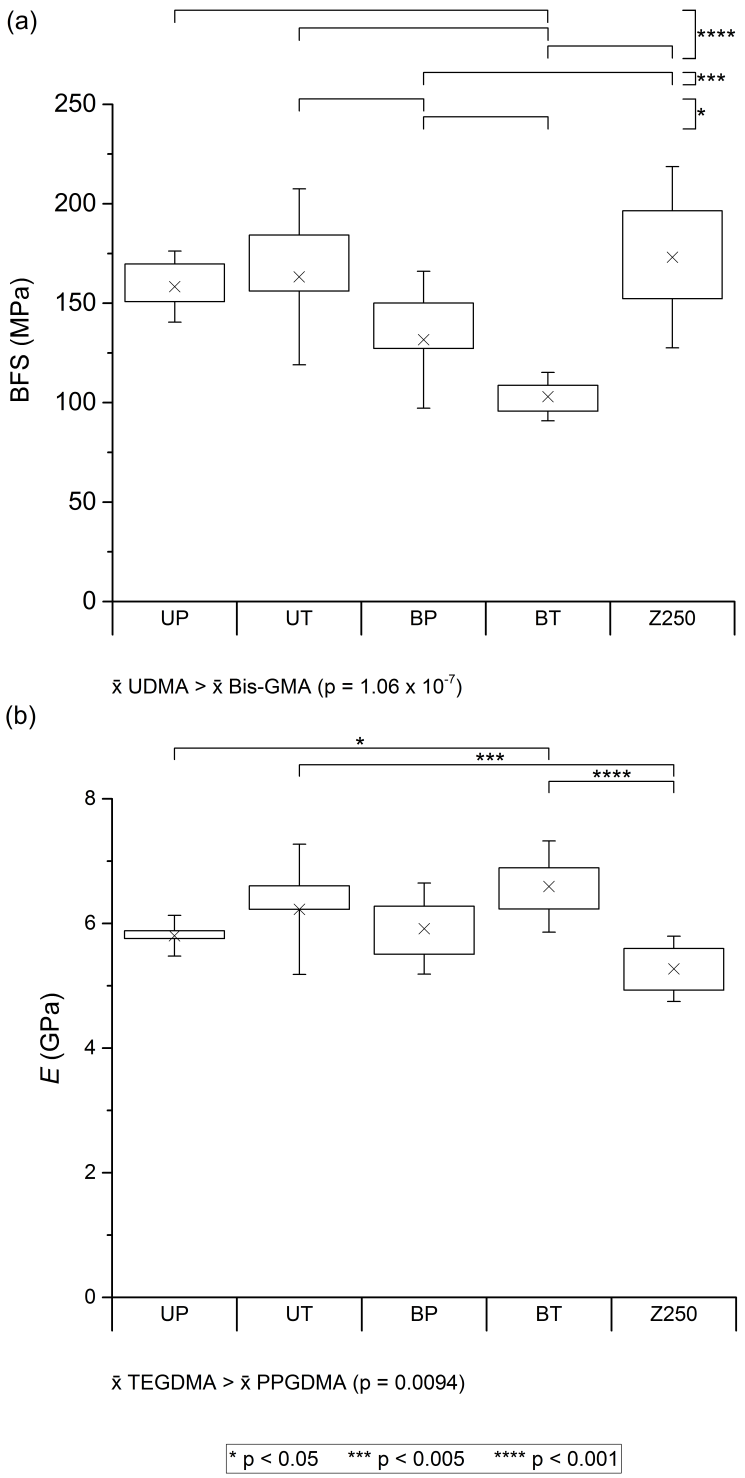

Figure 5.2. Mechanical properties of composites with varying monomers.

(a) Biaxial flexural strength and (b) modulus of tensile elasticity after storage in dH_2O at 37 ˚C for one week. Crosses represent mean, boxes represent 25–75 percentiles, error bars represent SD. The BPS of BP did not have normal distribution according to the Anderson-Darling test but had normal distribution according to others (Kolmogorov-Smirnov and Lilliefors tests). The *E* of UP and UT did not have normal distribution according to the Anderson-Darling test but had normal distribution according to the Kolmogorov-Smirnov normality test.

5.3.4 Cytocompatibility

5.3.4.1 Comparison of resazurin, WST-8 and MTS assays

The apparent cell density of HGF after being cultured in serum-free DMEM for 48 and 72 h is shown in Figure 5.3. An increase in apparent cell density from 30,000 to ~49,000 cells/cm^2 between 0 and 48 h was indicated by resazurin and WST-8 assays. MTS, however, reported a smaller increase in apparent cell density from 30,000 to 37,000 cells/cm^2. After 72 h, the resazurin assay reported a cell density of 113,000 cells/cm^2, much higher than the 74,000 cells/cm^2 reported by the WST-8 assay and the 45,000 cells/cm^2 reported by MTS. Due to the notable differences in cell densities measured in these control samples, subsequent data were normalised to the corresponding assay's control and time-point. The results from the cytocompatibility studies are reported in terms of 'relative metabolic activity' in order to emphasise the differences between assays.

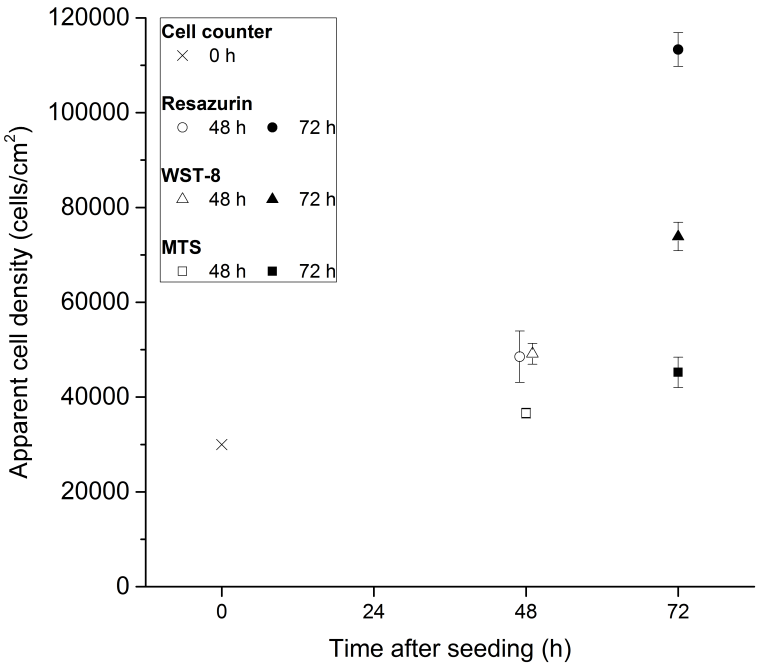

Figure 5.3. Initial seeding density of HGF.

Determined by cell counting (0 h, cross), and apparent density after culture in DMEM for 48 h (unfilled symbols) and 72 h (filled symbols), as assessed by resazurin (circle), WST-8 (triangle) and MTS (square) assays. Error bars represent SD.

5.3.4.2 Composite component cytocompatibility

The relative metabolic activity of HGF surviving exposure to liquid phase components, prepared at various concentrations, followed by a subsequent recovery period, is presented in Figure 5.4. Dashed lines represent the mean control value for pure DMEM, from each corresponding assay and time-point. All of the liquid phase components tested caused concentration-dependent reductions in cell number associated with increasing concentrations, as expected. The extent of this relationship, however, varied between assays. In all assays, every component at a concentration of 10 mM or higher caused complete loss of metabolic activity.

5.3.4.2.1 CQ

At the 48 h time-point, a direct correlation between CQ concentration and WST-8 activity was apparent, with ≤ 0.01 mM causing no significant decrease (Figure 5.4a). At 0.1, 1 or 10 mM, reductions in WST-8 activity of 17, 33 and 98% occurred, respectively. At most concentrations, similar levels (± 5%) of resazurin activity were measured after 48 h, but these did not change significantly by 72 h. By comparison, MTS activity was up to 15% higher after 48 h and further elevated after 72 h, at ~10–38% greater than the control, except at concentrations ≥ 10 mM. After 72 h, similar WST-8 activity to the control (± 7%) was measured at all concentrations except at concentrations ≥ 10 mM, which appeared to cause cell death.

5.3.4.2.2 DMAEMA, TEGDMA & UDMA

In contrast to CQ, 0.01 mM DMAEMA caused an 86–95% reduction in metabolic activity in all assays by 48 h and cell populations did not recover by 72 h (Figure 5.4b). ≥0.1 mM was sufficient to cause total inhibition of MTS, resazurin and WST-8 activity, clearly indicating that cell death had occurred. A concentration of 0.01 mM UDMA (Figure 5.4c) or TEGDMA (Figure 5.4f) was sufficient to inhibit all enzymes.

5.3.4.2.3 Bis-GMA

Bis-GMA appeared to have higher cytocompatibility than the other three monomers (Figure 5.4d). After 48 h, concentrations in the range of 0.001 and 0.01 mM appeared to have no effect on WST-8 metabolism, although activity increased by 7 and 66% upon increasing concentrations to 0.1 and 1 mM, respectively. Both other assays showed similar trends, except that at 0.001 and 0.1 mM, values reported by resazurin and MTS were lower by ~10–15% and ~23–28%, respectively. WST-8 activity increased by between 7 and 20% between 48 and 72 h, except at 10 mM, and activity at concentrations of 0.001–0.1 mM appeared to be greater than the corresponding

controls. The values recorded for resazurin activity were similar at both time-points (± 10%).

5.3.4.2.4 PPGDMA

The trends of HGF metabolic activity upon exposure to PPGDMA were more complex (Figure 5.4e), with all three assays giving varying results. MTS, resazurin and WST-8 metabolism were fully inhibited within 48 h by ≥10 mM PPGDMA and cells did not recover thereafter. A small increase in MTS and WST-8 activity occurred upon reducing concentration, though values remained well below those of the corresponding controls and cells did not appear to proliferate by 72 h. Interestingly, resazurin activity in PPGDMA solutions below 0.1 mM at 48 h was higher than for the control, later falling to control levels by 72 h. After 48 h, at 0.01–1 mM, PPGDMA caused reduction in WST-8 activity of 76, 85 and 92%, respectively, and these levels remained similar at 72 h. MTS metabolism was also similar. Resazurin activity at PPGDMA concentrations of 0.01 and 0.1 mM was 63 and 35% higher the control after 48 h, respectively. At 1 mM, it was comparable to the control. These values had fallen by 72 h, with resazurin activity at 0.01, 0.1 and 1 mM being ~12% greater, 7% lower and 80% lower than the control, respectively.

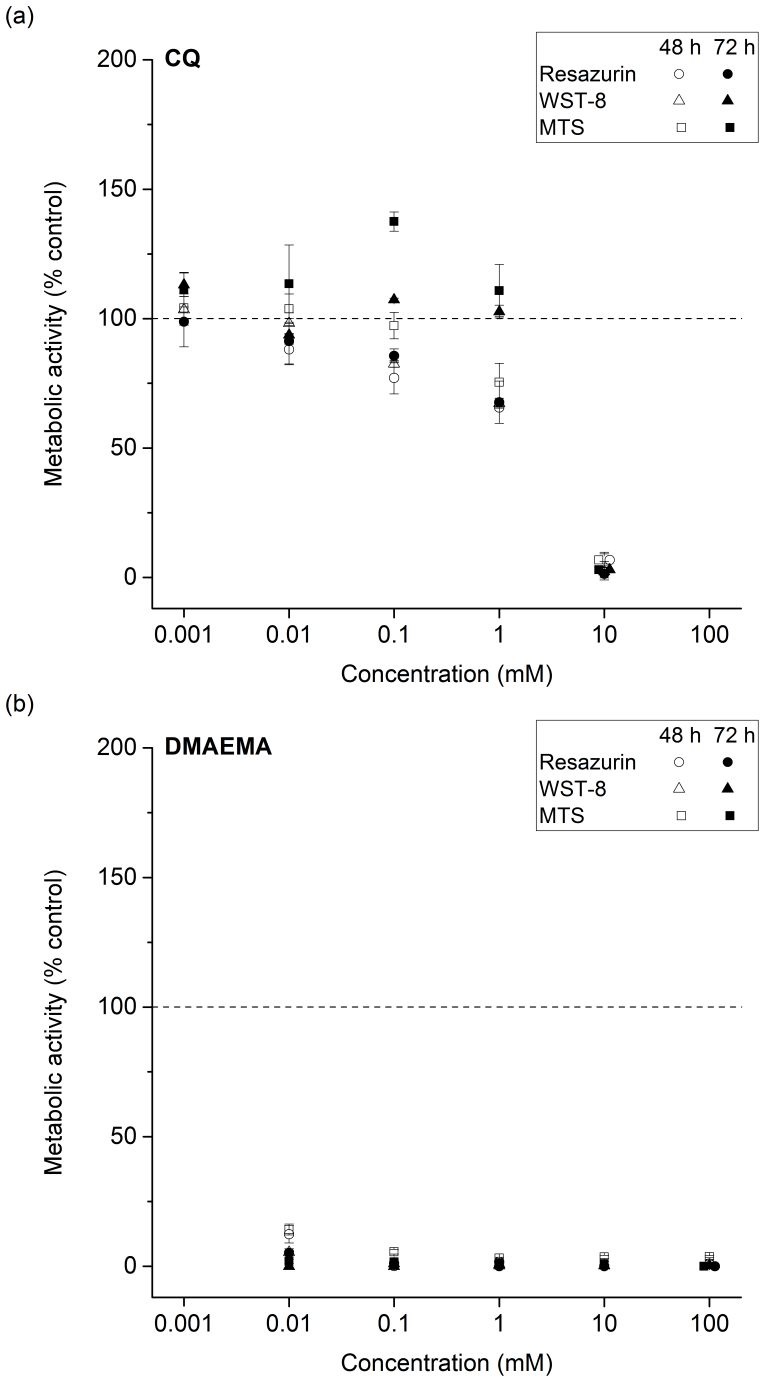

Figure 5.4. Relative metabolic activity of HGF after culture in liquid phase components.

* Continued overleaf *

(a) CQ, (b) DMAEMA, (c) UDMA, (d) Bis-GMA, (e) PPGDMA or (f) TEGDMA. Resazurin (circle), WST-8 (triangle) and MTS (square) assays were performed after 24 h culture in the solutions (48 h time-point, unfilled symbols), and after a subsequent 24 h recovery period in DMEM (72 h time-point, filled symbols). Component concentrations ranged from 0.001–10 mM (a and d) or 0.01–100 mM (b, c, e and f). Dashed lines represent the mean value of the control, error bars represent SD.

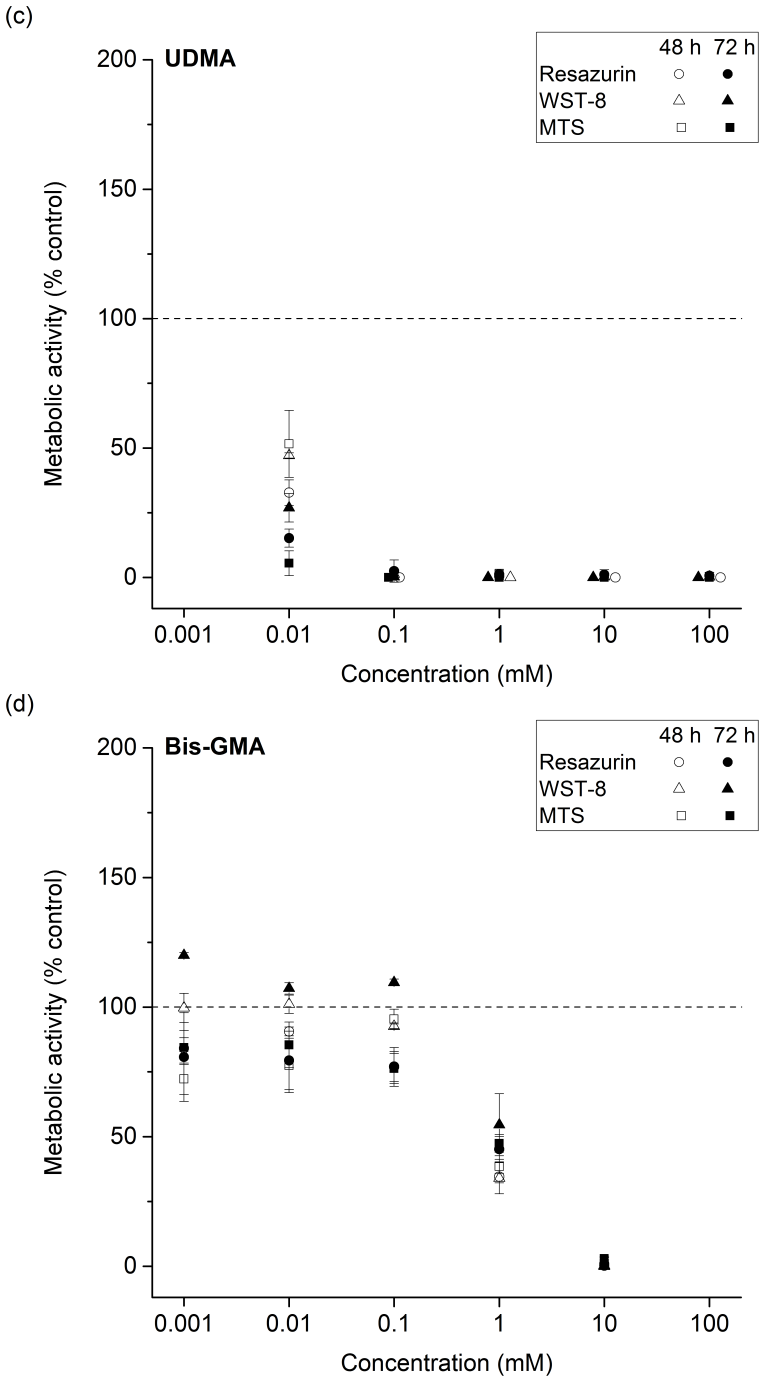

Figure 5.4 (continued). Relative metabolic activity of HGF after culture in liquid phase components.

* Continued overleaf *

(a) CQ, (b) DMAEMA, (c) UDMA, (d) Bis-GMA, (e) PPGDMA or (f) TEGDMA. Resazurin (circle), WST-8 (triangle) and MTS (square) assays were performed after 24 h culture in the solutions (48 h time-point, unfilled symbols), and after a subsequent 24 h recovery period in DMEM (72 h time-point, filled symbols). Component concentrations ranged from 0.001–10 mM (a and d) or 0.01–100 mM (b, c, e and f). Dashed lines represent the mean value of the control, error bars represent SD.

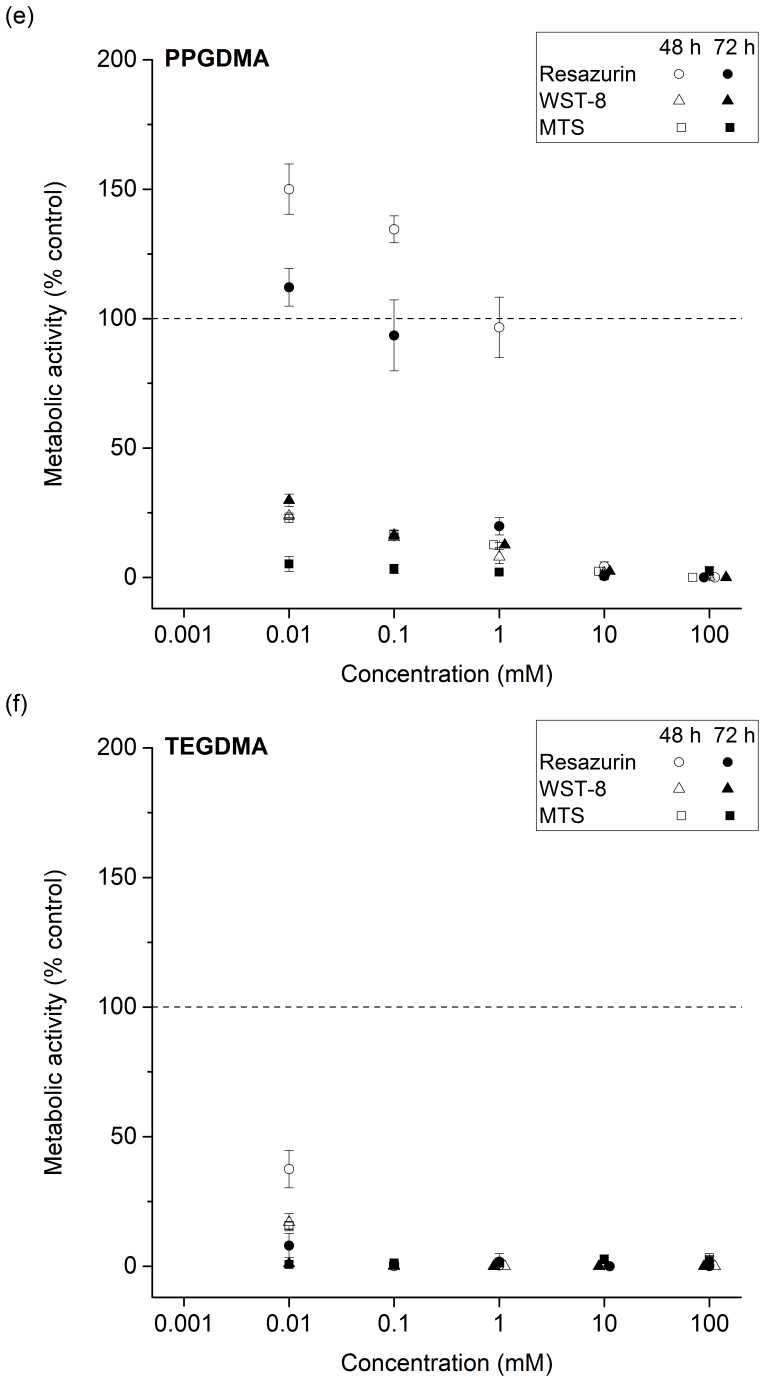

Figure 5.4 (continued). Relative metabolic activity of HGF after culture in liquid phase components.

(a) CQ, (b) DMAEMA, (c) UDMA, (d) Bis-GMA, (e) PPGDMA or (f) TEGDMA. Resazurin (circle), WST-8 (triangle) and MTS (square) assays were performed after 24 h culture in the solutions (48 h time-point, unfilled symbols), and after a subsequent 24 h recovery period in DMEM (72 h time-point, filled symbols). Component concentrations ranged from 0.001–10 mM (a and d) or 0.01–100 mM (b, c, e and f). Dashed lines represent the mean value of the control, error bars represent SD.

5.3.4.3 Composite extract cytocompatibility

HGF metabolic activity after culture in conditioned medium extracts of composites is presented in Figure 5.5. Similarly to the component assays, notable differences were observed between assays. From this point onwards, data are expressed as a percentage of the control for each corresponding extract (1 or 7 days) and assay time-point (48 or 72 h), in order to facilitate description and elucidation of trends.

A general downward trend in resazurin metabolism was observed after 24 h exposure to 1 day composite extracts (48 h time-point), in the following order: UP > UT ≥ BP > BT ≥ Z250. Despite WST-8 data differing slightly (UP ≈ UT > BP ≈ BT > Z250), both assays confirmed that the extracts from the deepest 1 mm of 4 mm thick composite specimens containing UDMA caused a lesser reduction in metabolic activity after 48 h than those containing Bis-GMA. This was statistically significant in the case of resazurin ($p = 0.001$). MTS showed no significant differences between experimental formulations. All assays indicated that Z250 had low cytocompatibility. In the case of all assays, metabolic activity varied from being similar to the control (UP) down to ~50% of the control (Z250). A small but significant reduction in resazurin activity was induced by TEGDMA extracts compared to PPGDMA extracts ($p < 0.01$), though WST-8 and MTS showed no clear trends with respect to the effect of diluent monomer.

Activity of all three enzymes after culture of HGF for 72 h in all material extracts had fallen to approximately 50% that of the control. Z250 was the only material with observable differences between assays, with resazurin activity remaining similar to after 48 h (~50%), but WST-8 activity falling from 53 to 37% and MTS activity falling from 53 to 33%, though these differences were not statistically significant.

As expected, resazurin and WST-8 indicated that 7 day extracts were more cytocompatible than 1 day extracts, as metabolic activity of HGF cultured in 7 day extracts returned to control levels by the 72 h time-point. The resazurin assay performed after 48 h on 7 day extracts gave similar trends to that performed on the corresponding 1 day extracts, though values were slightly higher. After 48 h incubation, for example, resazurin activity was ~75% relative to the control when HGF were cultured in 7 day BT extracts, compared to 56% in 1 day extracts. WST-8 activity in all material extracts was similar to the control or slightly elevated (up to 11%) after 48 h, except in the case of the 7 day extract of Z250, which caused significant reduction in WST-8 activity. Resazurin and WST-8 activity of HGF cultured in 7 day extracts had, in general, recovered by the 72 h time-point, though resazurin metabolism in BT and Z250 extracts remained slightly reduced at 89 and 82%, respectively. WST-8 activity

was between 10 and 31% greater than the control in all experimental formulation extracts after 72 h. In contrast, MTS activity in 7 day extracts was significantly different from that of resazurin and WST-8, at ~60–75% higher than the control at both time-points. MTS activity in 7 day Z250 extracts was similar to WST-8. 7 day extracts of UDMA-containing composites also appeared to have improved cytocompatible compared to Bis-GMA-containing composites in all assays (48 h resazurin, $p = 0.03$; 72 h WST-8, $p = 0.0008$; 72 h MTS, $p = 0.007$). Finally, WST-8 activity was significantly higher after exposure to 7 day extracts of PPGDMA-containing composites than TEGDMA-containing composites at 48 h ($p = 0.04$).

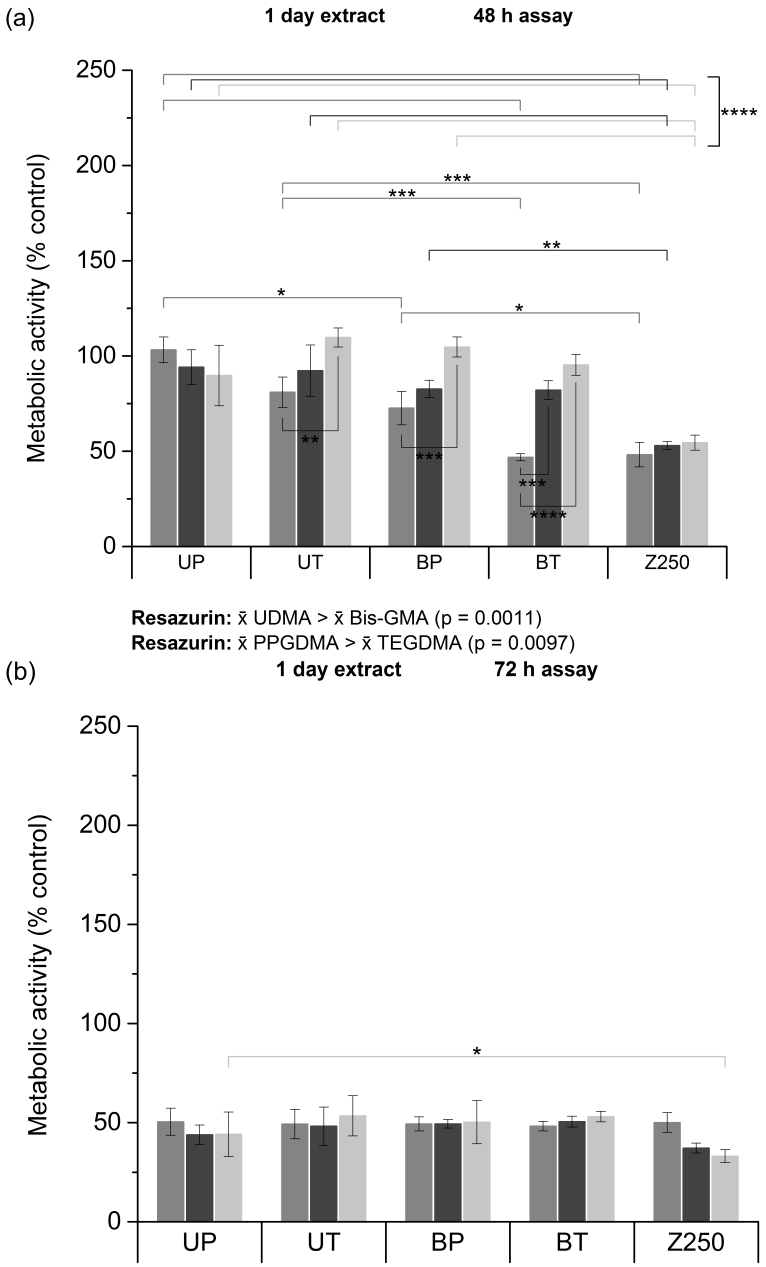

Figure 5.5. Relative metabolic of HGF after culture in composite extracts.

* Continued overleaf *

(a, c) 48 h or (b, d) 72 h culture in (a, b) 1 day or (c, d) 7 day extracts, assessed by resazurin (dark grey), WST-8 (black) and MTS (light grey) assays. Dashed lines represent the mean value of the control, error bars represent SD.

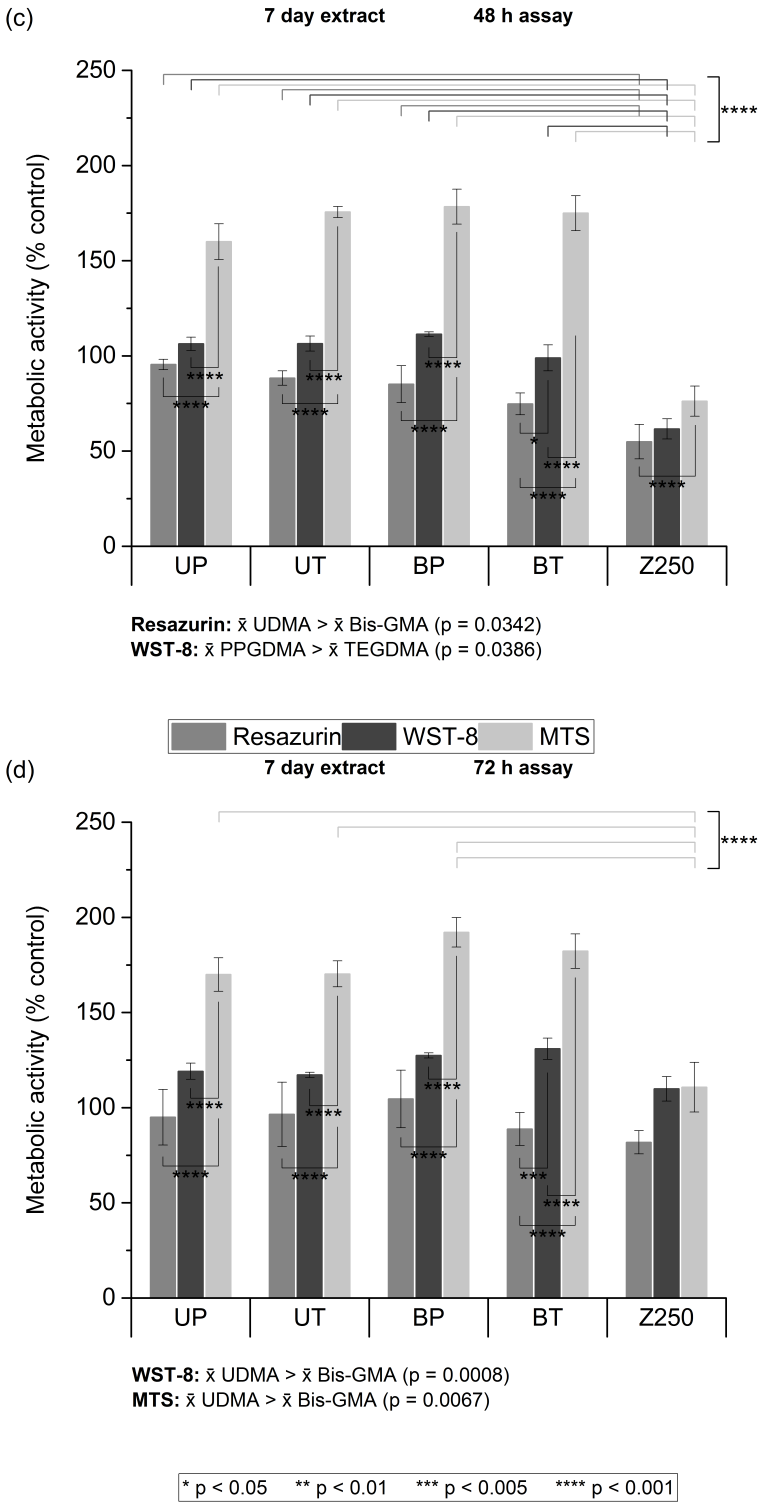

Figure 5.5 (continued). Relative metabolic of HGF after culture in composite extracts.

* Continued overleaf *

(a, c) 48 h or (b, d) 72 h culture in (a, b) 1 day or (c, d) 7 day extracts, assessed by resazurin (dark grey), WST-8 (black) and MTS (light grey) assays. Dashed lines represent the mean value of the control, error bars represent SD.

5.4 Discussion

In the present chapter, composites containing bulk monomer UDMA or Bis-GMA with diluent monomer PPGDMA or TEGDMA were compared in terms of their material characteristics and cytocompatibility. As expected, UDMA-containing experimental formulations had significantly higher conversion and slightly improved cytocompatibility compared to Bis-GMA-containing formulations. Similarly, PPGDMA-containing composites had higher conversion than TEGDMA-containing composites. The use of UDMA and PPGDMA as the sole bulk and diluent monomers did not detrimentally affect shrinkage or depth of cure, and this use of UDMA in place of Bis-GMA improved handling properties.

The proportions of OX-50 (10 wt%), $G_{0.7}$ (30 wt%), reactive fillers (variable) and G_7 (remainder of filler phase) used were determined by pilot studies, which found this general formulation to have optimal handling properties and wettability.

The differences in conversion of the four formulations followed the expected trends, based on differences in the chemical structures (Figure 2.4 and Figure 2.5) and physical characteristics (Table 2.4) of their constituent monomers. Despite being a slightly smaller molecule and subsequently having slightly higher double bond concentration (the ratio of double bonds per molecule to its molecular mass) than Bis-GMA, the lower glass transition temperature (T_g) and greater flexibility of UDMA enable more complete cross-linking[116]. Bis-GMA contains bulky aromatic groups which cause steric hindrance and very high viscosity (~80 times that of UDMA), which reduces flexibility and limits the likelihood of methacrylate groups binding to one another. Conversely, PPGDMA, which is over double the molecular mass of TEGDMA, achieves greater conversion because of its greater flexibility and lower double bond concentration.

The similar depth of cure of all formulations is likely due to the similar refractive indices of all the monomers, which was 1.48 ± 0.04, though results from using the standard protocol provide only limited information. BS EN ISO 4049:2009[103] utilises a 'scraping' method, which likely suffers from variability between different researchers and is only a rough and highly subjective measurement of composite hardness versus depth. It does not provide any information regarding the level of conversion at different depths, or the depth at which ≥50% conversion was achieved. As such, the standard requires that the depth value obtained is divided by 2 in order to give an estimate of the depth of cure, which appears to result in under-reporting of depth of cure values for certain formulations. In general, it may be considered that a value of ≥50% conversion

indicates that, on average, one methacrylate group per monomer molecule has reacted – enough to claim that that the composite has cured and has acceptable cytocompatibility[117]. The first double bond of a dimethacrylate molecule tends to polymerise faster than the second, since the propagating polymer is more flexible earlier on when less cross-linking has taken place. In order to overcome the limitations of the standard protocol, FTIR was used in the current chapter in order to more accurately assess the depth of cure by associating it with the conversion at various specified depths. In contrast to the similar depths of cure of all formulations obtained by the standard (mean 2.7 ± 0.25 mm), the FTIR-ATR-based method confirmed that UP, UT and BP had ≥ 50% conversion at 4 mm depth, whereas BT and Z250 had conversion below 50%. This facile technique therefore offers greater insight into the inter-related topics of monomer conversion and depth of cure than the current standard protocol.

The convenience and accuracy of the FTIR-ATR technique may be further exploited in order to overcome the high margin of error associated with the standard protocol for assessing shrinkage[18]. The standard protocol is based on measuring composite volume change and is highly sensitive to entrapment of air bubbles and instability of balance readings. While the standard protocol failed to elucidate any significant differences in the shrinkage of the composites, conversion-based calculations indicated that UDMA-containing composites have slightly higher conversion than Bis-GMA-based composites, as expected based on their chemistry. Equation 1 (p. 53) is, however, based on the assumption that one mole of C=C bonds typically undergoes polymerisation shrinkage of ~22.5 cm^3 [99]. It is important to note that this is a generalised value for methacrylates based on Bis-GMA-based monomers. It is unable to take into account possible differences arising from more complex physical properties, such as the flexibility or steric hindrance of different monomers. It also does not take into consideration that water may less readily penetrate some composites than others, based on pore size and the hydrophobicity of the materials. Despite this, the conversion calculation provides more reliable results without conflicting with those obtained using the standard protocol.

Despite their high conversion of 62–67.5% and slightly higher double bond concentration than composites containing Bis-GMA, those containing UDMA had acceptable shrinkage of 2.55–2.86 vol%, regardless of which measurement technique was employed. A possible explanation for this is that the shrinkage of dimethacrylates upon polymerisation may be more strongly affected by the first methacrylate group

bonding than by the second. Additionally, despite its higher conversion, PPGDMA had slightly lower shrinkage than TEGDMA, on average. This is attributed to its much higher Mr and the subsequent lower double bond concentration that arises from this.

A simplified version of BS EN ISO:2009 was used to estimate the water sorption of composites from their mass increase after storage in dH_2O for one week. This enabled use of less material than the standard recommends. Bis-GMA induced slightly lower mass increase than UDMA, which is likely due to the hydrophobicity of its aromatic groups. Similarly, propylene glycol groups on PPGDMA are more hydrophobic than ethylene glycol groups on TEGDMA. This, combined with TEGDMA's lower cross-linking density, resulted in greater water sorption in TEGDMA-containing composites.

The correlation between the conversion and BFS of experimental formulations was likely due to the improved entrapment of filler particles, which is likely to have occurred in composites with greater cross-linking. Furthermore, the interaction between the monomers and the short, aliphatic silane (3-(trimethoxysilyl)propyl methacrylate) coating on the fillers, which has relatively low hydrophobicity, is stronger with the aliphatic groups of UDMA, PPGDMA and TEGDMA than the aromatic groups of Bis-GMA. Z250 's higher BFS is likely due to differences in the fillers used, the composition of the liquid phase and the filler to liquid ratio, and no conclusions can be made without knowing its exact formulation. In comparison to previous studies, which have often explored *wt* ratios[28], a fixed *molar* ratio of bulk to diluent monomer was used, in order to enable direct comparison of conversion and cytocompatibility. The relatively low proportion of diluent monomer used in this study likely explains why Z250 had significantly higher BFS than BP and BT.

Although the densities of the monomers do not vary significantly, variations in M_r and viscosity result in noticeable differences in composite handling properties, as discussed in Chapter 2.3.1.1. This means that, when comparing composites with the same *molar* ratio of bulk to diluent monomer as opposed to *wt* ratio, handling properties were similar.

Despite the low solubility of most of the liquid phase components analysed in this study, it was possible to dissolve them in cell culture medium at up to 10 mM (CQ and Bis-GMA) or 100 mM (DMAEMA, PPGDMA, TEGDMA and UDMA). Most components remained fully dispersed in the medium, although CQ and TEGDMA did settle at high concentrations. In order to ensure complete dispersal of the components, test solutions were thoroughly mixed by vortexing immediately prior to adding them to well plates.

Due to the limitations of cytocompatibility assays and variability between the different enzymatic substrates available[115], the present study utilised three different assays (resazurin, WST-8 and MTS) in order to assess the cytocompatibility of composite liquid phase components and composite extracts. The reduction of all these three dyes is carried out by NADH and NADPH dehydrogenase enzymes in metabolically active cells, though the location of this activity varies, occurring within the mitochondria in the case of resazurin, in the cystoplasm in the case of MTS and extracellularly in the case of WST-8. It is important to take into consideration that the values obtained by these assays do not report the true cell density, as may be determined by cell counting via staining and imaging techniques such as a live/dead assay. They are, instead, an estimate of cell density based on the metabolic activity of the corresponding enzyme, extrapolated from a standard curve from various cell concentrations. The nature of such assays means that they rely on the assumption that relative metabolic activity remains constant with time after cell seeding. It can be seen in Figure 5.3, however, that different assays reported different cell densities over time, even in the controls, despite having the same initial seeding density. For this reason, the cytocompatibility of the composite components and extracts was reported in terms of metabolic activity as a percentage of the corresponding control, for each assay and time-point. The use of serum-free medium did not noticeably limit the proliferative potential of HGF over the short duration of these assays (up to 48 h), since apparent cell density values fell within the expected range for HGF based on typical culturing conditions with FBS.

CQ was shown to have good cytocompatibility. Given that it is present at low concentrations in the material, is unlikely to leach in large enough quantities to cause a toxic effect. DMAEMA was demonstrated to be highly cytotoxic. Unlike some other initiators such as DMPT, however, DMAEMAs methacrylate group enables it to become incorporated within the polymer, likely minimising its release.

A wealth of studies have shown that dental monomers such as Bis-GMA, UDMA and TEGDMA cause cytotoxic, genotoxic and apoptotic responses in a variety of cell types[33-37]. Presence of excessive reactive oxygen species have previously been shown to arrest cell cycle at different phases in different fibroblast types upon exposure to these monomers[35,118-122]. As well as delaying cell cycle progression, these monomers also have an impact on proliferation and cell survival, as well as causing inflammation and/or necrosis. TEGDMA has also been shown to act as a vasorelaxant[38-42] and to cause apoptosis and necrosis, which was associated with a reduction in cdc2, cyclin B1 and cdc25C expression and increase in p21 expression[43] and upregulation of

caspases[44]. Bis-GMA induces inflammation and necrosis by upregulating expression of prostaglandin, tumour necrosis factor-a and various cell surface antigens[123-125]. As discussed in 2.3.1.1, although Bis-GMA is typically synthesised via BPA-free routes and is widely used in composites, there are concerns over its ability to gradually degrade via hydrolysis to form BPA[32]. Furthermore, toxic monomers can be released by enzymatic degradation, as well as mechanical abrasion[37].

It was hypothesised that by increasing the length of the diluent monomer by using PPGDMA instead of TEGDMA, it would be possible to alleviate oxidative stress to some degree[126]. In the present short-term study, HGF metabolised resazurin significantly more efficiently after exposure to PPGDMA, either in solution or via composite extracts, than after exposure to TEGDMA or UDMA. HGF failed, however, to efficiently metabolise WST-8 and MTS after exposure to any of these components, even at low concentrations.

Bis-GMA had a lesser effect on metabolic activity of HGF than the other monomers, up to a concentration of at least 0.1 mM. Its TC_{50} value (the concentration at which 50% of cells survived) was in the range of ~0.5–1 mM, consistent with previous findings in HGF and HaCaT (keratinocyte cell line)[127] and an order of magnitude greater than observed in some other cell lines, such as L929[128,129]. This highlights the potential for variability, which can arise between different cell types and methods of material preparation, culture duration, seeding density and other factors. Although neither the longer-term cytotoxic effects nor the genotoxic effects of Bis-GMA were investigated here, previous studies have demonstrated that the use of Bis-GMA in dental materials is cause for concern. The use of alternative monomers with excellent mechanical properties and relatively high viscosity, but with lower viscosity and improved handling properties compared to Bis-GMA would therefore be ideal. The TC_{50} of UDMA and TEGDMA could not be directly compared to previous findings, since even at the lowest concentration tested, fewer than 50% of cells were viable after 48 h. The TC_{50} values of UDMA (≤ 0.01 mM) and TEGDMA (< 0.01 mM) were notably lower, however, than previously observed, at ~0.06–4 mM[119,127,129] and ~1–4.1 mM[127,129], respectively.

UDMA is also widely used in dental composites, typically in combination with Bis-GMA and/or similar high viscosity monomers. The use of UDMA has been shown to result in significantly higher conversion, more complete cross-linking and lower leaching of uncured monomer than Bis-GMA[112], as well as higher flexural strength and hardness[130]. It has therefore been suggested that UDMA may be used as the sole bulk monomer in orthodontic adhesives[28] and bone cements[131]. In the present Chapter, the

use of UDMA as the sole bulk monomer in a dental composite was investigated. It was hypothesised that its higher conversion would result in improved cytocompatibility due to reduced leaching of un-cross-linked monomers and initiators, such as the highly toxic DMAEMA. Despite UDMA being more cytotoxic than Bis-GMA to HGF in solution, the results of the 48 h resazurin and WST-8 assays suggest that 1 day extracts of UDMA-containing composites were more cytocompatible than those of Bis-GMA-containing composites. After a subsequent recovery period, however, all three assays showed similar metabolic activity after exposure to all materials, suggesting that UDMA is similarly cytotoxic but has a delayed action. These findings may result from a combination of the greater presence of Bis-GMA and diluent monomers in the extracts, due to Bis-GMA's poorer conversion, and UDMA's higher cytotoxicity.

Although water-soluble assays offer a convenient insight into the cytocompatibility of biomaterials, they have the drawback of being unable to differentiate between cells that are actively proliferating and cells that are in a quiescent state[132]. This is reflected in the over-estimation of cell density by the MTS assay in the present study. Overestimation and/or underestimation can also result from interference caused by the compound being analysed. Although resazurin[133], WST-8[134] and MTS[135] have all been previously reported to overestimate and/or underestimate cell number, MTS appears to be particularly affected. In the present Chapter, the MTS assay's significant underestimation of cell density in the control was most likely the cause of its overestimation of metabolic activity per cell.

Further complications arise from the fact that different studies utilise varying cell types. Given their differing phenotypes and susceptibility to cytotoxic and genotoxic effects[136], direct comparisons cannot be made. In addition, short-term cytocompatibility studies do not take into account possible genotoxic and mutagenic effects. Although it was beyond the scope of this study, future research into the longer-term cytotoxic and genotoxic effects of a wide range of commonly used composite components would be highly beneficial in elucidating the causes of the complex trends observed in this and other studies. Although an extensive range of such studies has been performed, the different parameters investigated between different research groups (material concentration, material preparation, extraction technique, cell type, assay, genes analysed and duration of study) make it difficult to directly compare results and definitively interpret them. Better understanding of the fundamental effects of each individual component is required in order to improve the biocompatibility of novel dental composites. A more systematic and wide-ranging approach would be beneficial in

establishing a library which comprehensively documents the effects of each component.

More comprehensive studies are therefore required to elucidate the longer-term effects of monomers and composite extracts on a wide range of markers of biocompatibility in a variety of relevant cell types. This includes analysis of expression of cell surface markers and genes implicated in oxidative stress and apoptotic response, in parallel with multiple metabolic activity assays, live/dead analysis, quantification of total DNA, e.g. via CyQUANT cell proliferation assay, and the study of changes to cell morphology via imaging techniques. This type of broad library approach would enable more targeted design of novel composites with improved biocompatibility for improved treatment of dental caries.

6 EFFECTS OF PHOTO- AND CO-INITIATORS ON MATERIAL PROPERTIES AND CYTOCOMPATIBILITY

6.1 Introduction to Chapter 6

As discussed in Chapter 2.3.1, the conversion, depth of cure and mechanical properties of composites are affected by the photoinitiators and co-initiators used, as well as their concentrations. In general, these properties improve as concentrations of these components are increased, up to a certain threshold, after which they either plateau or decline. There are, however, associated detrimental effects of high photoinitiators and co-initiator concentrations, such as poor cytocompatibility resulting from subsequent leaching of these small, toxic compounds, or discolouration and decline in aesthetics of the composite. The present chapter therefore focuses on optimising photo- and co-initiator compounds and concentrations for use in Chapter 7.

Furthermore, as mentioned in Chapter 2.3.1.3, PPD is able to act by both type I and type II photoinitiation mechanisms and has been shown to act synergistically when combined with CQ[51]. In Chapter 6.3.1, the conversion, depth of cure and mechanical properties of composites containing either CQ, PPD or a combination of both at a 1:1 molar ratio (total concentrations 20, 40 or 60 mM) are determined, with 60 mM DMAEMA as the co-initiator.

Since the conversion and cytocompatibility of composites is affected by the chemistry of the co-initiator used, these properties are assessed in composites containing either DMAEMA, DMPT, EDAB or Na-NTG-GMA at 60 mM in Chapter 6.3.2.

6.2 Formulations

Composites were prepared using the same filler phase and PLR as that in Chapter 5. This was combined with twelve dimethacrylate-based liquid phases prepared according to Chapter 3.1.1.1. These consisted of UDMA and PPGDMA at a molar ratio of 3.5:1, as in Chapter 5, with 100 ppm BHT and varying photo- and co-initiator concentrations. In the first set of studies, photoinitiator was varied. Varying CQ concentrations (20, 40 and 60 mM) were incorporated into three composites, with DMAEMA remaining constant at 60 mM. Similarly, PPD was incorporated into three composites alongside DMAEMA at the same concentrations. In addition, CQ and PPD were incorporated together into three composites, each at 10, 20 and 30 mM (total 20, 40 and 60 mM photoinitiator in each formulation). In the second set of studies, the co-initiator used

was varied. CQ was incorporated into three composites at 40 mM, alongside either DMPT, EDAB or Na-NTG-GMA at 60 mM (with comparison to the previously described formulation containing 40 mM CQ and 60 mM DMAEMA). Pastes were prepared according to Chapter 3.1.1.2 and disc specimens produced according to Chapter 3.1.1.3 were used for studies, except where otherwise indicated in specific method subsections. Formulations are summarised in Table 5.1.

Table 6.1. Chapter 6 experimental formulations.

Variable liquid phase parameters		
Photoinitiator(s)	**Photoinitiator concentration**	**Co-initiator (60 mM)**
CQ	20 mM 40 mM 60 mM	DMAEMA
CQ + PPD	10 mM each 20 mM each 30 mM each	DMAEMA
PPD	20 mM 40 mM 60 mM	DMAEMA
CQ	40 mM	DMPT EDAB Na-NTG-GMA
Fixed liquid phase parameters		
UDMA:PPGDMA molar ratio		3.5:1
BHT		100 ppm
Fixed filler phase and PLR parameters		
$GP_{0.7}$		30 wt%
GP_7		60 wt%
OX-50		10 wt%
PLR		40 vol% liquid

6.3 Results

6.3.1 Varying photoinitiator

6.3.1.1 Polymerisation properties

6.3.1.1.1 Conversion and depth of cure

The mean conversion at 1 mm depth of the nine formulations with varying photoinitiator type and concentration was 70.9 ± 3.1% (Figure 6.1a). In general, increasing total photoinitiator concentration from 20 to 60 mM appeared to result in very slightly increased conversion. These differences were statistically significant ($p \geq 0.05$) only between the formulations containing 10 mM CQ + 10 mM PPD and 30 mM CQ + 30 mM PPD ($p < 0.05$). The mean conversion values of all composites containing 40 or 60 mM photoinitiator were significantly higher than the mean values of those containing 20 mM, regardless of the photoinitiator used. Furthermore, the mean conversion values of

composites containing CQ or a combination of CQ + PPD were greater than that of composites containing only PPD.

The depths of cure of composites containing varying photoinitiator type and concentration are illustrated in Figure 6.1b. Composites containing CQ alone had a mean depth of cure of 2.72 ± 0.04 mm, regardless of CQ concentration. Composites containing 10 mM CQ + 10 mM PPD or 20 mM CQ + 20 mM PPD also had a mean depth of cure of 2.74 ± 0.04 mm, but this fell to a significantly lower 2.45 ± 0.05 mm in composites containing 30 mM CQ + 30 mM PPD ($p < 0.005$). Depth of cure of the formulation containing 20 mM PPD was poor, at 2.22 mm, but this rose to 2.58 and 2.67 mm as concentration was increased to 40 and 60 mM, respectively.

6.3.1.2 Mechanical properties

The mechanical properties of composites with different photoinitiator types and concentrations are shown in Figure 6.2. The mean BFS of all formulations was 163 ± 20 MPa. Though the BFS of composites containing only PPD appeared to increase slightly with increasing PPD concentration, this was not significant. There were no significant differences between BFS values of any formulation. In contrast, *E* increased in parallel with photoinitiator concentration, regardless of whether CQ, PPD or a combination was used, with mean values of each concentration having p values ≤ 0.0018. The mean *E* value of PPD-containing composites was significantly higher than the mean of CQ ($p = 1.09 \times 10\text{-}6$) or a combination ($7.1 \times 10\text{-}6$).

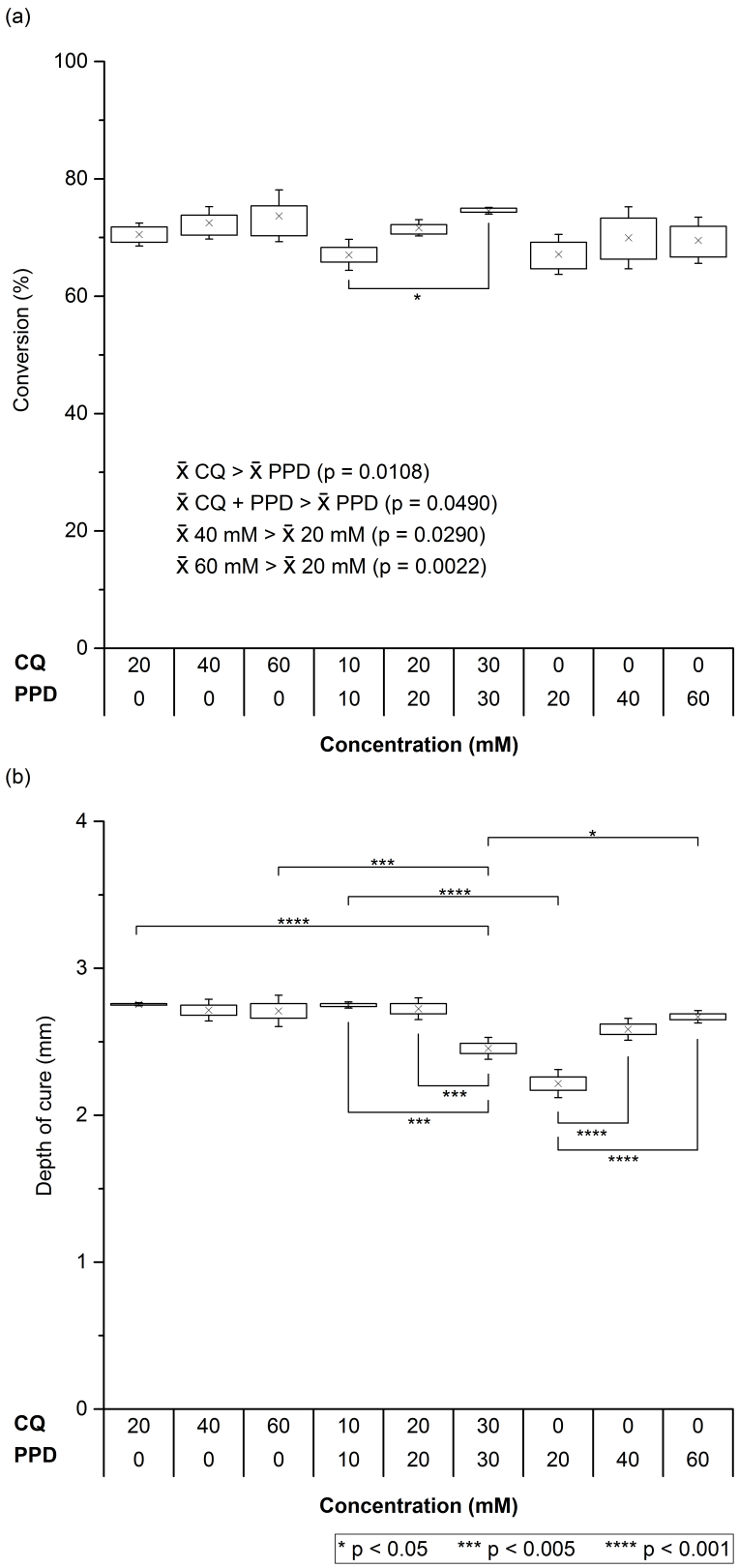

Figure 6.1. Polymerisation properties of composites containing varying photoinitiators. (a) Conversion and (b) depth of cure of composites containing varying photoinitiator type (CQ, PPD or both) and concentration (20, 40 or 60 mM total) at 1 mm depth. Crosses represent mean, boxes represent 25–75 percentiles, error bars represent SD.

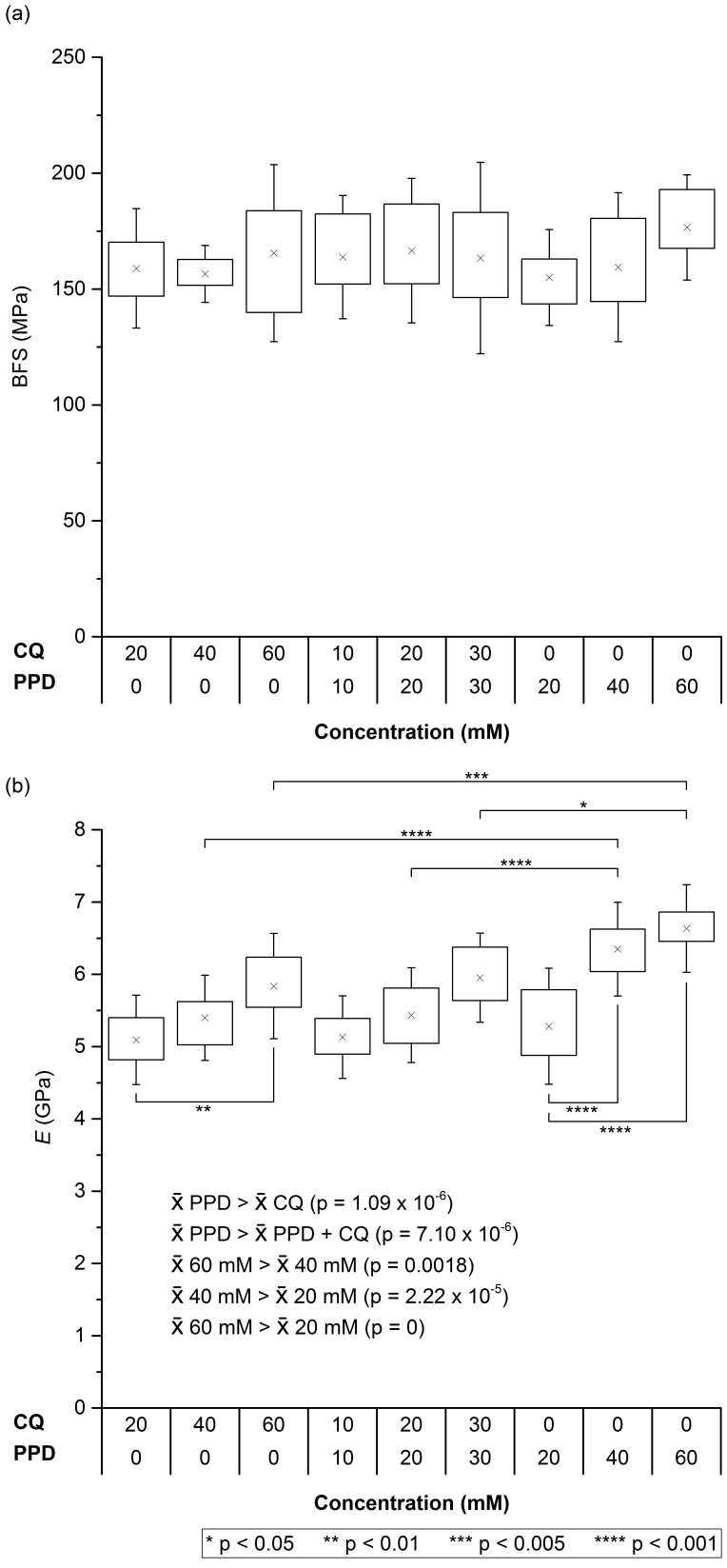

Figure 6.2. Mechanical properties of composites containing varying photoinitiators.
(a) BFS and (b) *E* of dry composites containing varying photoinitiator type (CQ, PPD or both) and concentration (20, 40 or 60 mM total). Crosses represent mean, boxes represent 25–75 percentiles, error bars represent SD.

6.3.2 Varying co-initiator

6.3.2.1 Conversion

There was no statistical difference between the conversion of experimental composites containing varying co-initiators at a fixed concentration of 60 mM, regardless of which photoinitiator or combination was used (Figure 6.3). Their mean value was 68.6 ± 3.82%, though Na-NTG-GMA had higher SD than DMAEMA, DMPT and EDAB. All experimental formulations had significantly higher conversion than Z250 ($p < 0.005$).

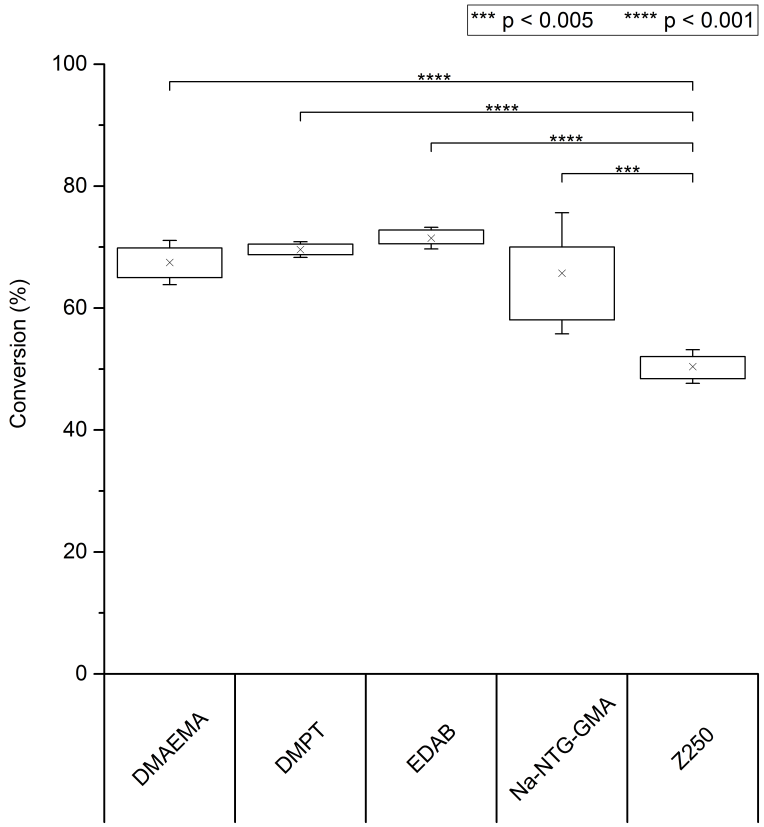

Figure 6.3. Polymerisation properties of composites containing varying co-initiators. Conversion of composites containing varying co-initiator type at 1 mm depth (DMAEMA, DMPT, EDAB or Na-NTG-GMA at 60 mM). Crosses represent mean, boxes represent 25–75 percentiles, error bars represent SD.

6.3.2.2 Cytocompatibility

The relative cell density of HGF following 48 h culture in extracts of composites containing various co-initiators is presented in Figure 6.4. WST-8 activity was significantly higher in all composite extracts compared to the extract- and serum-free DMEM control and was significantly higher in Na-NTG-GMA-containing composites compared to those containing DMAEMA, DMPT or EDAB.

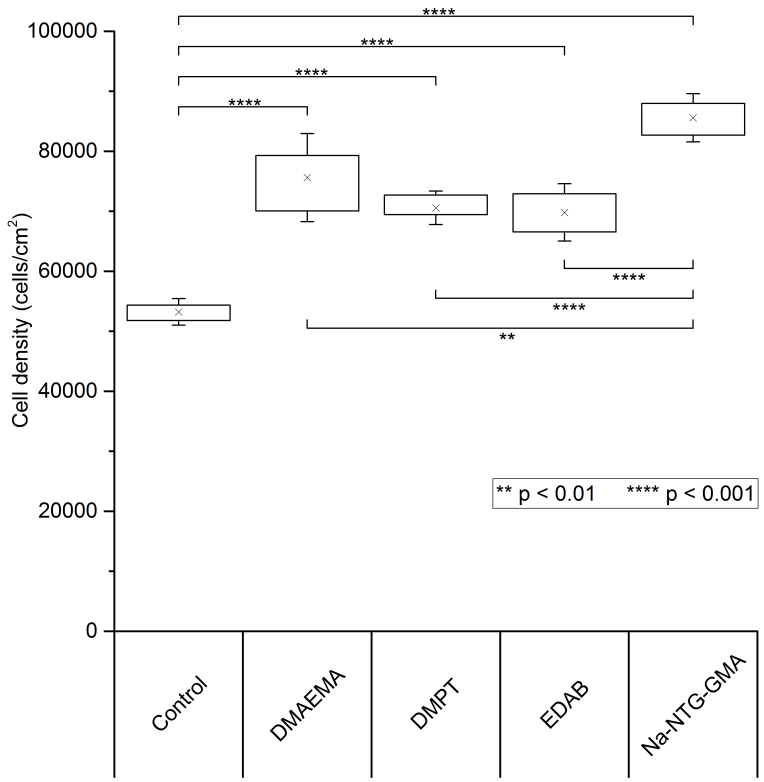

Figure 6.4. Cytocompatibility of composites containing varying co-initiators.
Cytocompatibility of extracts of composites containing varying co-initiator type at 1 mm depth (DMAEMA, DMPT, EDAB or Na-NTG-GMA at 60 mM), assessed using WST-8 assay. Crosses represent mean, boxes represent 25–75 percentiles, error bars represent SD.

6.4 Discussion

The physical properties of composites are directly determined by the efficiency of the polymerisation reaction, which in turn is determined by the type and concentration of photoinitiator and co-initiator. In order to optimise these properties and to improve understanding of the effect preliminarily investigated in the pilot studies (Chapter 4), photoinitiators CQ and PPD and co-initiators DMAEMA, DMPT, EDAB and Na-NTG-GMA were investigated in various combinations based on molar concentrations, as opposed to the constant wt% previously investigated.

It was hypothesised that increasing photoinitiator concentration would increase conversion up to a certain threshold, before plateauing[137]. A previous indication that CQ and PPD may work synergistically via their different photopolymerisation modes to improve depth of cure when combined together was also investigated[51]. As expected, a general increase in conversion was associated with an increase in photoinitiator concentration, though this trend was not statistically significant in most cases. The mean conversion value of all composites containing a total of 20 mM photoinitiator, however, was significantly lower than that of composites containing 40 or 60 mM. Furthermore, composites containing CQ with or without PPD had higher mean conversion than those containing only PPD. Depth of cure was consistently high in composites containing CQ at any concentration, whereas composites containing PPD with or without CQ had either similar or significantly lower depth of cure.

BFS was unaffected by photoinitiator type and concentration. In contrast, the mean *E* was significantly higher in composites containing PPD only than in those containing CQ or both. Since composites with high conversion and depth of cure are favourable and those with high *E* are at greater risk of brittle fracture, 40 mM CQ was deemed the most optimal photoinitiator type and concentration for further studies.

It was hypothesised that the cytocompatibility of extracts of composites would be affected by the co-initiator used, based on the size of the co-initiator and its ability to bind to the polymer, but that the conversion would not vary significantly when the same molar was used. As expected, there was no statistical difference in conversion of composites containing varying co-initiator at the same molar concentration, i.e. the same number of co-initiator molecules per specimen, regardless of the size of the molecule. WST-8 activity was elevated in all composite extracts compared to the control. Rather than improving cytocompatibility, it is more likely that this indicates a response to the co-initiator, though this study is inconclusive regarding whether this is

a positive or negative response. Future research should focus on better determining the cytocompatibility of composites containing different co-initiator types and concentrations. This should be done using multiple cytocompatibility assays, for the reasons discussed in Chapter 5, as well as studies on genotoxicity.

In theory, Na-NTG-GMA should be the most cytocompatible of the co-initiators tested, since it has the largest M_r and contains a methacrylate group, through which it can easily become incorporated into the polymer. It also has the potential to improve bonding to tooth mineral via Ca. Due to the inconclusiveness of this study, however, DMAEMA, which also contains a methacrylate group, was selected for continued use in Chapter 7, since it is more widely used as a co-initiator and the WST-8 activity of cells exposed to DMAEMA-containing composite extracts closer matched that of the control.

7 EFFECTS OF CALCIUM PHOSPHATES AND ANTIMICROBIAL AGENTS ON MINERAL FORMATION AND MATERIAL PROPERTIES

Note: Chapter 7 is the subject of the following publication and patent application (Refs. [104,113]):

Walters NJ, Liaqat S, Palmer G, Panpisut P, Mordan NJ, Ashley PF, Young AM. Rapid hydroxyapatite precipitation on dental composite surfaces. Under preparation for submission to *J Dent Res* 2016.

UCL Business. GB Patent Application No. 1313898.7. Aug 2013.

7.1 Introduction

Although favoured by clinicians for their excellent aesthetics and strength, the longevity of composites is affected by their ~2–6 vol% polymerisation shrinkage[138]. This is only partially compensated by ~1 vol% water sorption. Shrinkage exerts pressure on the remaining tissue, which can cause debonding of the restoration. This may be followed by the development of interfacial gaps between tooth and restoration which are susceptible to microbial microleakage. Acidic microbial waste products further expedite the demineralisation of the tooth. These factors can ultimately result in recurrent caries and failure of the restoration[139].

The aim of the present Chapter was to produce remineralising, antimicrobial composites to overcome these issues. The objectives in such materials are for CaPs to be released and precipitate between the tooth and restoration, minimising microleakage and enhancing the restoration interface, combined with antimicrobial protection. CaP release encourages greater water sorption, which may be regulated to create a tighter interface[68]. Use of hydrophilic components should then further enhance this interface and may even improve initial bonding strength.

Mobile antimicrobials such as CHXA[19,68] and silver nanoparticles[81] and immobile quaternary ammonium monomers[89] have been previously combined with CaPs in dental materials. In composites containing MCP, TCP and CHXA, TCP enhanced strength by preventing bulk loss of highly soluble MCP and enhancing CHXA release[19].

The present Chapter assessed whether εPL aids CaP release and HA precipitation and aimed to determine the individual and combined effects of MCP, TCP and εPL on composites stored in SBF, AS and dH_2O. SBF was used to simulate super-saturated

dentinal fluid, which is secreted by odontoblasts to remineralise dentinal tubules in response to caries[140]. The bio-inspired dental composites under development aim to mimic the natural remineralisation process that occurs in the dentinal tubulues and protect against microleakage in a similar manner at the tissue-restoration interface. Composites were stored in AS in order to prove that mineral formation would not occur on the aesthetic, exposed surface.

A liquid phase based on that developed in Chapter 5[101] was combined with MCP and/or TCP and/or εPL. The low viscosity and high hydrophilicity of the resulting composites were hypothesised to improve dentine bonding. It was also hypothesised that, due to its high solubility, εPL would expedite CaP diffusion and precipitation, enhancing HA nucleation, and that highly soluble MCP may be sufficient to induce mineral formation without requiring poorly soluble TCP, which detrimentally affects conversion and strength[68]. The combined effects of MCP and εPL could therefore prevent debonding, microleakage and restoration failure.

Materials were characterised in terms of conversion and initial τ to human dentine. Mass and volume change in SBF and dH_2O were quantified by gravimetric analysis over one week, the time period during which precipitates visibly formed, and composite surfaces analysed after one week using SEM, EDX and Raman spectroscopy. Since strength of remineralising composites typically declines upon immersion in liquid for up to one month due to component dissolution[68], BFS and modulus *E* were determined after 28 days storage in SBF or AS.

7.2 Formulations

Composites were prepared using a liquid phase with a fixed formulation, prepared according to Chapter 3.1.1.1. This was based on liquid phase UP (Chapter 5, Ref. [101]), except that the proportion of UDMA:PPGDMA was altered from 3.5:1 molar ratio (75.55:24.45 by weight) to 75:25 by weight. The PLR was also altered to 80:20 by weight. Six composites with varying filler phase formulations were analysed. The filler phases consisted of: OX-50 and $GP_{0.7}$ fixed at 10 and 30 wt%, respectively, along with 0 or 20 wt% MCPM, 0 or 20 wt% β-TCP and 0 or 10 wt% εPL. The remainder of each filler (10–30 wt%) phase consisted of GP_7. Pastes were prepared according to Chapter 3.1.1.2 and disc specimens produced according to Chapter 3.1.1.3 were used for studies, except where otherwise indicated in specific method subsections. Composites were designated abbreviations according to the quantity of reactive fillers and are summarised in Table 7.1. Note that 10 or 20 wt% in filler phase corresponds to 8 or 16

wt% in the composite as a whole, as reflected in the abbreviations. This ratio of filler particle sizes was selected for its optimal handling properties and wettability. Filtek Z250 was used for comparison.

Table 7.1. Chapter 7 experimental formulations.

Variable filler phase parameters			
Formulation	**Mass of reactive filler in composite (wt%)**		
	MCP	**TCP**	**εPL**
$M_0T_0\varepsilon_0$	-	-	-
$M_{16}T_{16}\varepsilon_0$	16	16	-
$M_0T_0\varepsilon_8$	-	-	8
$M_0T_{16}\varepsilon_8$	-	16	8
$M_{16}T_0\varepsilon_8$	16	-	8
$M_{16}T_{16}\varepsilon_8$	16	16	8
Fixed filler phase parameters			
$GP_{0.7}$	30 wt% of filler phase		
GP_7	20–60 wt% of filler phase		
OX-50	10 wt% of filler phase		
PLR	80:20 wt%		
Fixed liquid phase parameters			
UDMA:PPGDMA ratio	75:25 w/w		
CQ	40 mM		
DMAEMA	60 mM		
BHT	100 ppm		

7.3 Results

7.3.1 Conversion

All experimental composites had similar conversion (70.9 ± 1.6%) at 1 mm depth (Figure 7.1), ~40% higher than Z250 (50.4%). Conversion of $M_0T_{16}\varepsilon_8$ was lower than that of the other experimental formulations.

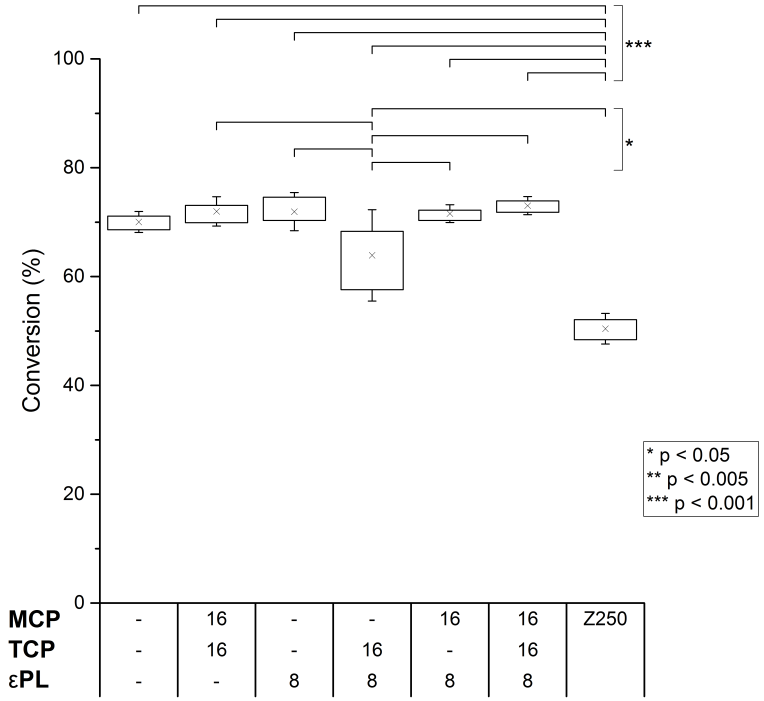

Figure 7.1. Conversion of composites containing varying levels of reactive fillers. Conversion of composites containing MCP (0 or 16 wt%), TCP (0 or 16 wt%) and εPL (0 or 8 wt%), with Filtek Z250 as a control. Crosses represent mean, boxes represent 25–75 percentiles, error bars represent SD.

7.3.2 Shear bond strength

τ (Figure 7.2) of composites to etched dentine without bonding agent followed complex trends. All reactive components caused decrease in τ, most significantly TCP. Increasing reactive filler content caused only slight reductions in handling properties, but TCP did not seem to affect this differently from MCP. Z250 had one of the poorest bonds (1.6 MPa), whereas experimental control $M_0T_0\varepsilon_0$ was strongest.

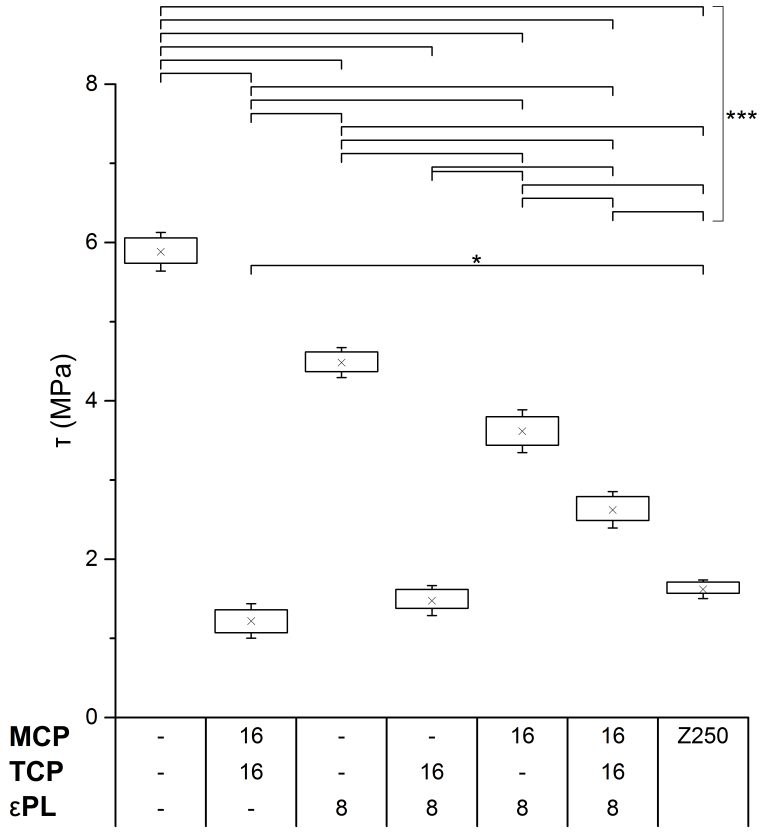

Figure 7.2. τ of composites applied directly to human dentine.

τ of composites containing MCP (0 or 16 wt%), TCP (0 or 16 wt%) and εPL (0 or 8 wt%), with Filtek Z250 as a control. Crosses represent mean, boxes represent 25–75 percentiles, error bars represent SD.

7.3.3 Mass and volume change

Mass and volume of all experimental formulations increased over one week in dH_2O or SBF (Figure 7.3a–d), with an initial burst increase within day one. Volume measurements had higher SD due to methodological limitations. $M_0T_0\varepsilon_0$ had low final mass or volume increase in both media (~0.5–0.8%). $M_{16}T_{16}\varepsilon_0$ increased 1.5 and 4.2 wt% and 2.9 and 5.9 vol% in dH_2O and SBF. $M_0T_0\varepsilon_8$ increased 3.6–3.9 wt% but only 1.3–1.7 vol%. $M_{16}T_0\varepsilon_8$ increased 4.2 wt% and 2.9 vol% in dH_2O, compared to 6.7 and 5.9 vol% in SBF. $M_0T_{16}\varepsilon_8$ increased ~4.8 wt% and 2.2 vol%, with little difference between media. $M_{16}T_{16}\varepsilon_8$ had the highest increases in both media, at 6.2–6.5% in dH_2O and 8.9–9.3% in SBF. Figure 7.3e–f notably shows that mass and volume increase of $M_{16}T_{16}\varepsilon_0$, $M_{16}T_0\varepsilon_8$ and $M_{16}T_{16}\varepsilon_8$ but not the other formulations was greater in SBF than dH_2O. These 'difference' values increased in a linear fashion until ~4 days ($M_{16}T_{16}\varepsilon_0$ and $M_{16}T_{16}\varepsilon_8$) or beyond ($M_{16}T_0\varepsilon_8$).

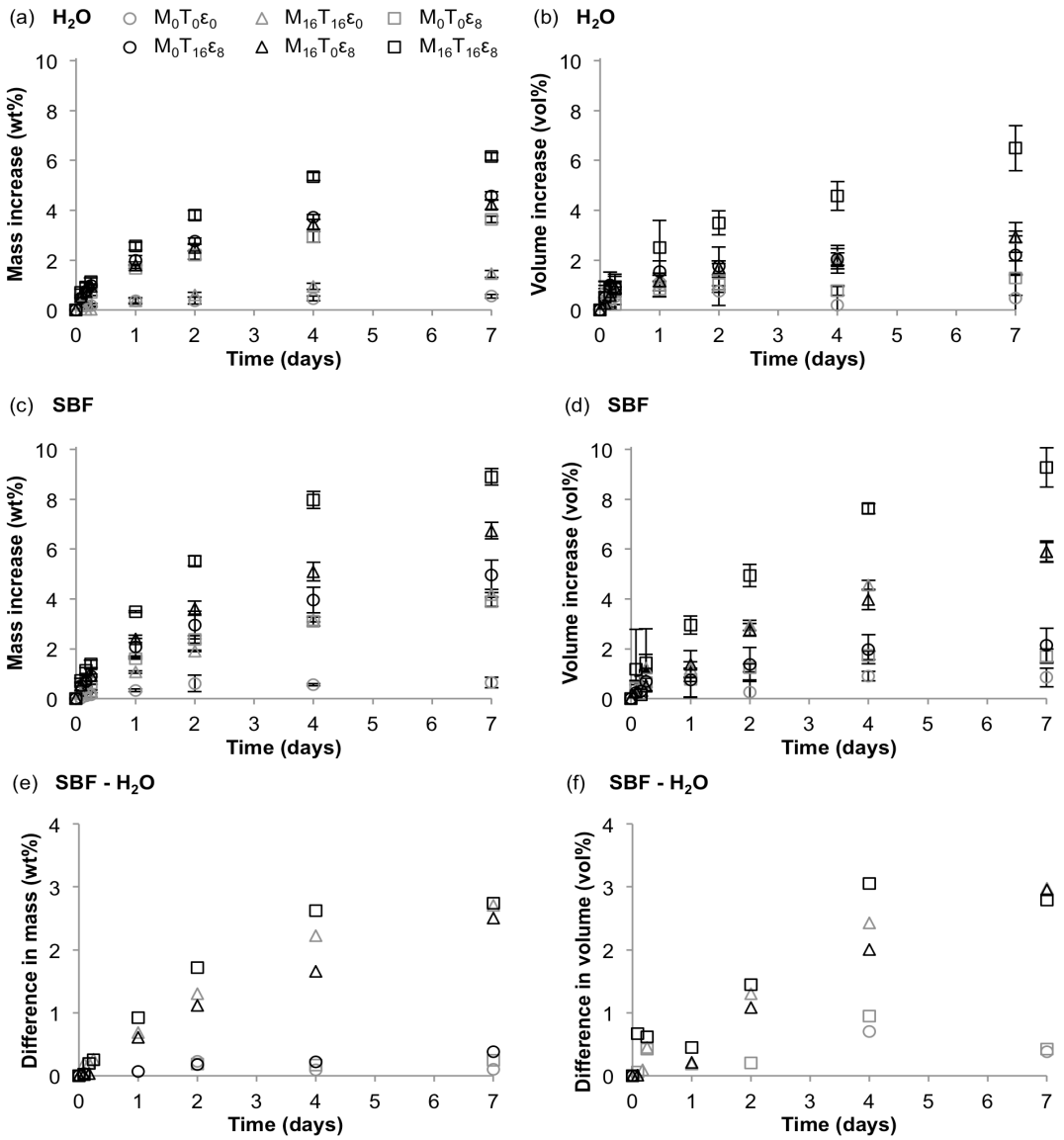

Figure 7.3. Mass and volume change of composites containing reactive fillers.

Increase in (a, c) mass (wt%) and (b, d) volume (vol%) of composites containing MCP (0 or 16 wt%), TCP (0 or 16 wt%) and εPL (0 or 8 wt%) over 7 days storage in (a, b) dH_2O or (c, d) SBF. Errors bars (a–d) represent SD.

7.3.4 SEM

Figure 7.4 shows composite surfaces imaged by SEM after one week in SBF. No precipitates were observed on $M_0T_0\varepsilon_0$ (a–b) or $M_0T_0\varepsilon_8$ (h). Presence of εPL in $M_0T_0\varepsilon_8$ caused greater pitting. Precipitates were observed on $M_0T_{16}\varepsilon_8$ (c–d), but visibility of pits indicated lack of a complete layer. In contrast, $M_{16}T_0\varepsilon_8$ (i–l) was fully covered in conjoined, ~3–8 μm diameter spherical crystals resembling HA (j–l), with a new layer forming on top. Cracks in the layer developed during specimen dehydration (j–k) and under exposure to electrons during microscopy (i). A similar, thinner layer formed on $M_{16}T_{16}\varepsilon_0$ (e–g). Cracks appeared to have propagated from pits (f). $M_{16}T_{16}\varepsilon_8$ (m–p) had significant CaP precipitate, though most crystals had smaller morphology, did not cover

the entire surface and pitting was more prominent. Around and particularly within pores, HA-like morphology was more apparent.

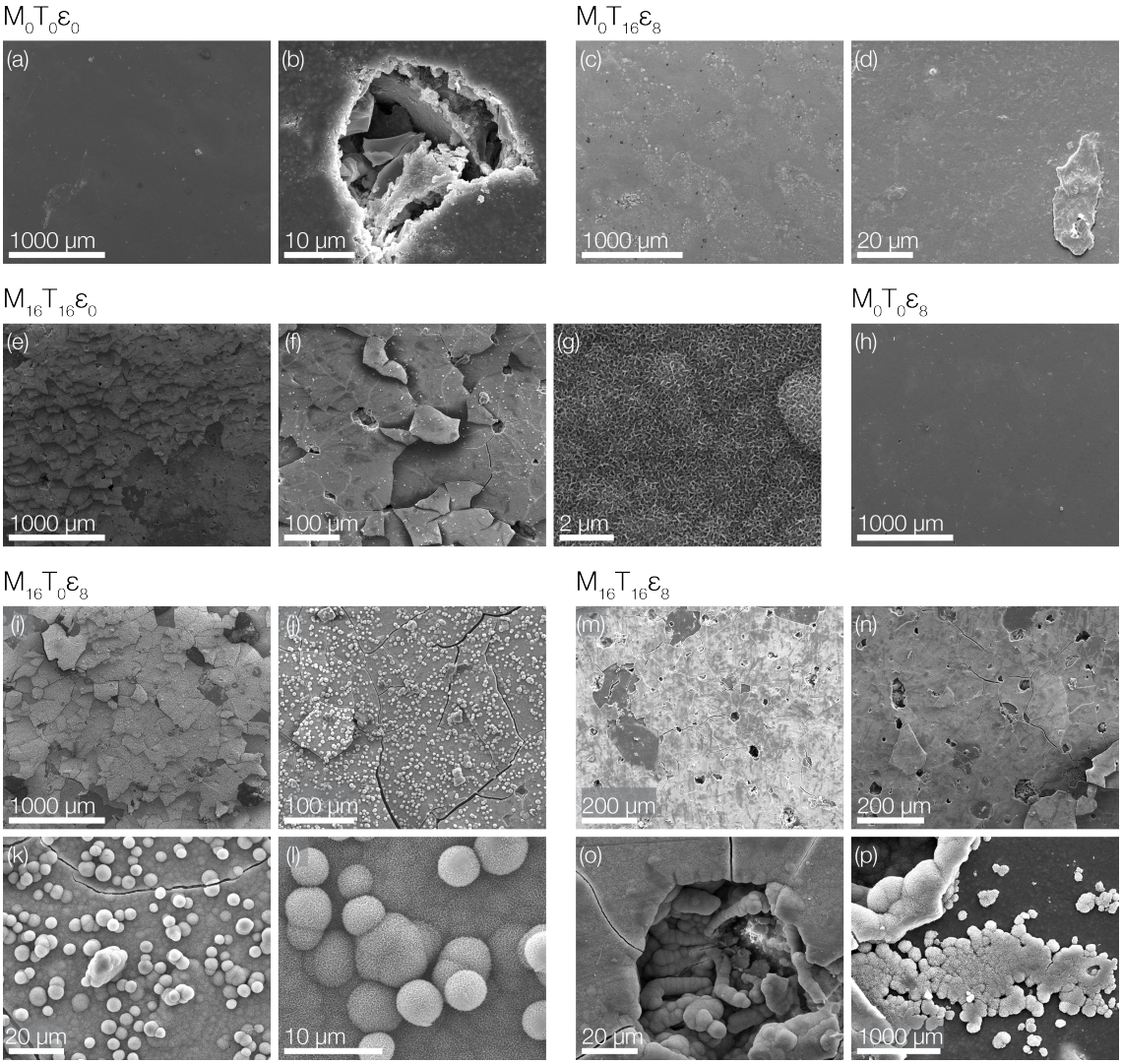

Figure 7.4. Scanning electron micrographs of composites after storage in SBF for 7 days. No CaP precipitation was observed on $M_0T_0\varepsilon_0$ (a, b) or $M_0T_0\varepsilon_8$ (h), though the latter had greater pitting. A thin layer of precipitate was observed on $M_0T_{16}\varepsilon_8$ (c, d), with pits still visible. $M_{16}T_0\varepsilon_8$ (i–l), by contrast, was covered with a continuous layer of merged spherulites of crystals which appeared likely to be HA, with a novel layer forming on top. $M_{16}T_{16}\varepsilon_8$ (m–p) had a similar HA-like layer, though it did not cover the entire surface and appeared thinner, due to the presence of pits. $M_{16}T_{16}\varepsilon_8$ (m–p) was only partially covered with a thin layer of precipitate similar to that observed on $M_0T_{16}\varepsilon_8$, with pores filled and surrounded by HA-like crystals.

7.3.5 EDX

Molar Si:Ca:P ratios obtained by EDX indicated presence of HA on $M_{16}T_{16}\varepsilon_0$ and $M_{16}T_{16}\varepsilon_8$ surfaces: $0.19^{\pm 0.04}$:$1.70^{\pm 0.04}$:$1^{\pm 0.05}$ ($M_{16}T_{16}\varepsilon_8$); $0.01^{\pm 0.01}$:$1.71^{\pm 0.01}$:$1^{\pm 0.02}$ ($M_{16}T_{16}\varepsilon_0$). EDX can detect some elements from several microns below the surface, but Si was almost completely absent from the surface of these specimens, indicating the presence of a relatively thick mineral layer. The Ca:P ratio very closely matches that expected for HA, based on the 5:3 (1.67) ratio of ions in HA ($Ca_5(PO_4)_3$).

7.3.6 Raman spectroscopy

Average Raman spectra of composite components, possible precipitates and composite surfaces after storage in SBF for one week are presented in Figure 7.5. All composites had distinct glass (1370, 1400 cm^{-1}) and polymer (874, 1448 cm^{-1}) peaks. These were, however, present to a lesser extent with CaP-containing composites than with $M_0T_0\varepsilon_0$ and $M_0T_0\varepsilon_8$. $M_{16}T_{16}\varepsilon_0$ and $M_{16}T_0\varepsilon_8$ had sharp HA peaks (959 cm^{-1}). $M_0T_{16}\varepsilon_8$ had a strong β-TCP double peak (947, 968 cm^{-1}). $M_{16}T_{16}\varepsilon_8$, by contrast, had a less prominent triple peak, indicating presence of both β-TCP and HA. Although εPL had a sharp (1442 cm^{-1}) and two very broad (~1010–1190, ~1235–1375 cm^{-1}) peaks, with composite surfaces these were below the detectable range.

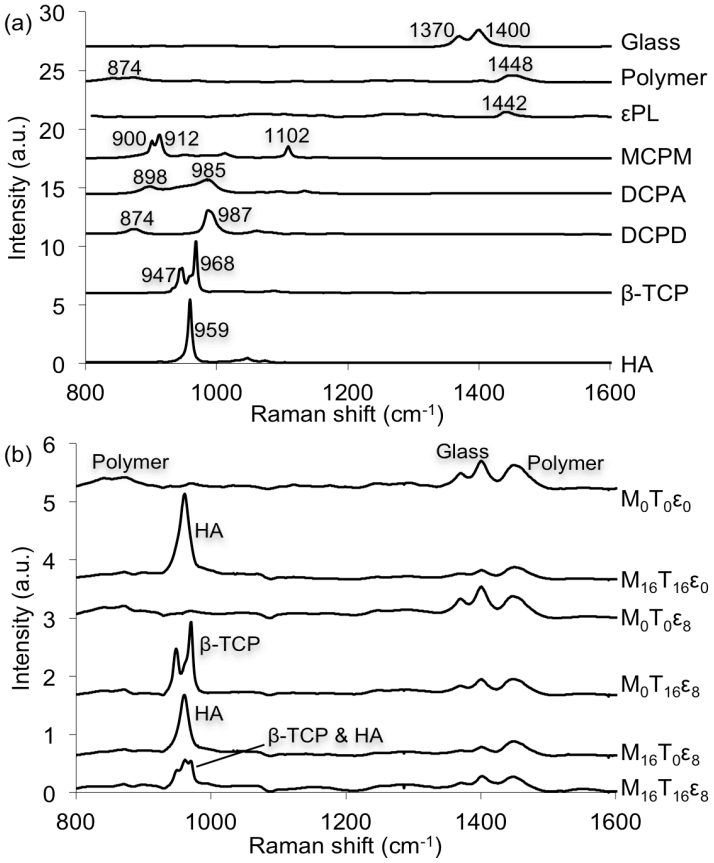

Figure 7.5. Raman spectra of composite components and surfaces after storage in SBF. (a) Pure composite components, possible CaP precipitates (glass, polymerised liquid phase, εPL, MCPM, β-TCP, DCPA, DCPD and HA) and (b) composite surfaces after 1 week's storage in SBF. The glass filler and polymerised liquid phase were visible in all spectra but gave significantly more prominent peaks in $M_0T_0\varepsilon_0$ than with CaP-containing composites. Sharp HA peaks were visible on the surfaces of $M_{16}T_{16}\varepsilon_0$ and $M_{16}T_0\varepsilon_8$, whereas $M_0T_{16}\varepsilon_8$ had β-TCP peaks. $M_{16}T_{16}\varepsilon_8$ had a mixture of HA and β-TCP on the surface.

7.3.7 Mechanical properties

BFS values were typically higher in AS than SBF, though this was not significant except in the case of $M_{16}T_{16}\varepsilon_0$ ($p < 0.001$). BFS (Figure 7.6a) was highest for Z250 (195, 183 MPa in AS, SBF), followed by experimental control $M_0T_0\varepsilon_0$ (173, 160 MPa). Addition of both CaPs without εPL caused no significant decline in BFS of $M_{16}T_{16}\varepsilon_0$ (167 MPa) compared to $M_0T_0\varepsilon_0$ in AS, but a significant decrease to 135 MPa in SBF. Three of the four composites containing εPL had significantly lower BFS than those lacking it after storage in both media. Values ranged from 67–86 MPa for $M_0T_0\varepsilon_8$, $M_0T_{16}\varepsilon_8$ and $M_{16}T_{16}\varepsilon_8$, with slightly higher values for those stored in AS than SBF. $M_{16}T_0\varepsilon_8$, however, had BFS of 134 and 102 kPa in AS and SBF, respectively. While these values were lower than those of εPL-free composites, they were significantly higher than those of composites containing both TCP and εPL.

The average *E* (Figure 7.6b) of experimental formulations stored in AS and SBF increased in a similar order to BFS and ranged from ~2.8 GPa for composites containing εPL alone or together with TCP ($M_0T_0\varepsilon_8$, $M_0T_{16}\varepsilon_8$, $M_{16}T_{16}\varepsilon_8$) to ~5.7 GPa for composites lacking εPL ($M_0T_0\varepsilon_0$, $M_{16}T_{16}\varepsilon_0$). In contrast to BFS, however, *E* values were slightly higher in SBF than AS, though this was not significant except in the cases of $M_{16}T_0\varepsilon_8$ ($p < 0.001$) and $M_{16}T_{16}\varepsilon_8$, ($p < 0.005$). Similarly to its BFS, the average *E* of $M_{16}T_0\varepsilon_8$ fell between these groups at 4.9 GPa, close to that of Z250 (5.9 GPa).

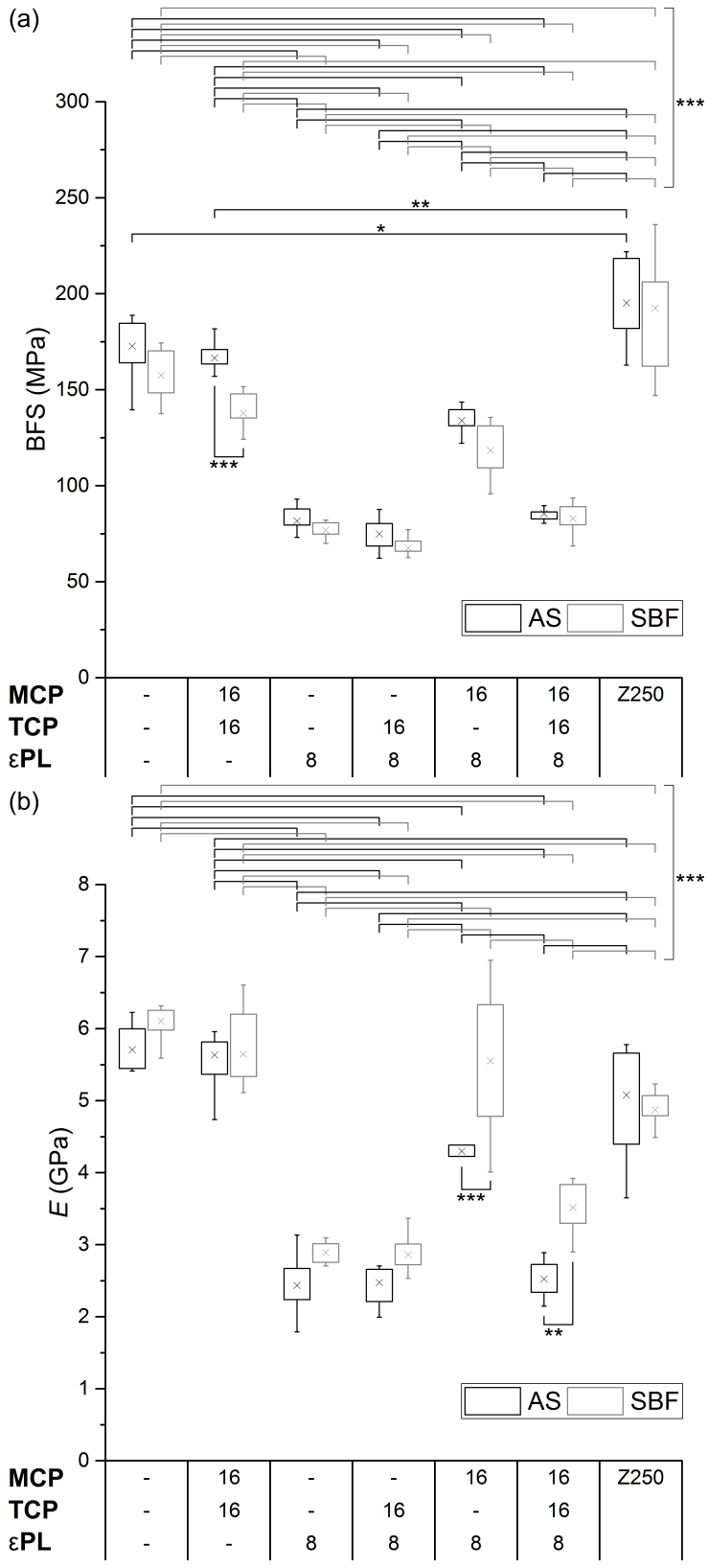

Figure 7.6. Mechanical properties of composites containing reactive fillers.

(a) BFS and (b) *E* of composites containing MCP (0 or 16 wt%), TCP (0 or 16 wt%) and εPL (0 or 8 wt%), with Filtek Z250 as a control after 28 days storage in AS (dark grey) or SBF (pale grey). Crosses represent mean, boxes represent 25–75 percentiles, error bars represent SD. $M_{16}T_{16}\varepsilon_0$ did not have normal distribution according to the Anderson-Darling test but had normal distribution according to others (Kolmogorov-Smirnov and Lilliefors tests).

7.4 Discussion

While previously developed composites containing MCP, TCP and chlorhexidine show great promise for more conservative treatment of dental caries[19], the individual effects of each CaP on strength, mass and volume change and HA precipitation had not yet been fully elucidated. Furthermore, use of broad spectrum antimicrobial εPL in dental composites has not been reported in the literature. It was hypothesised that εPL's high solubility would encourage water sorption, thereby expediting MCP release and HA precipitation, and enabling omission of TCP. Although its minimum inhibitory concentration is higher (1–20 μg/mL)[92,141] than that of chlorhexidine (0.6–4.9 μg/mL)[142], εPL release can exceed that of chlorhexidine by over an order of magnitude[113]. Furthermore, εPL is more biocompatible than CHXA and can safely be used at high doses.

Conversion at 1 mm depth was unaffected by presence of MCP and εPL, but was slightly reduced in $M_0T_{16}\varepsilon_8$. Although perceived handling properties of pastes did not vary noticeably, τ appeared to be associated with the hydrophilicity/hydrophobicity of the reactive fillers. MCP, εPL and particularly TCP each caused reduction in τ, though that of $M_{16}T_0\varepsilon_8$ was relatively high (2.2-fold compared to Z250).

Due to their high solubility, MCP and particularly εPL increased water sorption. This should aid CaP diffusion to the tissue-restoration interface. Greater mass than volume increase of $M_0T_0\varepsilon_8$ and $M_0T_{16}\varepsilon_8$ was due to water filling pores created upon εPL release. In contrast, greater volume than mass change of $M_{16}T_0\varepsilon_8$ and particularly $M_{16}T_{16}\varepsilon_0$ was caused by polymer expansion, caused by greater volumes of water filling voids left upon CaP release, combined with novel mineral formation, which resulted in thicker but less dense specimens. More rapid mass increases of $M_{16}T_0\varepsilon_8$ than $M_{16}T_{16}\varepsilon_0$ was due to greater solubility of εPL than TCP.

SEM, EDX and Raman demonstrated that storage of $M_{16}T_{16}\varepsilon_0$ and $M_{16}T_0\varepsilon_8$ in SBF caused rapid and substantial HA formation. Lack of MCP or TCP in Raman spectra implied that deposited layers were sufficiently thick to obscure detection of residual MCP or TCP. This was in contrast to $M_{16}T_{16}\varepsilon_8$, which appeared via SEM to only form a thin mineral layer, with HA-like morphology observed only around pores. This suggests that MCP is required for HA formation, that TCP is unable to transform to HA without MCP being present, due to its poor solubility, and that TCP and εPL each increase and expedite CaP release and subsequent precipitation. The lower degree of HA formation on $M_{16}T_{16}\varepsilon_8$ implied that too great a presence of soluble components (40 wt%) does not optimally foster HA transformation. One possible explanation is that too rapid release

of CaPs resulted in sudden over-saturation of SBF and precipitation within the solution, before nucleation on the composite could occur.

BFS of composites containing MCP with either TCP or εPL were weakened to a much lesser degree than those containing TCP and/or εPL without MCP, likely due to mineral formation within the composite. This may have been DCPA, as previously observed[68], or another CaP phase such as HA, and would require further investigation. HA-forming composites ($M_{16}T_{16}\varepsilon_0$, $M_{16}T_0\varepsilon_8$) had slightly higher BFS values after storage in AS than SBF, an artefact of the mechanical testing method. The added thickness of the specimens accounted for by newly formed mineral, which itself was likely porous and brittle, lead to artificial decreases in BFS values in SBF, due to the high sensitivity of the equation to specimen thickness (1 mm ± 10%). Composites containing MCP with εPL ($M_{16}T_0\varepsilon_8$, $M_{16}T_{16}\varepsilon_8$) had significantly higher *E* values after storage in SBF than AS, likely due to greater ion diffusion from highly saturated SBF into these formulations, resulting from greater release of these soluble components from the composites.

In summary, the present research has demonstrated the effectiveness of composites containing MCP with either TCP or εPL at forming HA deposits on composite surfaces. Of these two formulations, $M_{16}T_{16}\varepsilon_0$ absorbed less water and was therefore stronger, whereas $M_{16}T_0\varepsilon_8$ absorbed water more rapidly and therefore likely formed HA faster. It also had significantly higher τ, retained good mechanical properties in the range of some non-reactive commercial composites and had the extra advantage of containing antimicrobial agent εPL. Although further research into the antimicrobial effectiveness of εPL-containing composites is required, this study has demonstrated εPL's ability to induce rapid remineralisation. These findings also demonstrate that TCP is not required for HA transformation and that more soluble MCP is efficient at nucleating and converting to stable HA in the presence of εPL. Rapid formation of stable HA mineral within one week would likely improve the tooth-restoration interface, compensate for polymerisation shrinkage and protect against microbial microleakage. Furthermore, the antimicrobial action of εPL has the potential to protect against post-operative contamination, as well as subsequent microleakage and recurrent caries. This may allow more conservative and less painful treatment of dental caries by enabling restoration of teeth in which only infected (and not affected) dentine has been removed and would likely result in increased restoration durability.

8 CONCLUSIONS & FUTURE OUTLOOKS

Chapter 8 aims to concisely summarise the key findings of this thesis.

In Chapters 1 and 2, teeth, caries and restorative materials were introduced, with a focus on how innovative variants are being developed to overcome some of the drawbacks associated with composites. Chapter 3 detailed the materials and methods used throughout this set of studies, with the specific formulations described under each subsequent chapter.

Chapter 4 is a collection of a variety of preliminary studies which aimed to optimise the composite formulations prior to more detailed investigation in the following chapters. Chapters 5, 6 and 7 then go on to address the major aims of the project. The key observations are summarised below.

It can be concluded that UDMA significantly improved the conversion, BFS and depth of cure of composites compared to Bis-GMA, due to its greater flexibility and lower T_g. Its higher conversion also slightly improved cytocompatibility, likely due to reduced leaching of monomers. PPGDMA improved conversion relative to TEGDMA. The use of UDMA and PPGDMA in place of Bis-GMA and TEGDMA did not cause a detrimental increase in polymerisation shrinkage. Although the resazurin assay suggested that PPGDMA be more cytocompatible than TEGDMA, WST-8 and MTS assays proved inconclusive. Longer-term cytocompatibility and genocompatibility testing is therefore required. Furthermore, MTS significantly over-estimated metabolic activity, which emphasised the need to perform multiple types of analysis regarding biocompatibility.

These results suggest that careful consideration should be given to the polymerisation behaviour of the monomers used in dental composites, as well as their cytocompatibility. This is particularly true in the case of bulk fill materials, which aim to expedite the treatment of carious lesions by reducing the number of composite layers required, since the effect of monomer on conversion of the present composites was more pronounced at 4 mm than at 1 mm. Furthermore, the cytocompatibility test, which demonstrated that all formulations affect metabolic activity to different degrees, utilised specimens from the bottom 1 mm from a 4 mm stack. The deepest section of a restoration receives the lowest intensity of light during curing and as a result, can suffer from poor conversion if the constituent monomers lack flexibility. Given that this is also the most likely region of the composite to be in close proximity to pulp tissue, cytocompatibility is of particular importance for bulk fill materials.

The present research has also demonstrated the effectiveness of MCP at forming HA deposits on dental composite surfaces. TCP alone did not result in significant mineral formation, but when incorporated with MCP, it aided formation of substantial HA deposits. Similarly, εPL induced HA formation in MCP-containing composites. Incorporation of both TCP and εPL together with MCP resulted in reduced HA formation compared to when only one of these components was combined with MCP. The rapid formation of a stable HA surface layer within a one week period would likely improve the tooth-restoration interface, compensate for polymerisation shrinkage and protect against microbial microleakage. Furthermore, the antimicrobial action of εPL has the potential to protect against post-operative contamination, as well as subsequent microleakage and recurrent caries.

Overall, this project has been successful in improving the conversion, BFS and cytocompatibility of composites without detrimentally affecting shrinkage or depth of cure. Furthermore, composites which induced rapid and substantial surface HA formation were successfully developed. The water sorption and HA formation of these materials should help to improve the tissue-restoration interface and the presence of εPL should protect against microleakage. Such materials could be applied without requiring removal of affected dentine, allowing for the preservation of more healthy tissue and reducing the pain involved. This could be of particular benefit for paediatric patients in particular, given the high rate of caries in children[5], as well as those more sensitive to pain, as well as for patients in developing countries where access to equipment such as dental drills is limited. Given that the reactive fillers incorporated into these composites do not vary significantly in expense from standard glass fillers and that the failure rate of remineralisation and antimicrobial composites may be reduced compared to standard composites, this may result in a cost benefit, although this cannot be confirmed until long-term post-clinical evaluations can be conducted in order to determine the failure rate.

The major focus of future work should concern the antimicrobial effectiveness of these εPL-containing composites. Work has already begun on elucidating the effect of εPL against (confidential PhD thesis of Dr. Muhammad Adnan Khan). This will determine whether all of the εPL that is released from the composite exists in an active form. Additional future work will focus on further optimising the formulations to ensure an optimal balance between antimicrobial potential, mineral formation and mechanical properties. Studies on the wear resistance and aesthetics of the composites over time, as well as the shelf life of composite pastes is also required as the product is

commercialised and brought to the clinic. Finally, similar materials utilising a thermal initiator system are under development for orthopaedic treatments. Potential applications include vertebroplasty, for treatment of vertebral compression fracture, as well as maxillofacial surgery. The incorporation of strontium phosphate, growth factors such as bone morphogenetic protein 2, bisphosphonates or other therapeutic molecules may help to induce more complete integration between the orthopaedic composite and the surrounding bone tissue.

9 REFERENCES

1. Nanci A. Ten Cate's Oral Histology. 7 ed. Makati City: Elsevier Health Sciences; 2008. 1 p.
2. Atsu SS, Aka PS, Kucukesmen HC, Kilicarslan MA, Atakan C. Age-related changes in tooth enamel as measured by electron microscopy: implications for porcelain laminate veneers. J Prosthet Dent. 2005 Oct;94(4):336–41.
3. Vandana KL, Haneet RK. Cementoenamel junction: An insight. J Indian Soc Periodontol. 2014 Sep;18(5):549–54.
4. Loesche WJ. Role of *Streptococcus mutans* in human dental decay. Microbiol Rev. American Society for Microbiology (ASM); 1986;50(4):353.
5. National Institute of Dental & Craniofacial Research, National Institutes of Health, U.S. Department of Health & Human Services, editor. Dental caries (tooth decay) [Internet]. [cited 2016 Apr]. Available from: http://www.nidcr.nih.gov/DataStatistics/FindDataByTopic/DentalCaries/
6. Petersen PE. Sociobehavioural risk factors in dental caries - international perspectives. Community Dent Oral Epidemiol. 2005 Aug;33(4):274–9.
7. Bernardini F, Tuniz C, Coppa A, Mancini L, Dreossi D, Eichert D, et al. Beeswax as dental filling on a Neolithic human tooth. PLoS ONE. Public Library of Science; 2012;7(9):e44904.
8. Schmalz G, Arenholt Bindslev D. Biocompatibility of dental materials. Berlin: Springer Science & Business Media; 2008.
9. Agency for Toxic Substances Diseases Registry (ATSDR). Toxicological profile for mercury. Public Health Service, U.S. Department of Health and Human Services, Atlanta, GA; 1999.
10. Minamata convention on mercury – Text and annexes. United Nations Environment Programme; 2013.
11. Bowen RL. Dental filling material comprising vinyl silane treated fused silica and a binder consisting of the reaction product of bis pehnol and glycidyl acrylate. United States Patent Office. United States Patent Office; 3066112, 1962. pp. 1–3.
12. Albers HF. Tooth-colored restoratives: Principles and techniques. 9 ed. Ontario: BC Decker Inc; 2002.

13. Wolf H, Rateitschak-Pluss E. Color atlas of dental medicine: Periodontology. 3rd ed. Sttutgart: Thieme Medical Publishers; 2005.

14. Zimmerli B, Strub M, Jeger F, Stadler O, Lussi A. Composite materials: composition, properties and clinical applications. A literature review. Schweiz Monatsschr Zahnmed. 2010;120(11):972–86.

15. Mullen J, European Association for Paediatric Dentistry. History of water fluoridation. Br Dent J. 2005 Oct 8;199(7 Suppl):1–4.

16. Young AM, Rafeeka SA, Howlett JA. FTIR investigation of monomer polymerisation and polyacid neutralisation kinetics and mechanisms in various aesthetic dental restorative materials. Biomaterials. Elsevier; 2004;25(5):823–33.

17. Guida A, Hill RG, Towler MR, Eramo S. Fluoride release from model glass ionomer cements. J Mater Sci: Mater Med. Springer; 2002;13(7):645–9.

18. Leung D, Spratt DA, Pratten J, Gulabivala K, Mordan NJ, Young AM. Chlorhexidine-releasing methacrylate dental composite materials. Biomaterials. 2005 Dec;26(34):7145–53.

19. Mehdawi IM, Pratten J, Spratt DA, Knowles JC, Young AM. High strength re-mineralizing, antibacterial dental composites with reactive calcium phosphates. Dent Mater. 2013 Apr;29(4):473–84.

20. Newton T, Asimakopoulou K, Daly B, Scambler S, Scott S. The management of dental anxiety: time for a sense of proportion? Br Dent J. 2012 Sep;213(6):271–4.

21. Peumans M, Kanumilli P, De Munck J, Van Landuyt KL, Lambrechts P, Van Meerbeek B. Clinical effectiveness of contemporary adhesives: a systematic review of current clinical trials. Dent Mater. 2005 Sep;21(9):864–81.

22. Van Meerbeek B, De Munck J, Yoshida Y. Adhesion to enamel and dentin: current status and future challenges. Oper Dent. 2003.

23. Moszner N, Salz U, Zimmermann J. Chemical aspects of self-etching enamel-dentin adhesives: a systematic review. Dent Mater. 2005 Oct;21(10):895–910.

24. Moszner N, Salz U. Recent developments of new components for dental adhesives and composites. Macromolecular Materials and Engineering. 2007.

25. Van Landuyt KL, Snauwaert J, De Munck J, Peumans M, Yoshida Y, Poitevin A, et al. Systematic review of the chemical composition of contemporary dental adhesives. Biomaterials. 2007 Sep;28(26):3757–85.

26. Pashley DH, Tay FR, Breschi L, Tjäderhane L, Carvalho RM, Carrilho M, et al. State of the art etch-and-rinse adhesives. Dent Mater. 2011 Jan;27(1):1–16.

27. Sauro S, Watson TF, Mannocci F, Miyake K, Huffman BP, Tay FR, et al. Two-photon laser confocal microscopy of micropermeability of resin-dentin bonds made with water or ethanol wet bonding. J Biomed Mater Res Part B Appl Biomater. 2009 Jul;90(1):327–37.

28. Papakonstantinou AE, Eliades T, Cellesi F, Watts DC, Silikas N. Evaluation of UDMA's potential as a substitute for Bis-GMA in orthodontic adhesives. Dent Mater. 2013 Aug;29(8):898–905.

29. Ferracane JL. Hygroscopic and hydrolytic effects in dental polymer networks. Dent Mater. 2006 Mar;22(3):211–22.

30. Musanje L, Ferracane JL. Effects of resin formulation and nanofiller surface treatment on the properties of experimental hybrid resin composite. Biomaterials. 2004 Aug;25(18):4065–71.

31. Walter R, Swift EJ Jr, Sheikh H, Ferracane JL. Effects of temperature on composite resin shrinkage. Quintessence Int. 2009;40(10):843.

32. Rochester JR. Bisphenol A and human health: a review of the literature. Reprod Toxicol. 2013 Dec;42:132–55.

33. Ratanasathien S, Wataha JC, Hanks CT, Dennison JB. Cytotoxic interactive effects of dentin bonding components on mouse fibroblasts. J Dent Res. SAGE Publications; 1995;74(9):1602–6.

34. Schweikl H, Spagnuolo G, Schmalz G. Genetic and cellular toxicology of dental resin monomers. J Dent Res. 2006 Oct;85(10):870–7.

35. Schweikl H, Hiller K-A, Eckhardt A, Bolay C, Spagnuolo G, Stempfl T, et al. Differential gene expression involved in oxidative stress response caused by triethylene glycol dimethacrylate. Biomaterials. 2008 Apr;29(10):1377–87.

36. Batarseh G, Windsor LJ, Labban NY, Liu Y, Gregson K. Triethylene glycol dimethacrylate induction of apoptotic proteins in pulp fibroblasts. Oper Dent. 2014 Jan;39(1):E1–8.

37. Wisniewska-Jarosinska M, Poplawski T, Chojnacki CJ, Pawlowska E, Krupa R, Szczepanska J, et al. Independent and combined cytotoxicity and genotoxicity of triethylene glycol dimethacrylate and urethane dimethacrylate. Mol Biol Rep. 2011 Oct;38(7):4603–11.

38. Maddux WF, Abebe W, Schuster GS, Mozaffari MS. Effects of dental resin components on vascular reactivity. J Biomed Mater Res. 2002 Sep 15;61(4):572–80.

39. Abebe W, Pashley DH, Rueggeberg FA. Vasorelaxant effect of resin-based, single-bottle dentin bonding systems. J Endod. 2005 Mar;31(3):194–7.

40. Abebe W, Maddux WF. Roles of nitric oxide and prostacyclin in triethyleneglycol dimethacrylate (TEGDMA)-induced vasorelaxation. Dent Mater. 2006 Jan;22(1):37–44.

41. Basak F, Vural IM, Kaya E, Ulku C, Guven G, Cehreli SB, et al. Vasorelaxant effect of a self-etch adhesive system through calcium antagonistic action. J Endod. 2008 Oct;34(10):1202–6.

42. Guven G, Seyrek M, Vural IM, Cehreli ZC, Yildiz O. Vasodilatory effect of hydroxyethyl methacrylate and triethylene glycol dimethacrylate in rat aorta through calcium antagonistic action. J Endod. 2011 Mar;37(3):353–7.

43. Chang HH, Chang MC, Huang GF, Wang YL, Chan CP, Wang TM, et al. Effect of triethylene glycol dimethacrylate on the cytotoxicity, cyclooxygenase-2 expression and prostanoids production in human dental pulp cells. Int Endod J. 2012 Sep;45(9):848–58.

44. Huang F-M, Kuan Y-H, Lee S-S, Chang Y-C. Cytotoxicity and genotoxicity of triethyleneglycol-dimethacrylate in macrophages involved in DNA damage and caspases activation. Environ Toxicol. 2013 Dec 5.

45. Wiggins KM, Hartung M, Althoff O, Wastian C. Curing performance of a new-generation light-emitting diode dental curing unit. Journal of the American Dental Association. 2004.

46. Asmusen S, Arenas G, Cook WD, Vallo C. Photobleaching of camphorquinone during polymerization of dimethacrylate-based resins. Dent Mater. 2009 Dec;25(12):1603–11.

47. Datar RA, Rueggeberg FA, Caughman GB, Wataha JC, Lewis JB, Schuster GS. Effects of sub-toxic concentrations of camphorquinone on cell lipid metabolism. J Biomater Sci Polym Ed. Taylor & Francis; 2005;16(10):1293–302.

48. Neumann MG, Miranda WG, Schmitt CC, Rueggeberg FA, Correa IC. Molar extinction coefficients and the photon absorption efficiency of dental photoinitiators and light curing units. J Dent. 2005 Jul;33(6):525–32.

49. Hadis MA, Shortall ACC, Palin WM. Competitive light absorbers in photoactive dental resin-based materials. Dent Mater. 2012 Aug;28(8):831–41.

50. Brandt WC, Schneider LFJ, Frollini E, Correr-Sobrinho L, Sinhoreti MAC. Effect of different photo-initiators and light curing units on degree of conversion of composites. Braz Oral Res. 2010 Jul;24(3):263–70.

51. Park YJ, Chae KH, Rawls HR. Development of a new photoinitiation system for dental light-cure composite resins. Dent Mater. 1999 Mar;15(2):120–7.

52. Dunnick JK, Brix A, Sanders JM, Travlos GS. *N,N*-Dimethyl-*p*-toluidine, a component in dental materials, causes hematologic toxic and carcinogenic responses in rodent model systems. Toxicol Pathol. 2013 Jul 18.

53. Burton GW, Ingold KU. Autoxidation of biological molecules. 1. Antioxidant activity of vitamin E and related chain-breaking phenolic antioxidants in vitro. J Am Chem Soc. 1981.

54. Ferracane JL. Resin composite – State of the art. Dent Mater. 2011 Jan;27(1):29–38.

55. Matinlinna JP, Özcan M, Lassila LVJ, Vallittu PK. The effect of a 3-methacryloxypropyltrimethoxysilane and vinyltriisopropoxysilane blend and tris(3-trimethoxysilylpropyl)isocyanurate on the shear bond strength of composite resin to titanium metal. Dent Mater. 2004 Nov;20(9):804–13.

56. Fujita K, Ikemi T, Nishiyama N. Effects of particle size of silica filler on polymerization conversion in a light-curing resin composite. Dent Mater. 2011 Nov;27(11):1079–85.

57. Xu HHK, Sun L, Weir MD, Takagi S, Chow LC, Hockey B. Effects of incorporating nanosized calcium phosphate particles on properties of whisker-reinforced dental composites. J Biomed Mater Res Part B Appl Biomater. 2007 Apr;81(1):116–25.

58. Fong H. Electrospun nylon 6 nanofiber reinforced BIS-GMA/TEGDMA dental restorative composite resins. Polymer. Elsevier; 2004;45(7):2427–32.

59. Arikawa H, Kanie T, Fujii K, Takahashi H, Ban S. Effect of filler properties in composite resins on light transmittance characteristics and color. Dent Mater J. 2007 Jan;26(1):38–44.

60. Chen L, Yu Q, Wang Y, Li H. BisGMA/TEGDMA dental composite containing high aspect-ratio hydroxyapatite nanofibers. Dent Mater. 2011 Nov;27(11):1187–95.

61. Lin S, Cai Q, Ji J, Sui G, Yu Y, Yang X, et al. Electrospun nanofiber reinforced and toughened composites through in situ nano-interface formation. Comp Sci Technol. Elsevier; 2008;68(15):3322–9.

62. Garoushi S, Vallittu PK, Watts DC, Lassila LVJ. Polymerization shrinkage of experimental short glass fiber-reinforced composite with semi-inter penetrating polymer network matrix. Dent Mater. 2008 Feb;24(2):211–5.

63. Garoushi S, Kaleem M, Shinya A, Vallittu PK, Satterthwaite JD, Watts DC, et al. Creep of experimental short fiber-reinforced composite resin. Dent Mater. Nihon Shika Riko Gakkai, c/o Koku Hoken Kyokai Tokyo 170-0003 Japan; 2012;31(5):737–41.

64. Garoushi S, Säilynoja E, Vallittu PK, Lassila LVJ. Physical properties and depth of cure of a new short fiber reinforced composite. Dent Mater. The Academy of Dental Materials; 2013 Aug 1;29(8):835–41.

65. LeGeros RZ. Calcium phosphate-based osteoinductive materials. Chem Rev. 2008 Nov 12;108(11):4742–53.

66. Xia W, Razi M, Ashley PF, Abou Neel EA, Hoffman MP, Young AM. Quantifying effects of interactions between polyacrylic acid and chlorhexidine in dicalcium phosphate–forming cements. J Mater Chem B. 2014.

67. Abou Neel EA, Salih V, Revell PA, Young AM. Viscoelastic and biological performance of low-modulus, reactive calcium phosphate-filled, degradable, polymeric bone adhesives. Acta Biomaterialia. 2012 Jan;8(1):313–20.

68. Mehdawi IM, Abou Neel EA, Valappil SP, Palmer G, Salih V, Pratten J, et al. Development of remineralizing, antibacterial dental materials. Acta Biomaterialia. 2009 Sep;5(7):2525–39.

69. Combes C, Rey C. Amorphous calcium phosphates: synthesis, properties and uses in biomaterials. Acta Biomaterialia. 2010 Sep;6(9):3362–78.

70. Jean A, Kerebel B, Kerebel LM, LeGeros RZ, Hamel H. Effects of various calcium phosphate biomaterials on reparative dentin bridge formation. J Endod. 1988 Feb;14(2):83–7.

71. Al-Sanabani JS, Madfa AA, Al-Sanabani FA. Application of calcium phosphate materials in dentistry. Int J Biomater. 2013;2013:876132.

72. LeGeros RZ. Calcium phosphate materials in restorative dentistry: a review. Adv Dent Res. SAGE Publications; 1988;2(1):164–80.

73. Xu HHK, Weir MD, Sun L, Ngai S, Takagi S, Chow LC. Effect of filler level and particle size on dental caries-inhibiting Ca-PO(4) composite. J Mater Sci: Mater Med. 2009 Aug;20(8):1771–9.

74. Ginebra MP, Espanol M, Montufar EB, Perez RA, Mestres G. New processing approaches in calcium phosphate cements and their applications in regenerative medicine. Acta Biomaterialia. 2010 Aug;6(8):2863–73.

75. Skrtic D, Antonucci JM, Eanes ED, Eichmiller FC, Schumacher GE. Physicochemical evaluation of bioactive polymeric composites based on hybrid amorphous calcium phosphates. J Biomed Mater Res. 2000;53(4):381–91.

76. Dickens SH, Flaim GM, Takagi S. Mechanical properties and biochemical activity of remineralizing resin-based Ca–PO 4 cements. Dent Mater. Elsevier; 2003;19(6):558–66.

77. Zhao J, Liu Y, Sun W-B, Zhang H. Amorphous calcium phosphate and its application in dentistry. Chem Cent J. 2011;5:40.

78. Cheng L, Weir MD, Xu HHK, Kraigsley AM, Lin NJ, Lin-Gibson S, et al. Antibacterial and physical properties of calcium-phosphate and calcium-fluoride nanocomposites with chlorhexidine. Dent Mater. 2012 May;28(5):573–83.

79. Cheng L, Weir MD, Xu HHK, Antonucci JM, Kraigsley AM, Lin NJ, et al. Antibacterial amorphous calcium phosphate nanocomposites with a quaternary ammonium dimethacrylate and silver nanoparticles. Dent Mater. 2012 May;28(5):561–72.

80. Cheng L, Weir MD, Xu HHK, Antonucci JM, Lin NJ, Lin-Gibson S, et al. Effect of amorphous calcium phosphate and silver nanocomposites on dental plaque microcosm biofilms. J Biomed Mater Res Part B Appl Biomater. 2012 Jul;100(5):1378–86.

81. Melo MAS, Cheng L, Zhang K, Weir MD, Rodrigues LKA, Xu HHK. Novel dental adhesives containing nanoparticles of silver and amorphous calcium phosphate. Dent Mater. 2013 Feb;29(2):199–210.

82. Cheng L, Weir MD, Zhang K, Arola DD, Zhou X, Xu HHK. Dental primer and adhesive containing a new antibacterial quaternary ammonium monomer dimethylaminododecyl methacrylate. J Dent. 2013 Apr;41(4):345–55.

83. Melo MAS, Cheng L, Weir MD, Hsia R-C, Rodrigues LKA, Xu HHK. Novel dental adhesive containing antibacterial agents and calcium phosphate nanoparticles. J Biomed Mater Res Part B Appl Biomater. 2013 May;101(4):620–9.

84. Zhang N, Ma J, Melo MAS, Weir MD, Bai Y, Xu HHK. Protein-repellent and antibacterial dental composite to inhibit biofilms and caries. J Dent. 2015 Feb;43(2):225–34.

85. Imazato S, Russell RR, McCabe JF. Antibacterial activity of MDPB polymer incorporated in dental resin. J Dent. 1995 Jun;23(3):177–81.

86. Imazato S, Imai T, Russell RR, Torii M, Ebisu S. Antibacterial activity of cured dental resin incorporating the antibacterial monomer MDPB and an adhesion-promoting monomer. J Biomed Mater Res. 1998 Mar 15;39(4):511–5.

87. Li F, Majd H, Weir MD, Arola DD, Xu HHK. Inhibition of matrix metalloproteinase activity in human dentin via novel antibacterial monomer. Dent Mater. 2015 Jan 13.

88. Zhou C, Weir MD, Zhang K, Deng D, Cheng L, Xu HHK. Synthesis of new antibacterial quaternary ammonium monomer for incorporation into CaP nanocomposite. Dent Mater. 2013 Aug;29(8):859–70.

89. Zhang K, Cheng L, Wu EJ, Weir MD, Bai Y, Xu HHK. Effect of water-ageing on dentine bond strength and anti-biofilm activity of bonding agent containing new monomer dimethylaminododecyl methacrylate. J Dent. 2013 Jun;41(6):504–13.

90. Delihas N, Riley LW, Loo W, Berkowitz J, Poltoratskaia N. High sensitivity of *Mycobacterium* species to the bactericidal activity by polylysine. FEMS Microbiol Lett. 1995 Oct 15;132(3):233–7.

91. Lee J-H. Antimicrobial effect of medical adhesive composed of aldehyded dextran and ε-poly(L-lysine). J Microbiol Biotechnol. 2011 Nov 28;21(11):1199–202.

92. Shih I-L, Shen M-H, Van Y-T. Microbial synthesis of poly(epsilon-lysine) and its various applications. Bioresour Technol. 2006 Jun;97(9):1148–59.

93. Ye R, Xu H, Wan C, Peng S, Wang L, Xu H, et al. Antibacterial activity and mechanism of action of ε-poly-L-lysine. Biochem Biophys Res Coomun. 2013 Sep 13;439(1):148–53.

94. British Standard BS ISO 23317:2012, "Implants for surgery – *In vitro* evaluation for apatite-forming ability of implant materials." International Standards Organisation, Brussels, Belgium; 2012 p. 24.

95. Kokubo T, Takadama H. How useful is SBF in predicting in vivo bone bioactivity? Biomaterials. 2006 May;27(15):2907–15.

96. McKnight-Hanes C, Whitford GM. Fluoride release from three glass ionomer materials and the effects of varnishing with or without finishing. Caries Res. 1992;26(5):345–50.

97. Levine MJ, Aguirre A, Hatton MN, Tabak LA. Artificial salivas: present and future. J Dent Res. 1987 Feb;66 Spec No:693–8.

98. Rueggeberg F, Tamareselvy K. Resin cure determination by polymerization shrinkage. Dent Mater. 1995 Jul;11(4):265–8.

99. Patel MP, Braden M, Davy KW. Polymerization shrinkage of methacrylate esters. Biomaterials. 1987 Jan;8(1):53–6.

100. Loshaek S, Fox TG. Cross-linked polymers. I. Factors influencing the efficiency of cross-linking in copolymers of methyl methacrylate and glycol dimethacrylates. J Am Chem Soc. ACS Publications; 1953;75(14):3544–50.

101. Walters NJ, Xia W, Salih V, Ashley PF, Young AM. Poly(propylene glycol) and urethane dimethacrylates improve conversion of dental composites and reveal complexity of cytocompatibility testing. Dent Mater. 2016 Jan 4.

102. British Standard BS EN ISO 17304:2013, "Dentistry – Polymerization shrinkage: Method for determination of polymerization shrinkage of polymer-based restorative materials." British Standards Institute. International Standards Organisation, Brussels, Belgium; 2013 pp. 1–24.

103. British Standard BS EN ISO 4049:2009, "Dentistry – Polymer-based restorative materials." International Standards Organisation, Brussels, Belgium; 2009 pp. 1–38.

104. Walters NJ, Liaqat S, Palmer G, Panpisut P, Mordan NJ, Ashley PF, et al. Rapid hydroxyapatite precipitation on dental composite surfaces. Under preparation for submission to J Dent Res. 2016 Apr 5;:1–18.

105. Timoshenko S, Woinowsky-Krieger S. Theory of Plates and Shells. 2nd ed. New York: McGraw-Hill; 1959. 1 p.

106. Higgs WA, Lucksanasombool P, Higgs RJ, Swain MV. A simple method of determining the modulus of orthopedic bone cement. J Biomed Mater Res. 2001;58(2):188–95.

107. British Standard BS EN ISO 29022:2013, “Dentistry – Adhesion – Notched-edge shear bond strength test.” International Standards Organisation, Brussels, Belgium; 2013 pp. 1–24.

108. Liaqat S, Aljabo A, Khan MA, Ben Nuba H, Bozec L, Ashley PF, et al. Characterization of dentine to assess bond strength of dental composites. Materials. 2015 May;8(5):2110–26.

109. Liaqat S. Development of antibacterial-releasing dental composites with high strength and dentine bonding. Young AM, Bozec L, Ashley PF, editors. UCL Eastman Dental Institute; 2015. pp. 1–383.

110. International Standard ISO 10993-5:2009(E), “Biological evaluation of medical devices – Part 5: Tests for in vitro cytotoxicity.” International Standards Organisation, Brussels, Belgium; 2009 pp. 1–42.

111. British Standard BS EN ISO 10993-12:2012, “Biological evaluation of medical devices – Part 12: Sample preparation and reference materials.” International Standards Organisation, Brussels, Belgium; 2012 pp. 1–34.

112. Floyd CJE, Dickens SH. Network structure of Bis-GMA- and UDMA-based resin systems. Dent Mater. 2006 Dec;22(12):1143–9.

113. Business U. GB Patent Filing 1313898.7.

114. Chung KH, Greener EH. Correlation between degree of conversion, filler concentration and mechanical properties of posterior composite resins. J Oral Rehabil. 1990 Sep;17(5):487–94.

115. Williams DF. There is no such thing as a biocompatible material. Biomaterials. 2014 Dec;35(38):10009–14.

116. Sideridou I, Tserki V, Papanastasiou G. Effect of chemical structure on degree of conversion in light-cured dimethacrylate-based dental resins. Biomaterials. 2002 Apr;23(8):1819–29.

117. Lin NJ, Bailey LO, Becker ML, Washburn NR, Henderson LA. Macrophage response to methacrylate conversion using a gradient approach. Acta Biomaterialia. 2007 Mar;3(2):163–73.

118. Schweikl H, Altmannberger I, Hanser N, Hiller K-A, Bolay C, Brockhoff G, et al. The effect of triethylene glycol dimethacrylate on the cell cycle of mammalian cells. Biomaterials. 2005 Jul;26(19):4111–8.

119. Chang H-H, Chang M-C, Lin L-D, Lee J-J, Wang T-M, Huang C-H, et al. The mechanisms of cytotoxicity of urethane dimethacrylate to Chinese hamster ovary cells. Biomaterials. 2010 Sep;31(27):6917–25.

120. Chang M-C, Chen L-I, Chan C-P, Lee J-J, Wang T-M, Yang T-T, et al. The role of reactive oxygen species and hemeoxygenase-1 expression in the cytotoxicity, cell cycle alteration and apoptosis of dental pulp cells induced by BisGMA. Biomaterials. 2010 Nov;31(32):8164–71.

121. Olea N, Pulgar R, Pérez P, Olea-Serrano F, Rivas A, Novillo-Fertrell A, et al. Estrogenicity of resin-based composites and sealants used in dentistry. Environ Health Perspect. 1996 Mar;104(3):298–305.

122. Chang H-H, Chang M-C, Wang H-H, Huang G-F, Lee Y-L, Wang Y-L, et al. Urethane dimethacrylate induces cytotoxicity and regulates cyclooxygenase-2, hemeoxygenase and carboxylesterase expression in human dental pulp cells. Acta Biomaterialia. 2014 Feb;10(2):722–31.

123. Chang MC, Lin LD, Chuang FH, Chan CP, Wang TM, Lee JJ, et al. Carboxylesterase expression in human dental pulp cells: role in regulation of BisGMA-induced prostanoid production and cytotoxicity. Acta Biomaterialia. 2012 Mar;8(3):1380–7.

124. Kuan Y-H, Huang F-M, Lee S-S, Li Y-C, Chang Y-C. Bisgma stimulates prostaglandin E2 production in macrophages via cyclooxygenase-2, cytosolic phospholipase A2, and mitogen-activated protein kinases family. PLoS ONE. Public Library of Science; 2013;8(12):e82942.

125. Kuan YH, Li YC, Huang F-M, Chang Y-C. The upregulation of tumour necrosis factor-α and surface antigens expression on macrophages by bisphenol A-glycidyl-methacrylate. Int Endod J. 2012 Jul;45(7):619–26.

126. Tamura A, Fukumoto I, Yui N, Matsumura M, Miura H. Increasing the repeating units of ethylene glycol-based dimethacrylates directed toward reduced oxidative stress and co-stimulatory factors expression in human monocytic cells. J Biomed Mater Res A. 2014 Jun 10.

127. Moharamzadeh K, Van Noort R, Brook IM, Scutt AM. Cytotoxicity of resin monomers on human gingival fibroblasts and HaCaT keratinocytes. Dent Mater. Elsevier; 2007;23(1):40–4.

128. Kostoryz EL, Tong PY, Chappelow CC, Eick JD, Glaros AG, Yourtee DM. In vitro cytotoxicity of solid epoxy-based dental resins and their components. Dent Mater. 1999 Sep;15(5):363–73.

129. Thonemann B, Schmalz G, Hiller K-A, Schweikl H. Responses of L929 mouse fibroblasts, primary and immortalized bovine dental papilla-derived cell lines to dental resin components. Dent Mater. Elsevier; 2002;18(4):318–23.

130. Barszczewska-Rybarek IM. Structure-property relationships in dimethacrylate networks based on Bis-GMA, UDMA and TEGDMA. Dent Mater. 2009 Sep;25(9):1082–9.

131. Deb S, Aiyathurai L, Roether JA, Luklinska ZB. Development of high-viscosity, two-paste bioactive bone cements. Biomaterials. 2005 Jun;26(17):3713–8.

132. Rampersad SN. Multiple applications of Alamar Blue as an indicator of metabolic function and cellular health in cell viability bioassays. Sensors (Basel). 2012;12(9):12347–60.

133. O'Brien J, Wilson I, Orton T, Pognan F. Investigation of the Alamar Blue (resazurin) fluorescent dye for the assessment of mammalian cell cytotoxicity. Eur J Biochem. 2000 Sep;267(17):5421–6.

134. Semisch A, Hartwig A. Copper ions interfere with the reduction of the Water-Soluble Tetrazolium Salt-8. Chemical research in toxicology. ACS Publications; 2014;27(2):169–71.

135. Wang P, Henning SM, Heber D. Limitations of MTT and MTS-based assays for measurement of antiproliferative activity of green tea polyphenols. PLoS ONE. Public Library of Science; 2010;5(4):e10202.

136. Lapp CA, Schuster GS. Effects of DMAEMA and 4-methoxyphenol on gingival fibroblast growth, metabolism, and response to interleukin-1. J Biomed Mater Res. 2002 Apr;60(1):30–5.

137. Yoshida K, Greener EH. Effect of photoinitiator on degree of conversion of unfilled light-cured resin. J Dent. 1994 Oct;22(5):296–9.

138. Labella R, Lambrechts P, Van Meerbeek B, Vanherle G. Polymerization shrinkage and elasticity of flowable composites and filled adhesives. Dent Mater. 1999 Mar;15(2):128–37.

139. Kahler B, Kotousov A, Swain MV. On the design of dental resin-based composites: a micromechanical approach. Acta Biomaterialia. 2008 Jan;4(1):165–72.

140. Smith AJ, Cassidy N, Perry H, Bègue-Kirn C, Ruch JV, Lesot H. Reactionary dentinogenesis. Int J Dev Biol. 1995 Feb;39(1):273–80.

141. Badaoui Najjar M, Kashtanov D, Chikindas ML. Natural antimicrobials ε-poly-l-lysine and Nisin A for control of oral microflora. Probiotics and Antimicrobial …. 2009.

142. Li F, Weir MD, Fouad AF, Xu HHK. Time-kill behaviour against eight bacterial species and cytotoxicity of antibacterial monomers. J Dent. 2013 Oct;41(10):881–91.